RESEARCH & DEVELOPMENT

IMPROVEMENT OF MATERIAL CRITERIA FOR HIGHWAY EMBANKMENT CONSTRUCTION

Mehrdad Hassani, PhD Candidate

Miguel A. Pando, PhD, PE

Rajaram Janardhanam, PhD

Department of Civil and Environmental Engineering

University of North Carolina at Charlotte

1. Report No. FHWA/NC/2015-05	2. Government Accession No.	3. Recipient's Catalog No.	
4. Title and Subtitle Improvement of Material Criteria for Highway Embankment Construction		5. Report Date March 2019	
		6. Performing Organization Code	
7. Author(s) Mehrdad Hassani, PhD Candidate, Research Assistant Miguel A. Pando, Ph.D, P.E. Rajaram Janardhanam, Ph.D		8. Performing Organization Report No.	
9. Performing Organization Name and Address Department of Civil and Environmental Engineering University of North Carolina at Charlotte 9201 University City Boulevard Charlotte, NC 28223-0001		10. Work Unit No. (TRAIS)	
		11. Contract or Grant No.	
12. Sponsoring Agency Name and Address Research and Development Unit 104 Fayetteville Street Raleigh, North Carolina 27601		13. Type of Report and Period Covered Final Report January 2015 – March 2019	
		14. Sponsoring Agency Code 2015-05	
Supplementary Notes:			

16. Abstract

Performance of the highway embankments has been investigated based on two main concerns; slope stability and deformation. To examine embankment performance, parameters obtained from both total stress analysis (TSA) and effective stress analysis (ESA) have been considered, that is stability and deformation have been each investigated under two states of TSA and ESA. This also necessitates that soil strength properties are obtained at both TSA and ESA conditions. The scope considers only failures and settlements related to compacted embankment and not due to poor foundation soil conditions. A set of unconsolidated-undrained (UU) triaxial tests has been used to obtain total stress soil strength properties, and a set of consolidated-undrained (CU) triaxial tests with pore pressure measurements has been considered to achieve effective stress soil strength properties. Sixteen embankment geometric sections have been considered in total. For the highway embankment deformation analysis, two-dimensional plane strain conditions were assumed. Among all cases, not even one case showed TSA factor of safety lower than the minimum value of 1.3. In many of these cases FS is well above the minimum value. Results of the stability analysis based on ESA parameters were completely different from those of obtained using TSA parameters, as in the effective stress stability analyses many cases were found having FS lower than 1.3. For the effective stress slope stability analysis, shallow failure must be checked as it is a case with high possibility. There are some findings that might give grounds to the idea that soils with higher PI such as Soil 2 Lee an A-7-6 AASHTO class perform slightly better under rain-induced inundation conditions. This is in opposition to the criterion of limiting material PI as material selection criteria which is currently used by the NC state standard. This might at least cast doubt on the NCDOT material selection specification of limiting PI to 15% in the North Carolina coastal area. Providing suitable vegetation cover (to reduce infiltration and promote runoff) as well as drainage measures for the highway embankments could be very helpful to avoid detrimental effects of presence of water in the body of embankment.

17. Key Words Highway Embankment, Slope Stability, Deformation, Shallow Slope Failure, Case History, Compaction, Soil Strength, UU triaxial test, CU triaxial test, Soil		18. Distribution Statement		
19. Security Classif. (of this report) Unclassified		20. Security Classif. (of this page) Unclassified	21. No. of Pages 215	22. Price

Form DOT F 1700.7 (8-72)   **Reproduction of completed page authorized**

DISCLAIMER

The contents of this report reflect the views of the author(s) and not necessarily the views of the University. The author(s) are responsible for the facts and the accuracy of the data presented herein. The contents do not necessarily reflect the official views or policies of either the North Carolina Department of Transportation or the Federal Highway Administration at the time of publication. This report does not constitute a standard, specification, or regulation.

ACKNOWLEDGMENTS

EXECUTIVE SUMMARY

This report serves as the final report for the NCDOT research project 2015-05 on improvement of material criteria for highway embankment construction. This report is divided into 10 chapters and 3 appendices. Literature review on the necessary research issues is followed by investigation of the performance of highway embankments built with typical soils found in the piedmont region of North Carolina.

Performance of the highway embankments has been investigated based on two main concerns; slope stability and deformation. To examine embankment performance, parameters obtained from both total stress analysis (TSA) and effective stress analysis (ESA) have been considered, that is stability and deformation have been each investigated under two states of TSA and ESA. This also necessitates that soil strength properties are obtained at both TSA and ESA conditions. The scope considers only failures and settlements related to compacted embankment and not due to poor foundation soil conditions. A set of unconsolidated-undrained (UU) triaxial tests has been used to obtain TSA soil strength properties, and a set of consolidated-undrained (CU) triaxial tests has been considered to achieve ESA soil strength properties. Rate of the axial strain in UU triaxial tests was 1%/minute. Failure criterion of generated pore pressure during shear stage equal to zero was adopted in the CU triaxial tests. Brief search on minimum factor of safety (FS) against sliding was accompanied by an extensive search on allowable settlement for highway embankments. Sixteen embankment geometric sections have been considered in total. Limit equilibrium method was used for stability analysis. For the highway embankment deformation analysis, two-dimensional plane strain conditions were assumed. Elasticity modulus has been selected meticulously; and initial model was improved by the hypothesis of taking into account differences in elasticity modulus within embankment depth based on the average of horizontal stresses.

Detailed tables are presented as the result of slope stability analyses and deformation analyses. Wherever seemed feasible and reasonable, regression equations were represented to introduce values of FS or deformation based on embankment geometric parameters and soil strength parameters. A set of dimensionless formulae has been generated for ease of use as well.

Among all cases, not even one case showed TSA factor of safety lower than the minimum value of 1.3. In many of these cases FS is well above the minimum value. A table is presented which provides descriptive information of acceptable cases based on TSA deformation criterion.

Results of the stability analysis based on ESA parameters were completely different from those of obtained using TSA parameters, as in the effective stress stability analyses many cases were found having FS lower than 1.3. For the effective stress slope stability analysis, shallow failure must be checked as it is a case with high possibility. A descriptive table is presented which may be used as means of acceptance zone/cases based on effective stress analysis stability criterion.

There are some findings that might give grounds to the idea that soils with higher PI such as Soil 2 Lee (a soil with AASHTO A-7-6 class) perform slightly better under rain-induced inundation conditions. This is in opposition to the criterion of limiting material PI as material selection criteria which is currently used by the NC state standard. Of course, it is noted that among tested soils Soil 2 Lee has PI=21 which still keeps it in the acceptable range of $PI \leq 25$ for piedmont area of NC. However, this may cast doubt on the NCDOT material selection specification of limiting PI to 15% in the North Carolina coastal area.

TABLE OF CONTENTS

LIST OF FIGURES

LIST OF TABLES

LIST OF ABBREVIATIONS AND SYMBOLS

AASHTO	American Association of State Highway and Transportation Officials
ASTM	American Society for Testing and Materials
USDOT	United States Department of Transportation
NCDOT	North Carolina Department of Transportation
NC	North Carolina
MC	moisture content (same as water content) of soil sample, also denoted by w, unit: %
w	moisture content of soil sample, unit: %
OMC	optimum moisture/water content obtained in a standardized laboratory compaction test, unit: %, also denoted by W_{opt}
g_m	total / moist unit weight of material, unit: kN/m^3
g_d	dry unit weight of material, unit: kN/m^3
$g_{d\max}$	maximum dry unit weight obtained in a standardized laboratory compaction test, unit= kN/m^3
RC	relative compaction which is the ratio of dry unit weight (or dry density if expressed in terms of mass per unit volume) achieved after compaction in the field to $g_{d\max}$
PI	plasticity index
LL	liquid limit
m	meter
ft	foot/feet
in	inch/inches
H	height of highway embankment
S	side slope of highway embankment; stated as ratio of horizontal step to vertical step, for instance for 4H:1V embankment, S would be equal to 4
TSA	total stress analysis
ESA	effective stress analysis
UU	unconsolidated-undrained triaxial test
CU	consolidated-undrained triaxial test
FS	factor of safety in slope stability analysis
D	maximum crest deformation of embankment, unit: centimeters
f_{UU}	total stress friction angle of soil material obtained from UU triaxial test, unit: degrees
C_{UU}	total stress cohesion of soil material obtained from UU triaxial test, unit: kPa
E_{UU}	modulus of elasticity of soil material obtained from UU triaxial test, unit: kPa
f'	effective stress friction angle of soil material obtained from CU triaxial test, unit: degrees
C'	effective stress cohesion of soil material obtained from CU triaxial test, unit: kPa
E_{CU}	modulus of elasticity of soil material obtained from CU triaxial test, unit: kPa
C_D	dimensionless cohesion
E_D	dimensionless modulus of elasticity

UNITS CONVERSION INDEX

This report is written mainly based on the SI units which uses Newton as the unit for force measurement and meter as the unit for distance measurement. It is noted that U.S. DOTs are in a transition period from Imperial units to SI units; however, as NCDOT is still dealing with Imperial units; the following table might be useful for the users.

Imperial units	SI units	Unit type
1 inch	2.54 cm	Distance
1 foot = 12 inch	30.48 cm = 0.3048 m	Distance
1 lb	0.454 kg	Mass
1 lb-f	0.454 kg-f = 4.452 N	Force
1 psf	47.92 Pa	Stress
1 psi	6900 Pa $\approx$ 7 kPa	Stress
1 pcf	16.03 kgf/m^3 = 157.23 N/m^3	Unit weight

1. INTRODUCTION

Although good knowledge and extensive research is available regarding general aspects of the highway embankments such as global stability, construction routine, and settlement, it seems there is still an important need to better understand some special aspects of these structures.

For example, shallow slope failure seems to be a common current mode of failure that needs to be investigated more meticulously. Shallow slope failure appears to be related to the appearance of water in the embankment body, or more accurately in the embankment side slopes. In other words, shallow or surficial failures are usually induced by heavy rainfall.

Performance of highway embankments is mainly related to two concerns of slope stability, and deformation. That is, to investigate performance of embankments not only failure possibility, but also deformation behavior must be examined. Also, each of these concerns must be viewed from two viewpoints; total stress analysis (TSA), and effective stress analysis (ESA). Under TSA condition, embankment soil is assumed unsaturated which may represent conditions right after construction of an embankment. Under ESA condition, it is assumed that embankment soil is vulnerable to saturation due to the rainfalls; thus, this state might be alternatively called rain-induced condition analysis. ESA condition might not happen at the construction time but is likely to occur during the service time of an embankment.

However, it seems besides slope stability and immediate deformation, we could mention another concern which must be addressed in terms of performance of embankments. This concern seems to be "creep" of the highway embankment. Creep of saturated clays has been studied extensively as part of the consolidation behavior of clays. However; it is important to point out that in those cases, creep refers to the secondary consolidation of a saturated soil that has first undergone a one-dimensional consolidation phase. For the purposes of this research, creep might refer to long-term soil deformation under constant load.

Before an embankment is built, it seems two important questions must be answered; that embankment will be built with what type of material? and that how this embankment will be built? Therefore, embankment material selection criteria and embankment construction specifications

which are currently executed must be reviewed. This important task is presented in the literature review chapter.

However, extensive survey of the literature revealed that embankment material selection criteria and embankment construction specifications may be very different among agencies in the U.S. The use of plasticity index (PI) as material selection criteria for embankments is limited to a few states, but the possibility of incidence of large undesirable long-term deformations due to use of material with high PI should be investigated. As mentioned earlier, this concern may be addressed using laboratory long-term one-dimensional creep tests under constant loading.

We also need to investigate any possible relationship between shallow slope failure and material selection criteria, also between shallow slope failure and construction specifications. For this purpose, we need to gain good knowledge about case histories of shallow slope failure. This task is also presented in the literature review chapter.

After literature review, research methodology is explained in chapter three. As mentioned before performance of embankment should be reviewed using both total stress analysis (TSA) parameters, and effective stress analysis (ESA) parameters. That is stability and deformation each need to be investigated in two conditions; TSA and ESA. This also necessitates that we obtain soil strength properties at both TSA and ESA conditions. To find TSA soil strength properties a set of unconsolidated-undrained (UU) triaxial tests has been designed, and to achieve ESA soil strength properties a set of consolidated-undrained (CU) triaxial tests with pore pressure measurements has been considered.

TSA might apply to when an embankment has just been constructed (right after embankment construction); embankment soil is unsaturated, similar to the state of soil specimen in a UU triaxial test. On the other hand, under the ESA state it is assumed that embankment soil is vulnerable to saturation due to the rainfalls. This situation is similar to the soil specimen in a CU triaxial test (after consolidation stage / before shear stage). Results of the laboratory attempt are presented in chapters five, six, and seven.

Chapters eight and nine present slope stability analysis and deformation analysis respectively. Utilized methods, assumptions, parameters are explained and discussed. Finally, chapter ten

presents summary and conclusions. A few appendix chapters at the end of report provide detailed information regarding laboratory tests or analysis tasks.

At the end, objectives of this research study are listed as following:

- Improving material selection criteria for highway embankment,

- Survey of the current practices followed by U.S. state DOTs,

- Comprehensive laboratory investigation on compacted borrow soils that are representative of NCDOT current construction practices; to obtain: classification and index properties, engineering properties, and shear strength properties,

- Define acceptable zones for slope stability and deformation considerations in the moisture content - dry unit weight domain.

2. LITERATURE REVIEW

An extensive literature review has been carried out to better guide different aspects of this research project. The literature review chapter is subdivided into the following topics: i) U.S. states requirements for highway embankment material selection and construction, ii) case histories of road/highway embankment failure, iii) minimum factor of safety for highway embankments, and iv) settlement of the highway embankment.

2.1. U.S. States Specifications on Highway Embankment Material Selection and Construction Requirements

In this section a review of the specifications and requirements set by U.S. states regarding highway embankment material selection and construction is presented. Reviewed components regarding material selection include material gradation / classification, and Atterberg limits. Reviewed components regarding construction include any requirements on minimum field dry unit weight and relative compaction, moisture control, and lift thickness. Material presented in this section are obtained from Hassani et al. (2017), a report submitted to NCDOT as part of the current project.

2.1.1. Requirements on Material Gradation

After intensive review of the state standards it is noted that only a few of them have minor requirements set for material gradation. These include Colorado, Ohio, Rhode Island, South Carolina and Utah. In all cases, these requirements are very general; for instance, South Carolina specifies that A-7 group soil shall not be used. Pennsylvania also sets some requirements only for the fine-grained portion of the embankment material. Figure 2.1 shows states imposing requirements on gradation. It is noted that two U.S. separate states, that is Alaska and Hawaii are also shown on the map.

All states mention a maximum allowable particle size suitable for the upper layers of embankment. They usually forbid using particles larger than 4 to 6 inches in the upper 1 or 2 feet, and also disallow use of large rock fragments and stones in the top few feet of the highway embankment.
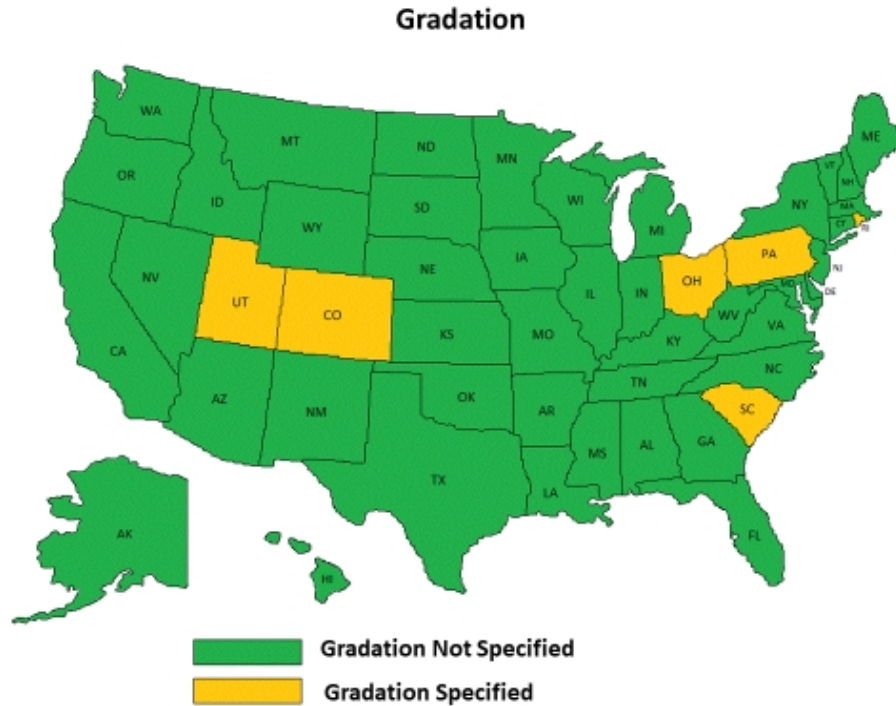
Gradation

Figure 2.1. States imposing requirements on gradation as material selection criterion (Hassani et al. 2017)

2.1.2.   Requirements on Material Atterberg Limits

Seven states including Delaware, Louisiana, North Carolina, Ohio, Pennsylvania, Texas and Washington have specifications on the Atterberg limits required for the material used in embankments. Figure 2.2 shows states imposing requirements for Atterberg limits.

Instead of setting a maximum plasticity index, Delaware has specified a maximum liquid limit of 40%. Louisiana sets a minimum PI of 11% and a maximum of 25% for what they classify as usable soil for embankment construction. North Carolina's current specifications require that the plasticity index stay below 15% for coastal area, and below 25% for piedmont and western area. Pennsylvania specifies that embankment material can consist of both fine-grained portion and granular portion, then it states some conditions regarding gradation, and Atterberg limits of the fine-grained portion which are listed in Table 2.1. In Texas, for a material to be considered as granular the following shall hold: $LL \leq 45$, $PI \leq 15$. Texas also correlates acceptable relative compaction to the PI of the soil being compacted. In Washington, as borrow material becomes finer, the PI shall be limited to a lower value. This state is probably one of the strictest states with $PI = 0$ for material having more than 35.1% passing sieve No. 200. Table 2.1 summarizes information for U.S. states which use Atterberg limits as embankment material selection criteria.

Table 2.1. Summary of states specifying Atterberg limits as material selection criteria (Hassani et al. 2017)

State	Specification
Delaware	LL of borrow ≤ 40
Iowa	PI > 10, for select cohesive soils
Louisiana	$11 \leq PI \leq 25$
North Carolina	PI ≤ 15 for coastal area; PI ≤ 25 for piedmont and western area
Ohio	LL < 65
Pennsylvania	for soil (fine-grained portion): LL < 65; if $41 < LL < 65$: PI $\geq$ LL-30
Texas	LL ≤ 45, PI ≤ 15 for granular material
Washington	if $12.1 \leq P_{200} \leq 35$, PI ≤ 6 if $35.1 < P_{200}$, PI $= 0$
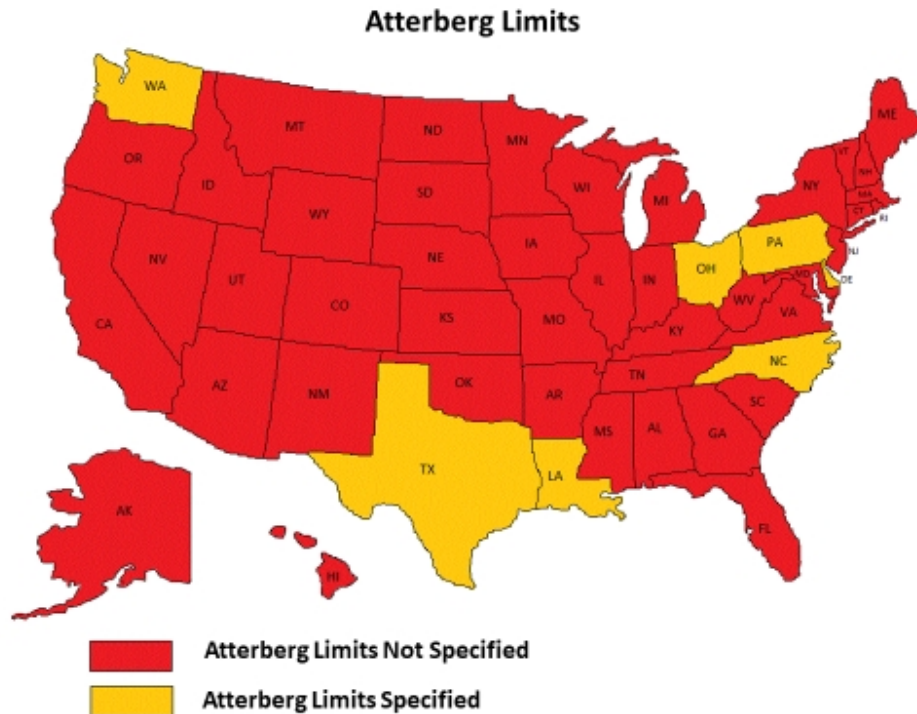
Figure 2.2. States imposing requirements on Atterberg limits as borrow material selection criteria
(source: Hassani et al. 2017)

Of course, in some specific portions of the embankment, like bridge approaches, or for the select borrow which is usually of higher quality than common borrow, plasticity index requirement may be stricter (in this case lower). However, requirements pertaining to the bridge approaches or to the select borrow are not covered completely in this report.

2.1.3.   Requirements on Minimum Field Dry Unit Weight and Relative Compaction

Nine states (Colorado, Delaware, Georgia, Indiana, Maryland, Michigan, Ohio, Pennsylvania and South Carolina) have specifications limiting the minimum dry unit weight of material placed in highway embankment. Of these states, Colorado, Delaware, Georgia, Indiana and Ohio limit the dry unit weight to a minimum value of 90 lbs/ft^3. Michigan and Pennsylvania limit the unit weight to a minimum of 95 lbs/ft^3. Maryland and South Carolina limit the minimum unit weight to 100 lbs/ft^3.

The majority of states require achieving a minimum relative compaction specified with respect to a laboratory standard compaction test, such as Standard Proctor (AASHTO T 99) or Modified Proctor (AASHTO T 180). Of course, a vast number of states use local standards, which represent AASHTO standards with a level of minor modification.

Of all the 50 states reviewed, 33 states somehow state that maximum laboratory dry density ($\gamma_{d\max}$) shall be obtained in accordance with AASHTO T 99, which uses Standard Proctor energy. 23 of these states necessitate reaching exactly the minimum relative compaction of 95%, while others range from minimum RC of 90% to 102%. AASHTO and FHWA also require compacting embankments to RC $\geq$ 95% while $\gamma_{d\max}$ obtained at standard energy level. This fact may justify the high number of states sticking to AASHTO T 99. Number of states accepting AASHTO T 180, Modified Proctor energy, is equal to eight. Half of them require minimum RC of exactly 95% while others range within 90% to 95%.

Five of the states combine standard and modified energy in quality control process, correlating level of compacting energy to factors like material gradation or selected minimum RC in the plans. Two states of Kansas and Nebraska test the quality of embankment compaction according to the roller status. Compaction is considered accomplished by them for example when tamping feet of the roller walks out of the surface, or when a specific number of passes is obtained. No information regarding compaction energy could be found for the two states of Minnesota and Mississippi. They have only stated relative compaction level. Table 2.2 summarizes compaction energy level distribution among states and Figure 2.3 shows compaction energy level specifications by each state across the U.S.

Table 2.2. Summary of compaction energy required by states (Hassani et al. 2017)

Energy Level	Number of States
Standard Proctor	33
Modified Proctor	8
Standard/Modified Proctor	5
roller controlled	2
not mentioned	2
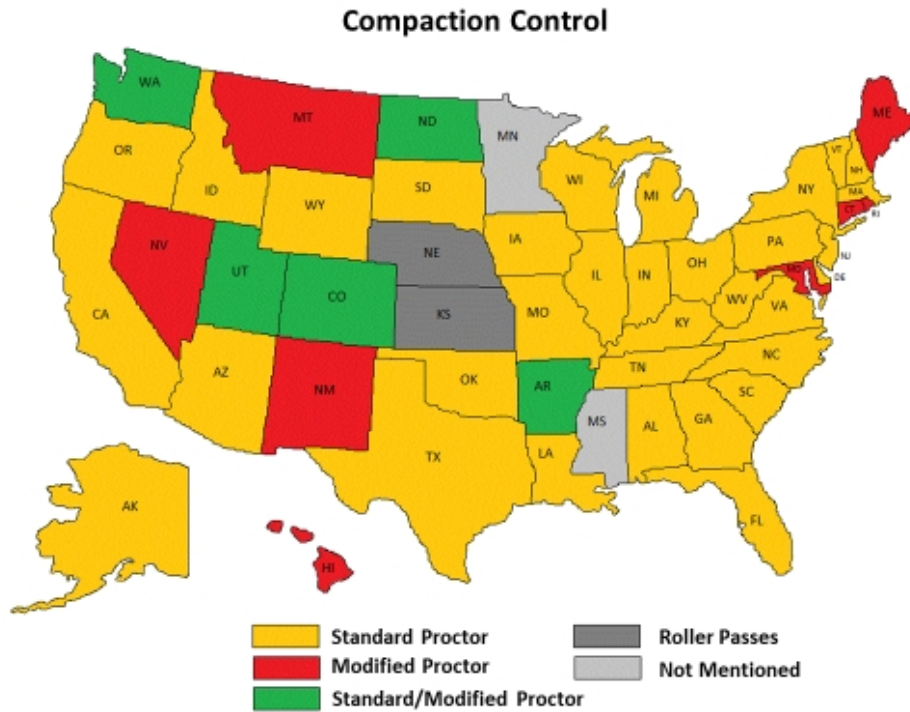
Figure 2.3. Compaction energy specifications by state (Hassani et al. 2017)

2.1.4. Requirements on Moisture Control

Twenty seven (27) states have specified some kind of criteria as the moisture content control. These requirements are in most of cases as an acceptable range for placing moisture content. The requirements differ based on the material gradation, Atterberg limits of material, moisture content of material itself, and level or energy of compaction.

Ten (10) states have specified acceptable moisture content in the range of ±2% of optimum moisture content. This high number seems to be related to the same specification set by Federal and AASHTO standards.

Twenty three (23) states have not specified any to designate moisture content of the embankment layers. Of course, all of them imply that material moisture content shall be in a range that minimum field density requirement is achievable.

2.1.5. Requirements on Lift Thickness

A lift thickness of 8" in loose state is required by 31 states, while two of the agencies require same 8" lift thickness but measured after compaction. Majority of the states consider lift thickness in loose state as only five states of Florida (6" or 12" depending on gradation), Maryland (8"), Pennsylvania (6"/8" for granular material), Rhode Island (12"), West Virginia (6") set lift thickness requirement measured after compaction. Only Indiana uses a compound lift placement measurement as 6" after compaction and 8" in loose state.

It is noted that maximum accepted lift thickness is 12", while the minimum is 4" loose measurement in Washington that is for the top 2 feet of embankment. Depending on material gradation, compaction class or position of layer, some states have different placing layer thicknesses.

All states have mentioned lift thickness as an easy to use, smooth and whole number, whether loose or compacted, except New York where lift thickness shall be obtained via charts with the load per wheel of compacting equipment as input. Lift thickness specifications requirement is summarized and illustrated in Figure 2.4. This figure shows 7 states having lift thicknesses equal to 12"; out of which only Rhode Island referring to compacted state and the rest indicating loose state.
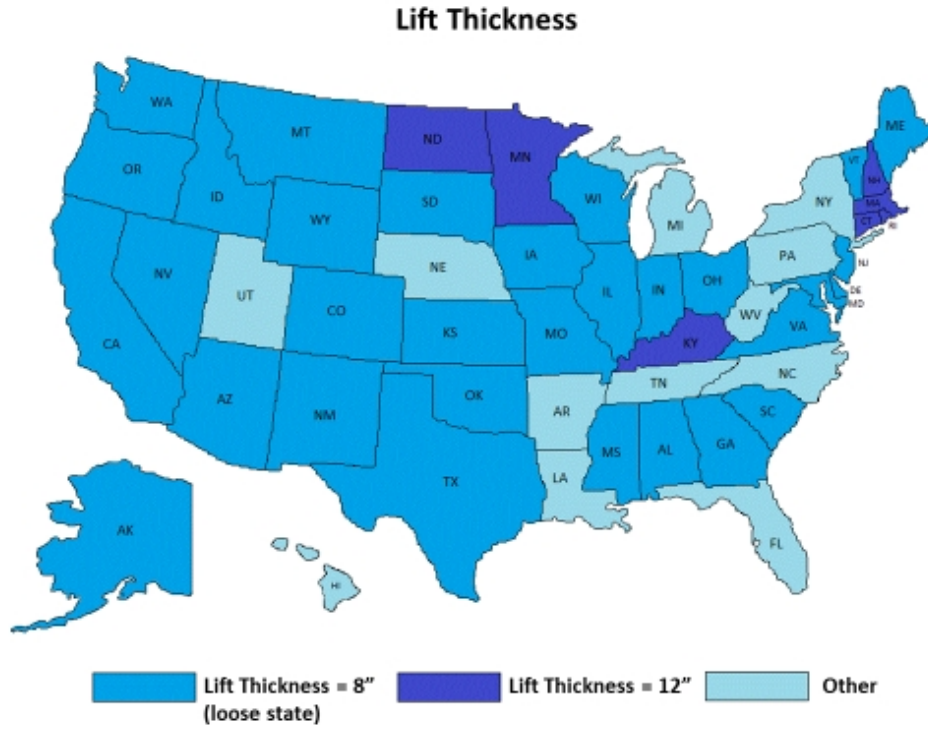
Lift Thickness

Figure 2.4. Variation of lift thickness specifications by state (Hassani et al. 2017)

2.2. Case Histories of Road/Highway Embankment Failure

Since providing support for a pavement system above natural ground is the function of a highway embankment, an embankment has failed when it causes unrest or damage to the roadway. Level of failure could be different; as in the case of slides resulting from instability of the embankment or the underlying foundation materials the failure may be spectacular and catastrophic. However, the subtle failure has been seen more predominantly. Creep and/or consolidation of the embankment or the underlying foundation materials may produce failure by the gradual development of excessive differential settlements of the pavement surface, causing rutting, dips, or cracks. Hence, highway embankment performance is tied to the stability and the deformation of both the embankment and the underlying foundation materials (NCHRP 1971).

However, the main purpose of this section is to present a summary of case histories of embankment failure in which the failure surface involves only the embankment. According to Khan et al. (2015) shallow failure is a major issue for embankment slopes constructed with high plastic clayey soils. As it will be indicated in the following subsections, the depth of the shallow slope failures varies with soil type and slope geometry, but generally ranges between 0.9 and 2 m (3-7 ft) (Loehr et al. 2007; Briaud 2013).

Case histories of embankment failure are presented in the following sections. We first present embankment failures occurred in North Carolina, and then we present failures reported in other places. At the end of this section a table summarizing most important facts about case histories is presented.

2.2.1. I-540 at Davis Drive, North Carolina

Figure 2.5 shows an example of longitudinal cracking caused due to strength loss after wetting-drying cycles, on NC I-540 at Davis Drive. According to the local reports, this crack is caused by presence of moisture and "collapse" of embankment soil happening after cycles of wetting and drying. Site soil is attributed to be similar to the Soil 2 Lee of the current project, a highly plastic silt with LL= 58 and PI= 21.

Figure 2.5. Longitudinal cracking caused by strength loss after wetting-drying cycles, NC I-540 @ Davis Drive (source: "Geotextile for Pavement Stabilization" presentation by NCDOT office)

2.2.2. Haywood County, North Carolina

In August of 2006 debris flow initiated as embankment failure on a development road at elevation 4580 ft near the northwest-facing slopes of Eaglenest Ridge in Haywood County, North Carolina. The mountain track is 90 ft wide at its widest point. If there was a house at the location where the debris is deposited, it would be destroyed. According to the North Carolina Geological Survey (NCGS) staff members, the debris flow was probably triggered because of the heavy rains associated with the remnants of Tropical Storm Ernesto. Field contractors reported 6.5 inches of rain during a 12-hour period prior to the debris flow. The report by North Carolina Geological Survey (2006), lists the possible factors leading to the embankment failure as: woody debris and graphitic-sulfidic bedrock fragments in the embankment; a steep embankment slope placed on a steep natural slope overlying a steeply inclined, weathered bedrock surface; and, a possible seepage zone beneath the embankment (North Carolina Geological Survey 2006). Some tension cracks are shown in Figure 2.6.

The bedrock beneath embankment is a graphitic-sulfidic bedrock which seems has been excavated by blasting to construct the road prism. It should be noted that the graphitic-sulfidic

bedrock is one of the problematic rock types well-known as prone to acid runoff and instability in embankments.

But NCGS geologic and geotechnical expertise also had some recommendations to prevent further slope failures and acid runoff in the development area. They proposed two solutions which both neutralize the acidic runoff and improve the stability of the embankment; reconstructing the embankment in compacted lifts treated with lime and limestone, and encapsulating the acidic material in lime and limestone. Of course, it is difficult to establish vegetation on an embankment constructed with graphitic-sulfidic rock material, and most probably vegetation alone will not prevent future slope failures (North Carolina Geological Survey 2006).

Figure 2.6. View of cracks in embankment, Haywood County, North Carolina
(source: North Carolina Geological Survey 2006)

2.2.3.   Great Smoky Mountains National Park

Some other cases of graphitic-sulfidic problematic bedrocks in North Carolina are worth mentioning (North Carolina Geological Survey 2006). In August 2006 a rockslide occurred in a similar graphitic-sulfidic rock type that caused the Blue Ridge Parkway to close. In May 2003 Swain County had heavy rains followed by six damaging debris flows, of which five originated in embankments that contained sulfidic rock.

In December 1990, the chlorinator building for the Bryson City municipal water system was destroyed due to a debris flow that originated in a road embankment underlain by graphitic-sulfidic rock (North Carolina Geological Survey 2006).

Acidic runoff from sulfidic bedrock can decrease the natural pH of stream waters and cause fatality to aquatic life. This happened in 1963 during reconstruction of U.S. Highway 441 near Newfound Gap in the Great Smoky Mountains National Park (North Carolina Geological Survey 2006).

According to a report by Appalachian Landslide Consultants which was prepared for the Jackson County Planning Department (Appalachian Landslide Consultants 2013), the most common type of road embankment failure seen in western North Carolina is slope failures from the shoulders of the road, as Figure 2.7 illustrates. These are the areas often compacted improperly. Sometimes utilities are buried in the outside shoulders and refilled without enough compaction. In such cases, uncompacted soil provides a pathway for water to flow along the utilities or between the more compacted soil of the road bed and the less compacted soil of the shoulder.

Figure 2.7. Embankment failure from the shoulder of roadway (Appalachian Landslide Consultants 2013)

2.2.4.   Maryland Study by Aydilek and Ramanathan

Aydilek and Ramanathan (2013) studies 48 slope failures in highway embankments. They state that most of the failures occur in embankments made of highly plastic soils, but coarser embankment material like gravel or sand are also susceptible to failure. They also reported that, in Maryland which was their study area, 46% of the failures along highway slopes occurred on slope angles between 20° (2.7H:1V) and 30° (1.7H:1V). Regarding elevation of the failed slopes it is noted that six (6) were shorter than 10m, eleven (11) were between 10m-30m, 27 had elevations between 30m to 90m, and four (4) were higher than 90m. They further noted that among 48 slope failures in highway embankments, 90% were surficial erosion failures, and 80% occurred during or after rainfall.

2.2.5.   Embankment Failures During the Historic October 2015 Flood In South Carolina

From October 2-5 in 2015, Hurricane Joaquin resulted in extensive rainfall of more than 50 cm in most parts of the midlands of South Carolina, which was more than 1000-year design rainfall. The flooding resulted in more than 40 embankment failures across the state and caused 19 fatalities (Tabrizi et al. 2017). One of the failed embankments is the Lake Elizabeth Dam located in Richland county, a lake with its spillway gates located along the Wilson roadway in Columbia. The failure of this dam was reported on October 6, 2015, which matches with local reports stating that the failure of the road embankment happened 1.5 day after the rainfall. Figure 2.8 shows Lake Elizabeth Dam before failure, right after failure and long time after failure.

For this dam, the height of crest overtopping is reported equal to 1 m; this value is in fact the difference between maximum head above breach invert and breach depth (Tabrizi et al. 2017). For this case as a roadway embankment, it seems this number means at the time of failure the height of water on top of pavement was 1 m. Field investigation and sampling classified the lake soil as SC (clayey sand) with 70.9% of sand and 24% of fine particles (silt and clay).

However, the author interpretation is that because of the fact that failure happened 1.5 day after the rainfall, the roll of water penetrating beneath/through the embankment body cannot be overemphasized. Having enough time, embankment soil becomes saturated and starts to lose shear strength. The lateral force of the large volume of water was also helping to push water through

upper levels of the embankment. Eventually, the embankment soil and its foundation that have lost strength initiate failure and this also helps to break the pavement system.

(a) [photo credit: Google Maps]

(b) [photo credit: Tabrizi et al. (2017)]

(c) [photo credit: Mehrdad Hassani]
Figure 2.8. Lake Elizabeth Dam, (a) before flooding failure, (b) shortly after failure, (c) long time after failure on March 2018

2.2.6.   U.S. Highway 287, Texas

According to Khan et al. (2015), in September 2010 surficial movements and a cracked shoulder due to rainfall were observed on the southbound slope of U.S. Highway 287 in Texas. Figure 2.9 shows an illustration of the cracked shoulder. They constructed three recycled plastic pin (RPP) reinforced sections as long as 15.25 m (50 ft) and left two sections unreinforced as control sections. The studied slope consisted of 3H:1V fill slope with a height of 9.15 m (30 ft). The local Eagle Ford formation is composed of residual soils, clay, and weathered shale. Dominant mineral of the soil is montmorillonite which has shrink/swell characteristics. Slope soil was categorized as high-plastic clayey soil (CH), with liquid limit (LL) and plasticity index (PI) of the topsoil ranging between 48-79 and 25-51, respectively.

In this study, it was discovered that instrumented equipment started moving after a rainfall. Moreover, it was seen that control sections had significantly greater settlement (total settlement) at the crest than the reinforced sections. The maximum settlement was 35 cm (3.8% of H) in one of the control sections while reinforced sections had maximum and minimum settlements of 13 cm (1.4% of H) and 5 cm (0.5% of H) respectively.

However, the failure mechanism could be explained as follows. The highly plastic clay soil having montmorillonite, makes the soil highly susceptible to swelling and shrinkage during wetting and drying cycles. Wright (2005) states that fully softened strengths (which is lower than peak strength) may eventually develop in high-plastic clays, generally in field condition, after exposure to the wetting/drying cycles and provide the governing strength for first-time slides in both excavated and fill slopes. Moreover, it is well known that the cohesion of soil almost disappears in the fully softened state (Wright 2005; Duncan et al. 2014). The wetting and drying cycles may have caused the near-surface soil to soften, resulting in the movement of the slope and causing shoulder cracks. The cracks may have provided an easy path for water to intrude into the slope, which eventually saturated the soil near the crest during rainfall.

Figure 2.9. Surficial movement and cracked shoulder due to rainfall on U.S. Highway 287, Texas
[photo credit: Khan et al. 2015]

2.2.7.   I-70 Emma Field, Missouri

The I70-Emma field is located on U.S. Interstate 70 approximately 65 miles west of Columbia, Missouri. The slope is an approximately 6.8 m (22 ft) high embankment with 2.5H:1V side slopes. The soil is composed of mixed lean and fat clays with scattered cobbles and construction rubble. Prior to being selected for a reinforcement RPP project, the embankment had experienced recurring surficial slides in four areas of the embankment denoted as S1, S2, S3, and S4, as depicted in Figure 2.10. Depth of sliding masses was ranging from approximately 0.9 m (3 ft) to 1.5 m (5 ft). In the back analysis process it was assumed that soil would have a negligible cohesion intercept in the long-term. This case history is reported by Parra et al. (2003).

Slide areas S3 and S4 were left unreinforced as control sections. During spring of 2001, the site experienced higher than normal rainfall. Both control slides (S3 and S4) failed in late Spring of 2001 around the time when only small movements were observed in the stabilized sections. The continuously screened piezometers and tensiometers also indicated that increased pore water

pressures were observed during Spring 2001, that is when control slide failed. The observed movements from instrumented equipment correspond closely with the rainfall pattern at the site.
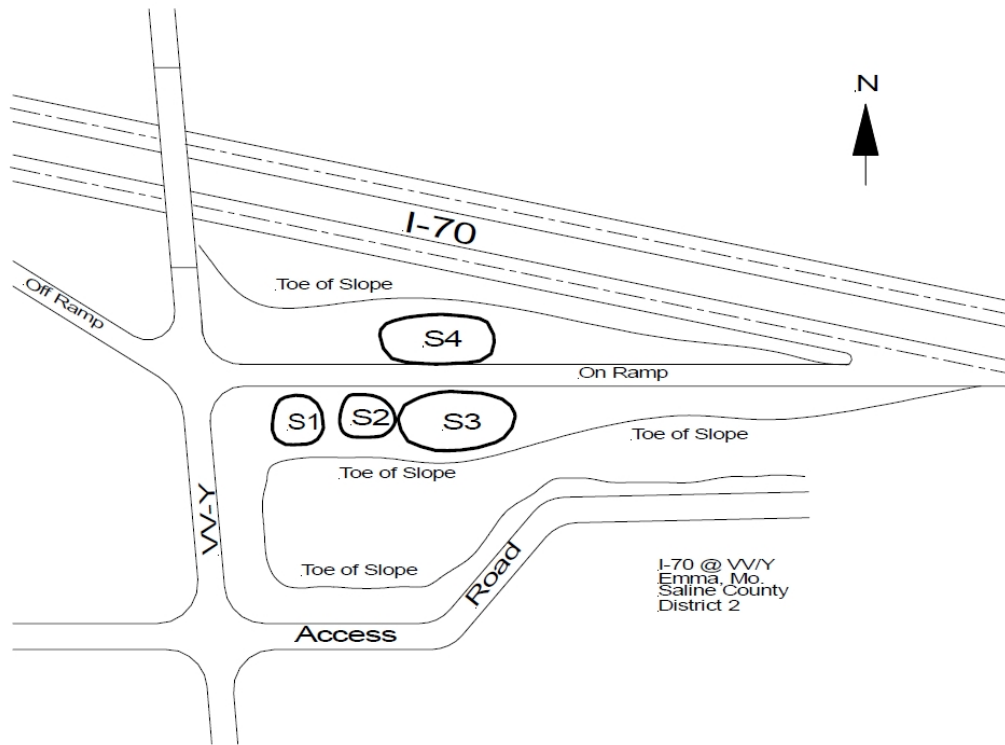
Figure 2.10. Plan view of I70-Emma field recurring surficial failures (from Parra et al. 2003)

2.2.8. I-435 Kansas City Field, Missouri

The I435-Kansas City site also reported by Parra et al. (2003) is located at the intersection of Interstate 435 and Wornall Road in southern Kansas City, Missouri near the Missouri-Kansas border. The embankment is a zoned-fill embankment consisting of a 1.0 m (3 ft.) to 1.5 m (5 ft) surficial layer of mixed of lean to fat clay with soft to medium consistency, overlying a stiffer compacted clay shale. The embankment is approximately 9.6 m (31.5 ft) high with side slopes of 2.2H:1V. The embankment had experienced at least two surficial slides along the interface between the upper clay and the lower compacted shale prior to being selected for a stabilization project. The most recent slide took out a large amount of the ornamental vegetation as well as 4-6 inches of gardening mulch which were part of neighborhood beautification project.

The maximum moments of the instrumented reinforcing members closely correlate with the movements in the slope. Maximum bending moments increased between April and July 2002 during a period of above average rainfall in the area.

I435-Kansas city study site has been review also by Loehr et al. (2007) and embankment has been characterized as follows: embankment with lean, soft to medium clay (CL) over stiff to very stiff clay shale (CH) fill.

2.2.9. US-36 Stewartsville, Missouri

The slope is located over the US36-Stewartsville and is approximately 8.8 m (29 ft) high with an inclination of 2.2H:1V. According to Loehr et al. (2007) this site is an excavated slope with soft to stiff lean clay (CL) over stiff to very stiff fat clay (CH). As a common phenomenon for all reinforced slopes of this type, it was observed that as precipitation increased, both lateral displacement and mobilized bending moment of reinforcing members increased in early 2004.

2.2.10. Summary of Embankment Failure Case Histories

In this section, aforementioned failures are depicted on the map of Atterberg limits requirements and compaction requirements respectively. It is noted that these maps were introduced in the section that reviews specifications on highway embankment.

In fact, we are trying to find any possible relationship between failures and imposed requirements by the states. It seems reviewing this information does not lets us make a strong conclusion about any possible pattern among failures. Of course in most of the cases, failures happen in fields where use Standard Proctor energy as field quality control. But since high percentage of 66% (33 out of 50) of U.S. states already use standard energy as compaction quality control, we cannot necessarily attribute shallow failures to the locations where use Standard Proctor.
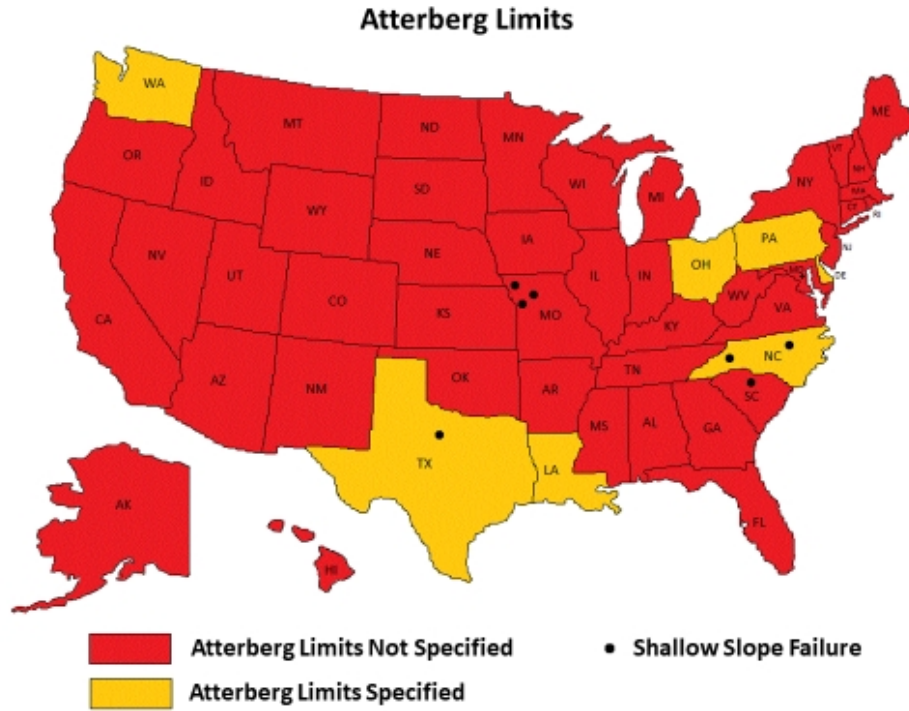
Atterberg Limits

Figure 2.11. Failure cases on the map of Atterberg limits requirements

Compaction Control
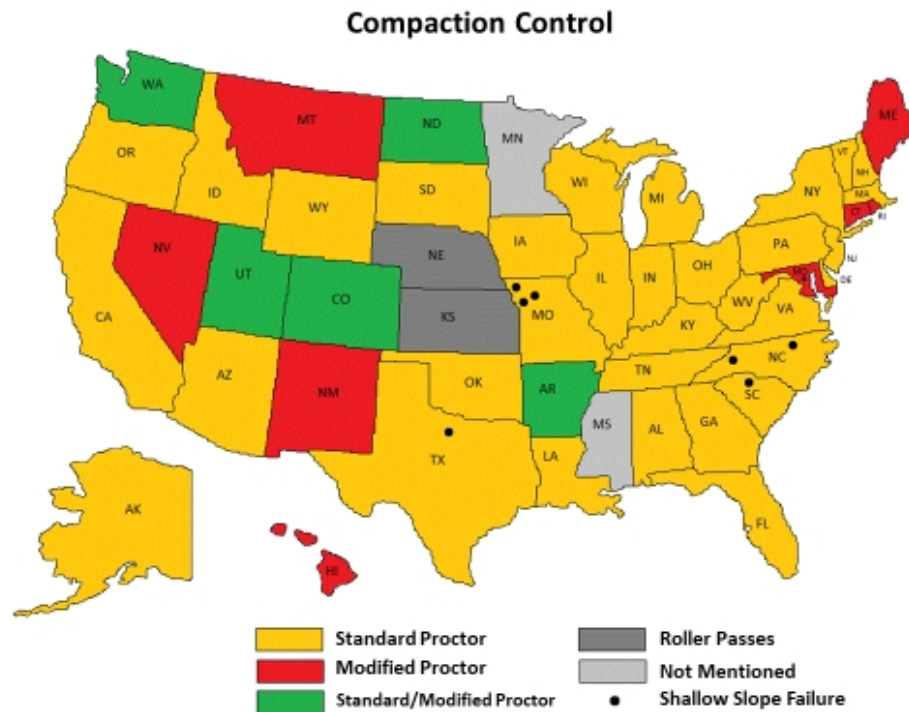
Figure 2.12. Failure cases on the map of compaction requirements

At the end of this section a table summarizing most important and paramount facts about case histories is presented. Figure 2.13 and Figure 2.14 also show distribution of shallow slope failures

presented in the summary table with respect to embankment height (feet), and embankment side slope (degrees) respectively. In these figures embankment height is in feet and embankment side slope is in degrees. It can be seen that big portion of failures have occurred in embankments higher than 35 ft.
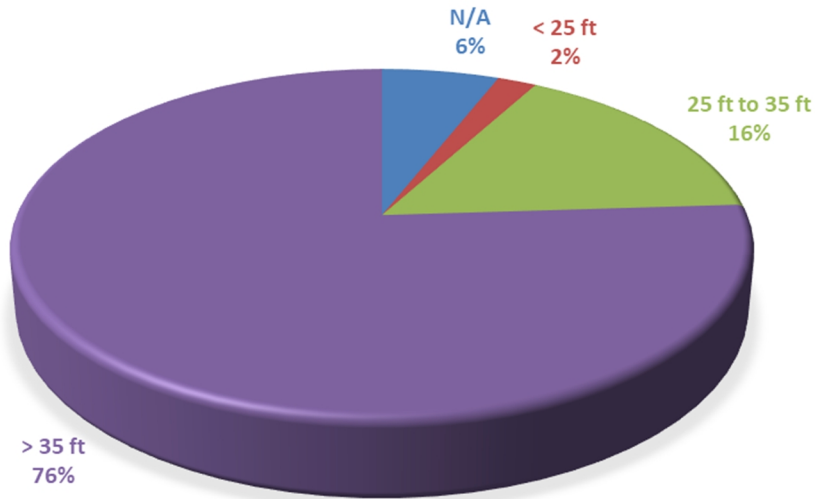
Figure 2.13. Shallow slope failure distribution with embankment height (feet)
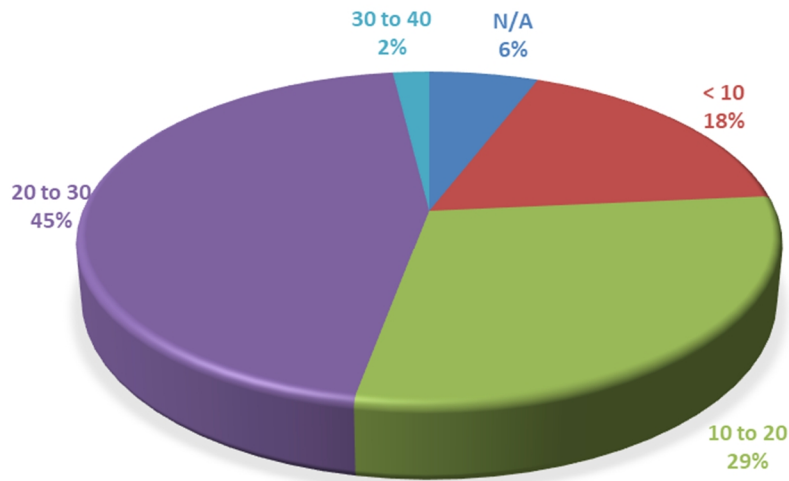
Figure 2.14. Shallow slope failure distribution with embankment side slope (degrees)

Table 2.3. Summary of case histories

case history	n	H	S (slope)	soil description (material)	field compaction requirement (construction)	failure description
I-540 at Davis Drive, NC	1	N/A	N/A	similar to the Soil 2 Lee, a highly plastic silt with LL= 58 and PI= 21	RC ≥ 95%, Standard Proctor	longitudinal cracking caused due to strength loss after wetting-drying cycles
Embankment failures from the shoulder of roadway, NC	1	N/A	N/A	silty and clayey soil	RC ≥ 95%, Standard Proctor	most common type of road embankment failure seen in western North Carolina; shallow slope failures; poor compaction near utility buried outside shoulders; triggered by rainfall
Maryland investigation	43	refer to text	refer to text	N/A	RC ≥ 92%, Modifies Proctor	most of the failures occur in embankments made of highly plastic soils; 46% of the failures on steep slope angles between 20° (2.7H:1V) and 30° (1.7H:1V); 90% surficial erosion failures; 80% occurred during or after rainfall
Lake Elizabeth Dam, SC	1	N/A	N/A	clayey sand with 24% fine	RC ≥ 95%, Standard Proctor	1.5 day after the historic rainfall; embankment soil and foundation and pavement were washed away
U.S. Highway 287, Texas	1	9.15 m (30 ft)	3H:1V	high-plastic clayey soil (CH); LL= 48-79 and PL= 25-51; with shrink/swell characteristics	RC ≥ 98%*, Standard Proctor	instrumented equipment started moving after a rainfall; wetting and drying cycles may have caused the top soil to soften, resulting in the movement of the slope and causing shoulder cracks; cohesion of soil almost disappears in the fully softened state
I-70 Emma field, Missouri	1	6.8 m (22 ft)	2.5H:1V	mixed lean and fat clays with scattered cobbles and construction rubble	RC ≥ 95%, Standard Proctor	depth of surficial slides was ranging from 0.9 m (3 ft) to 1.5 m (5 ft); control sections failed after higher than normal rainfall; increased pore water pressures at time of failure
I-435 Kansas city field, Missouri	1	9.6 m (31 ft)	2.2H:1V	lean, soft to medium clay (CL) over stiff to very stiff clay shale (CH)	RC ≥ 95%, Standard Proctor	maximum bending moments of instrumented reinforcing members increased during a period of above average rainfall;
US-36 Stewartsville, Missouri	1	8.8 m (29 ft)	2.2H:1V	soft to stiff lean clay (CL) over stiff to very stiff fat clay (CH)	RC ≥ 95%, Standard Proctor	as precipitation increased, both lateral displacement and mobilized bending moment of reinforcing members increased

Table Note: n: number of failures, * Also depends on the range of soil PI

2.3.   Minimum Factor of Safety for Highway Embankments

Traditional factors of safety for embankment at the end-of-construction condition are 1.3 to 1.5 (NCHRP 1989). For the purpose of this project FS=1.3 is selected as the minimum FS for both TSA and ESA conditions.

2.4.   Settlement of the Highway Embankment

In the technical literature dealing with highway embankments one can observe that large portion of the available literature focuses on the settlement of embankment foundation and ignores settlement of the embankment itself.

The amount of settlement which is an immediate response to the embankment loading is termed initial settlement. This settlement is compensated during embankment construction; when next layers of fill are placed the embankment is brought up to the design grade level. Thus, initial settlement does not affect the final embankment elevation (Ladd and Foott 1977).

Soriano (2013) states that for high embankments founded on firm ground (hard soils or rocks), long-term settlements and deformations can also cause some problems. This can happen due to creep deformations of the fill material of the embankment.

If post-construction settlements are uniform and are in the order of 0.3 to 0.6 m (1 to 2 ft) during the economic life of a roadway, and occur slowly over a period of time, and do not occur next to a pile-supported structure, they are considered acceptable. If post-construction settlement occurs over a long period of time, it provides the possibility of repair of any pavement distress caused by embankment settlement. The repair could also happen when the pavement is resurfaced. Although rigid pavements have performed well after 0.3 to 0.6 m (1 to 2 ft) of uniform settlement, flexible pavements are usually selected where there is question whether the post-construction settlements are uniform or not. However, some U.S. states utilize a flexible pavement when predicted settlements exceed 150 mm (6 in.) (NCHRP 1975; Stark et al. 2004).

Virginia manual of instructions states that total vertical settlement of embankment fill and underlying native soil shall be less than 2 inches over the initial 20-years, and less than 1 inch over the initial 20-years within 100 ft of bridge abutments (Virginia DOT 2014).

North Carolina DOT (2012) defines the rut as "a surface depression in the wheel path(s) or at the edge of pavement. Rutting comes from a pavement deformation in any of the pavement layers or in the subgrade, usually caused by consolidation or lateral movement of the materials due to traffic loads. Movement in the mix in hot weather or inadequate compaction during construction is the main cause of rutting". It also reports rutting 1 inch deep or greater as a severe rut.

Soriano (2013) reports on the geotechnical investigation of the construction of some embankments for the A24 motorway in north of Portugal. Vertical displacements after 22 months of observation have been very small, less than 0.1% of the embankment heights, that means "allowing to forecast a good performance in the future".

At the end of this section some points about the settlement of highway bridge approaches are presented. These studies at least imply that in other sections of an embankment (which is the subject of the current research project) the settlement can be in the same order or a little more than following values.

NCHRP (1990) suggests a differential settlement of 13 mm (0.5 inch) is likely to require maintenance in highway bridge approaches.

When approach slabs are not used, many scholars [Zaman et al. 1994; Stark et al. 1995; Long et al. 1998] suggest the allowable differential settlements at the embankment-structure interface to be between 12 and 75mm (0.5 - 3 in.).

Samtani and Nowatzki (2006b) reports that according to NCHRP (1983) differential vertical movements of 2 to 4 inches (50 to 100 mm), depending on span length, appear to be acceptable, assuming that approach slabs or other provisions are made to minimize the effects of any differential movements between abutments and approach embankments.

Finally, summary of some of the provided information is presented in Table 2.4. It is noted that the value of one inch (1 in.) is selected as the allowable nonuniform settlement for highway embankments in this research project.

Table 2.4. Summary of the literature review on allowable settlement for highway embankments

Reference	Reported/Allowable settlement	Description
NCHRP (1975)	0.3 to 0.6 m (1 to 2 ft)	allowable uniform settlements, but not next to a pile-supported structure
	150 mm (6 in)	in this case flexible pavement is selected by some U.S. states
NAVFAC (1986a)	0.1-0.2% of H in 3 to 4 years 0.3-0.6% of H in 15 to 20 years	range of secondary compression as a source of embk settlement; significant only in high embankments; larger values in each range belong to fine-grained plastic soils
Virginia DOT (2014)	50 mm (2 in)	total vertical settlement; embankment fill and underlying native soil; over the initial 20 years
	25 mm (1 in)	total vertical settlement; embankment fill and underlying native soil; over the initial 20 years; within 100 ft of bridge abutments
Khan et al. (2015)	3.8% of H	in a control section; total vertical settlement; indicated failure;
	0.5-1.4% of H	in reinforced sections; total vertical settlement; indicated good performance;
Soriano (2013)	0.1% of H	allowing to forecast a good performance in future; within 22 months after construction
	0.5-1.0% of H	some recommended side slopes; during the first 5-10 years of operation
North Carolina DOT (2012) *	25 mm (1 in)	considered severe rut in the pavement
NCHRP (1990) *	13 mm (0.5 inch)	differential settlement for highway bridge approaches
Zaman et al. 1994; Stark et al. 1995; Long et al. 1998 *	12-75 mm (0.5-3 in)	at embankment-structure interface; when approach slabs are not used

* Some of the cases mentioned in the table are not directly related to allowable settlement for highway embankments, but they can be eye-opener in this regard

2.5.   **Summary and Conclusion**

At the end of literature review chapter, important facts that we learn from literature about highway embankments, as well as found gaps are presented. In fact, the current research project tries to cast light on some of these gaps.

- Embankment material selection criteria and embankment construction specifications may vary considerably from state to state in the U.S.

- The use of PI as material selection criteria for embankments is limited to a few states, but the possibility of unwanted long-term deformations should be investigated when material with PI greater than 10 is used.

- Conventional field compaction acceptance criteria based on RC does not provide any information relating to embankment slope stability and/or embankment allowable settlement.

- Slope stability failure through highway embankment alone is not very common.

- Few cases of failures through embankment, involved shallow or surficial failures and usually induced by heavy rainfall.

- Reviewing case history failures which are recently dominated by shallow failure, does not lets us make any strong conclusion. In fact, most of the failures happen in fields where use Standard Proctor energy as field quality control, but since high percentage of U.S. states use standard energy, we cannot necessarily attribute shallow failures to the locations where use Standard Proctor.

- Behavior of the instrumented reinforcing members show that failures occur after heavy rainfalls and recorded movements also increase after heavy rainfalls.

- Wetting and drying cycles may cause the top layers of soil to soften, crack and finally loose strength and fail.

- Geotechnical literature is very sparse in terms of allowable settlement for the highway embankments.

3. RESEARCH METHODOLOGY

3.1. General Research Methodology / Work Plan Used in the Project

As stated earlier, performance of embankments is mainly tied to two concerns; stability and deformation. It was also mentioned that embankment performance should be examined for both TSA parameters and ESA parameters.

General research methodology used in this project consists of the idea that we will be striving to find out regions on the moisture content-dry unit weight domain which meet criterion for minimum factor of safety against sliding as well as criterion for allowable deformation of embankment. In other words, behavior of soil samples all over the moisture content-dry unit weight domain should be scrutinized. Figure 3.1 schematically illustrates general research methodology used in the project. This figure which is on the moisture content-dry unit weight domain, shows an acceptance zone based on slope stability analysis, an acceptance zone based on deformation analysis, and an overall acceptance zone. Shown in this figure is also the zero void air curve or saturation line, which represents location of saturated soil samples. This curve also serves as a limiting border on the moisture content-dry unit weight domain.
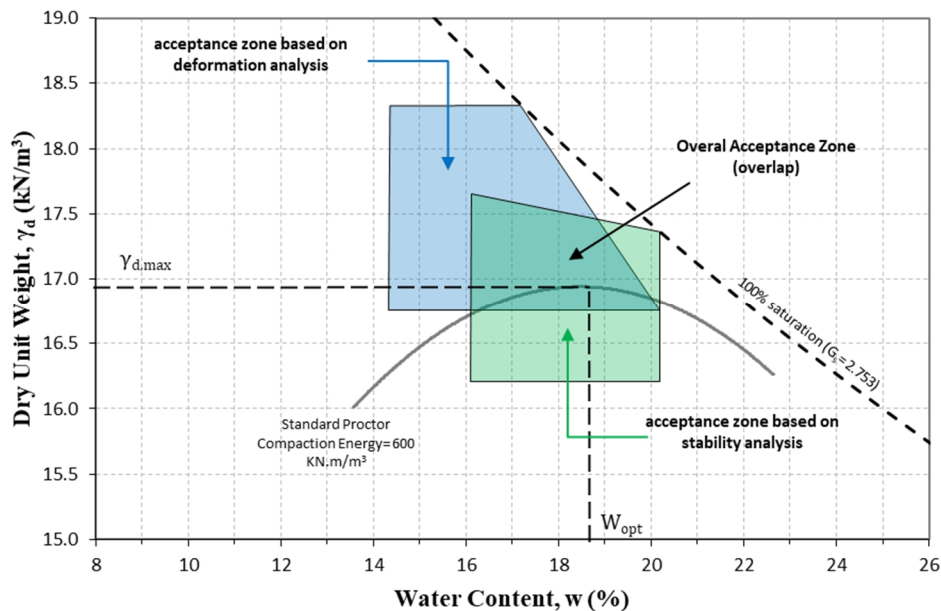
Figure 3.1. Schematic general research methodology used in the project

To reach this goal, soil samples having different moisture contents were prepared, then they were compacted at Standard Proctor or Modified Proctor energy levels, following the ASTM related standards. For more meticulous investigation of the engineering properties, it was decided to include an intermediate compactive energy level as well. Covering both wet-of-optimum and dry-of-optimum sides of each compaction curve needs minimum of five data points. Knowing that there are three energy levels, this method needs minimum of fifteen data points, making this method more or less known as 15-points method in the sparse literature. It is noted that this concept is in fact only applicable for TSA, and not for the ESA. This fact will be explained more later in this section. The concept of having enough data points around optimum moisture content (OMC) at each compacting energy is schematically illustrated in Figure 3.2.

As stated earlier, performance of embankments could be attributed to two concerns; stability and deformation. In fact, factor of safety against instability, and deformation characteristics of embankments built with soil samples/data points shown in Figure 3.2 must be investigated.
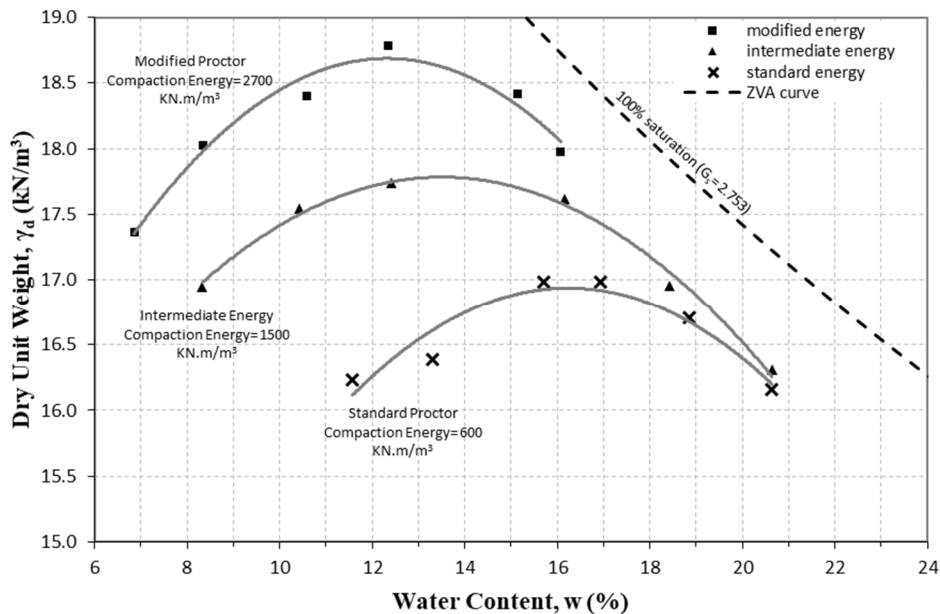
Figure 3.2. Schematic illustration of 15-points method; having enough data points around OMC at each compacting energy level

On the other hand, considered embankments must be such that they represent geometries commonly found in the field. Based on the information obtained from literature review and common state of practice currently used in the field, it was decided to consider embankment sections listed in Table 3.1. Table 3.1 lists different cases of embankment side slope angle and

embankment height which have been considered in this project. Four side slopes of 1H:1V, 2H:1V, 3H:1V, and 4H:1V in combination with four heights of 10ft, 20ft, 30ft, and 40ft lead to 16 embankment sections/geometries in total. Obviously, embankment sections considered for both slope stability analysis and deformation analysis will be the same.

Table 3.1. Different considered side slopes and heights for embankment geometries

Slope	Slope angle (deg)	Height (ft./m)
1H:1V	45	10 / 3.00
2H:1V	27	20 / 6.10
3H:1V	18	30 / 9.10
4H:1V	14	40 / 12.20

Figure 3.3 illustrates some of the numerous geometries that will be considered for the slope stability and deformation analyses in the project. In all of these sections embankment height is equal to 40 ft but the side slope is varying. Shown in this figure is also uniformly distributed external load which will be explained later in this chapter.
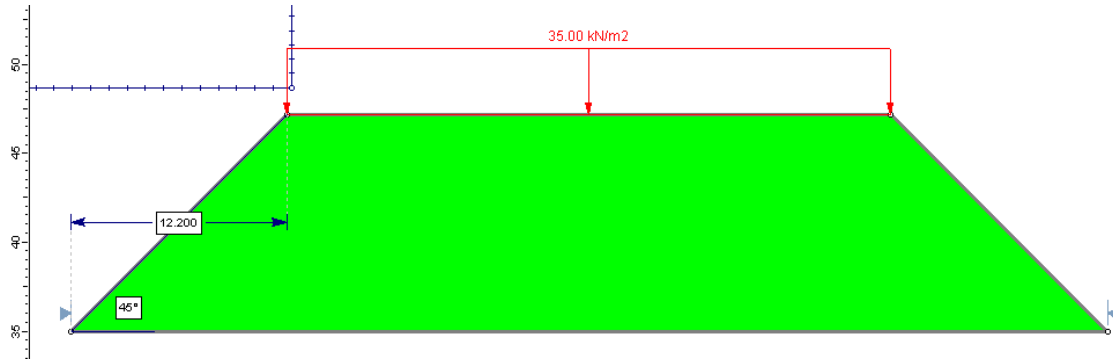
(a) side slope: 1H:1V, height= 40 ft (12.2 m)
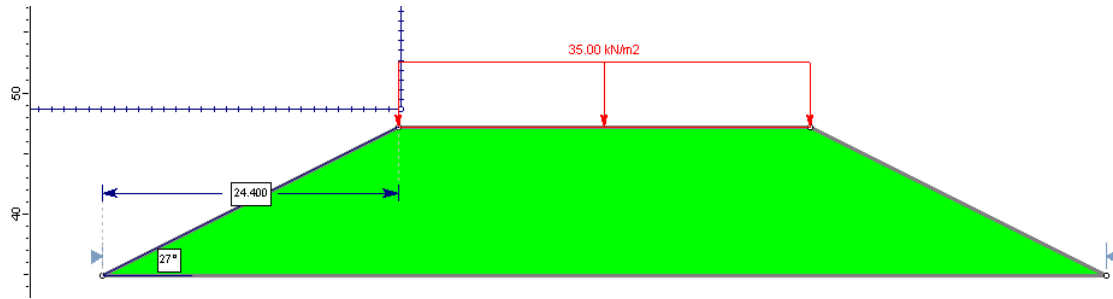
(b) side slope: 2H:1V, height= 40 ft (12.2 m)
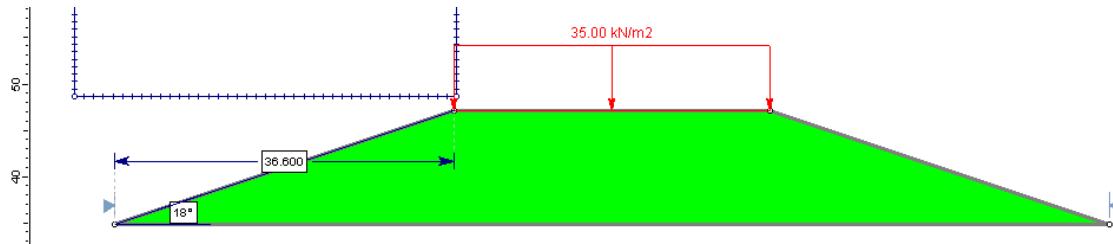
(c) side slope: 3H:1V, height= 40 ft (12.2 m)
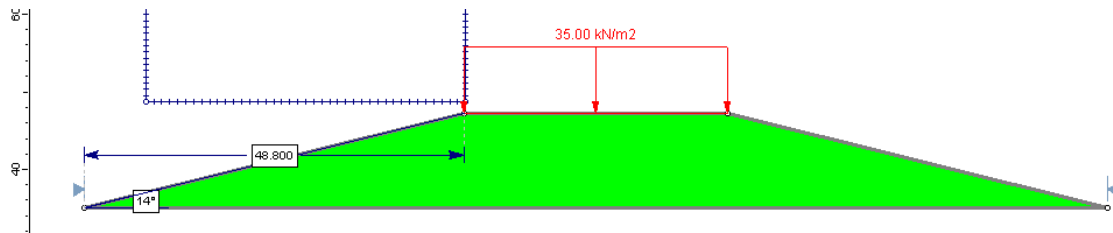
(d) side slope: 4H:1V, height= 40 ft (12.2 m)

Figure 3.3. Typical embankment geometries for embankment with height = 40 ft (12.2 m)

To present even a more lucid understanding of the used research methodology, it is noted that for each test soil, strength properties of data points on Figure 3.2 are attributed to embankment sections of the type shown in Figure 3.3. In fact for the ESA, where saturated samples are encountered, strength properties of data points located on the zero void air curve (saturation line) will be attributed to the embankment sections. Then slope stability analysis and deformation analysis will be performed.

However, it is also noted that performance of the highway embankments could be looked at from two different viewpoints; TSA and ESA. For the TSA state, embankment soil is assumed unsaturated both on the surface and deep into the embankment; this state may be representative of situations right after construction of the embankment. On the other hand, for the ESA state it is assumed that embankment soil is vulnerable to saturation due to the rainfalls. This situation might happen even locally.

As mentioned before, knowledge on the strength properties of utilized material is also essential in this research. Soil strength parameters will be obtained by means of laboratory triaxial tests. Methodology to obtain soil strength parameters will be explained in the next section.

The existence of two viewpoints also necessitates that we obtain soil strength properties for both TSA and ESA conditions. To find total stress soil strength properties, a set of unconsolidated-undrained triaxial tests has been designed, and to achieve effective stress soil strength properties, a set of consolidated-undrained triaxial tests with pore pressure measurements has been considered.

In fact, 15-points method is only applicable for TSA, and not for the ESA. Obviously, for the ESA we only encounter soil samples which are saturated and hence located on the zero void air curve. This is why the research procedure is slightly different for ESA (with CU triaxial parameters) than that of for TSA (UU triaxial parameters). As mentioned, for the ESA strength properties of data points located on the zero void air curve (saturation line) will be attributed to the embankment sections.

Figure 3.4 is provided to help understanding the governing research methodology / research flow in the project.

```
                    ┌────────────────────────────────────┐
                    │   Study of the Highway Embankments  │
                    │                  /                  │
                    │   Improving Material Selection Criteria │
                    └────────────────────────────────────┘
```

slope stability analysis

deformation analysis

TSA

ESA

TSA

ESA

UU triaxial parameters were used – 15 points method utilized

CU triaxial parameters were used

CU triaxial parameters were used

OUTPUT

OUTPUT

OUTPUT

OUTPUT

- FS regression equations for each soil
- FS regression equation for all soils

- Descriptive table for acceptance zone/cases
- FS tables (in main body)

- Descriptive table for acceptance zone/cases
- Regression equations for each soil
- Regression equation for all soil samples
- Deformation tables (Appendix A)

NOTE FS and deformation regression equations are presented in two forms: dimensioned and dimensionless

Figure 3.4. Schematic governing research methodology / research flowchart in the project

It is also noted that the scope will consider only failures and settlements related to compacted embankment and not due to poor foundation soil conditions. In other words, embankment foundation is assumed to be decent and impeccable.

3.2. Obtaining Strength Parameters

To obtain total stress and effective stress strength parameters of the soil, it is decided to use UU triaxial test and CU triaxial test respectively. Laboratory UU triaxial tests and CU triaxial tests will help us achieve strength parameters such as friction angle, cohesion and elasticity modulus.

Friction angle and cohesion terms might be known as soon as Mohr-Coulomb failure envelop of the soil material is known. Obviously, for one to be able to draw the failure line, more than one triaxial test and the minimum of three is required. This necessitates creating minimum of three identical soil specimens for each particular point located on the moisture content-dry unit weight domain. Confining cell pressures (S_C), or effective confining cell pressures (S'_C) in the case of CU triaxial tests, will differ in the three consecutive tests and could be as 25kPa, 50 kPa and 100 kPa respectively. Figure 3.5 illustrates different steps needed to obtain three samples and to perform a triaxial test.

(a) pushing tubes into the soil sample
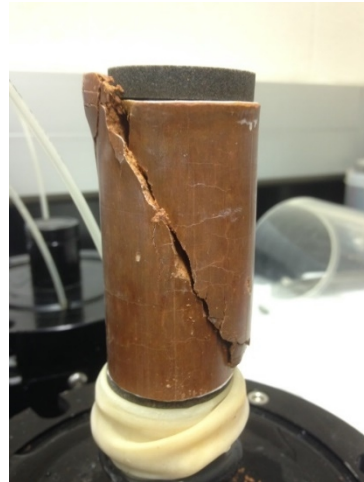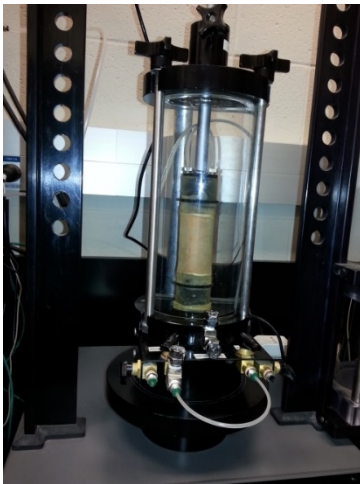
(b) UU triaxial test

(c) broken sample after the test

Figure 3.5. Illustration of different steps needed to perform a triaxial test

It is expected that the shear strength envelop would exhibit linear behavior over the range of confining cell pressures that will be used for the laboratory UU and CU triaxial tests. It is noted that shear strength envelop is the tangent line over the Mohr Circles which are drawn in shear stress (t) versus normal stress (S_n) space. However, using the well-known method proposed by Duncan et al. (1980), we can get the strength parameters more easily by having the failure points on p-q space rather than S_n-t space, and by using the following set of equations. The concept is also illustrated in Figure 3.6, and equations are listed in equation (3-1).
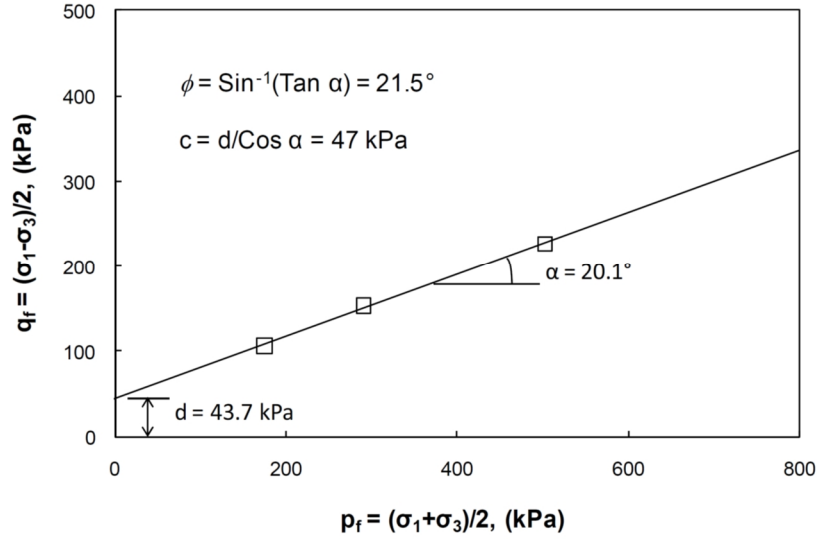
Figure 3.6. Method to get strength parameters from failure line in p-q space (from Chen 2010)

$$p_f = \frac{s_{1f} + s_{3f}}{2}, \; q_f = \frac{s_{1f} - s_{3f}}{2}, \; f = \sin^{-1}(\tan a), \; c = d/\cos a \qquad (3\text{-}1)$$

where s_{3f} is minor principal stress at failure, s_{1f} is major principal stress at failure, and a and d are respectively slope and intercept of the failure line in p-q space.

3.3. Obtaining Elasticity Modulus for Deformation Considerations

Elasticity modulus of the soil is a parameter that is required for deformation analysis. Elasticity modulus can be obtained from laboratory triaxial tests. Figure 3.7 shows a typical stress-strain curve from a triaxial compression test. According to Das (2008) different elasticity moduli might be defined as follows.

- Initial tangent modulus, E_i

- Tangent modulus at a given stress level, E_t

- Secant modulus at a given stress level, E_s

According to Das (2008), in ordinary geotechnical problems when the modulus of elasticity for a given soil is quoted, it is meant to be the secant modulus from zero to about half the maximum deviator stress which is denoted by E_{50}. It is common in geotechnical literature to infer stiffness of soil specimens from measurements of the secant modulus E_{50} (Chen 2010; Wiebe et al. 1998). Hence, in this project E_{50} has been used for deformation calculations in both TSA and ESA.
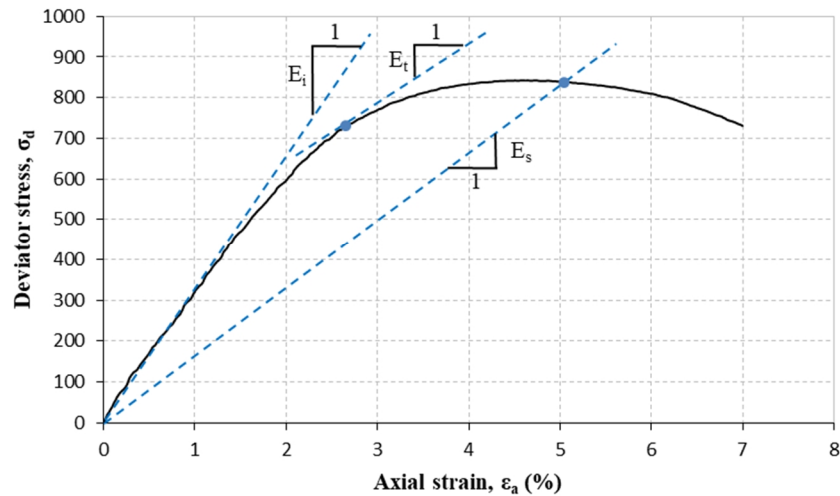
Figure 3.7. Schematic definition of different soil moduli from triaxial test results (modified from Das 2008)

3.4. Embankment Loading

According to NCHRP (1971) the design load used to investigate the stability and deformation of an embankment is the weight of the overlying embankment and pavement materials. Traffic loads does not seriously affect embankments except for the upper few feet.

Same document reports that heavy loads imposed by hauling and paving equipment which are used only during embankment construction might create major problems in some cases. Wheel loads from this equipment may produce high stresses in the compacted soil, even higher than the stresses anticipated from traffic loads after the road is in service condition. In many states, examples of stability failures caused by heavy construction equipment in compacted embankments that had already met compaction requirements can be reported. Almost all of the cited problems have been occurred in <u>silty materials which are extremely sensitive to moisture and density conditions</u>.

NCHRP (2004) which deals with geofoam applications in highway embankments has used a uniform surcharge equal to 21.5 kPa (450 lb/ft^2) to model pavement system. To model traffic surcharge, it has also taken values from ASSHTO (2002) which is Standard Specifications for Highway Bridges. Based on the ASSHTO recommendation of using 0.67 m (2 ft) of an 18.9 kN/m^3 (120 lb/ft^3) soil layer at the top of embankment to represent traffic load, traffic surcharge is 12.6 kPa (263 lb-ft^2). Therefore, the total surcharge representing pavement and traffic is 21.5 kPa plus 12.6 kPa or 34.1 kPa, which is rounded up to 35 kPa (730 lb/ft^2). This value will be applied as a uniformly distributed load on top of the embankment.

4. INDEX TESTS RESULTS OF TEST SOIL SAMPLES

This report revolves around the five NC piedmont soil samples. Figure 4.1 shows location of five piedmont soil samples received from NCDOT. To perform classification of the received soil samples ASTM standard have been followed. Gradation curves of the five piedmont soil samples are shown in Figure 4.2. Table 4.1 also lists classification information of these soil samples.
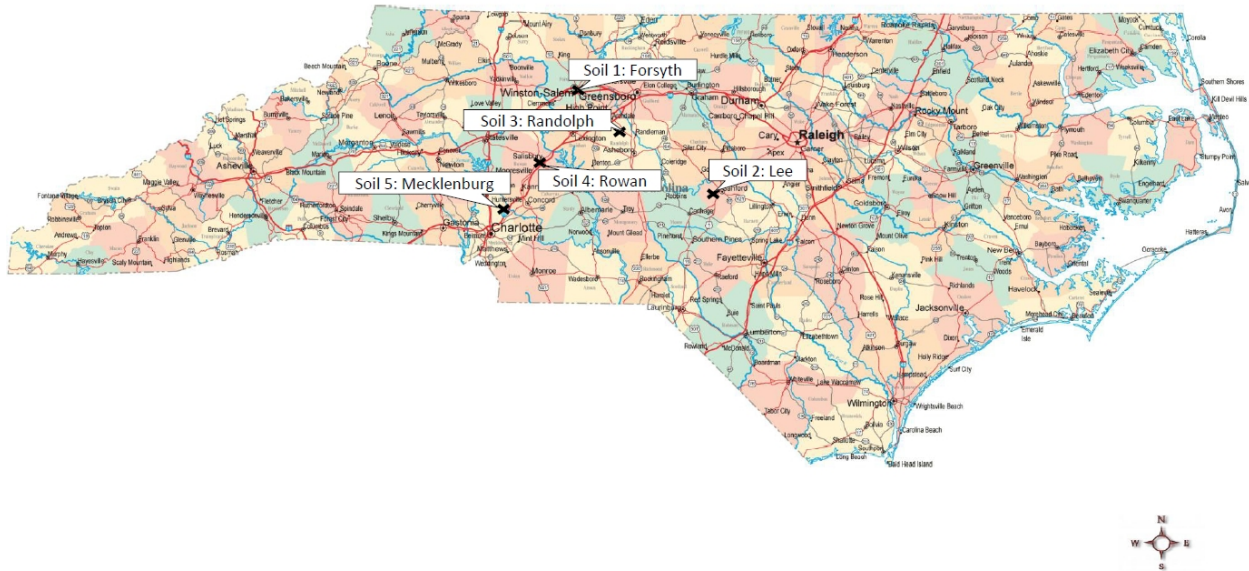
Figure 4.1. Location of piedmont soil samples received from NCDOT
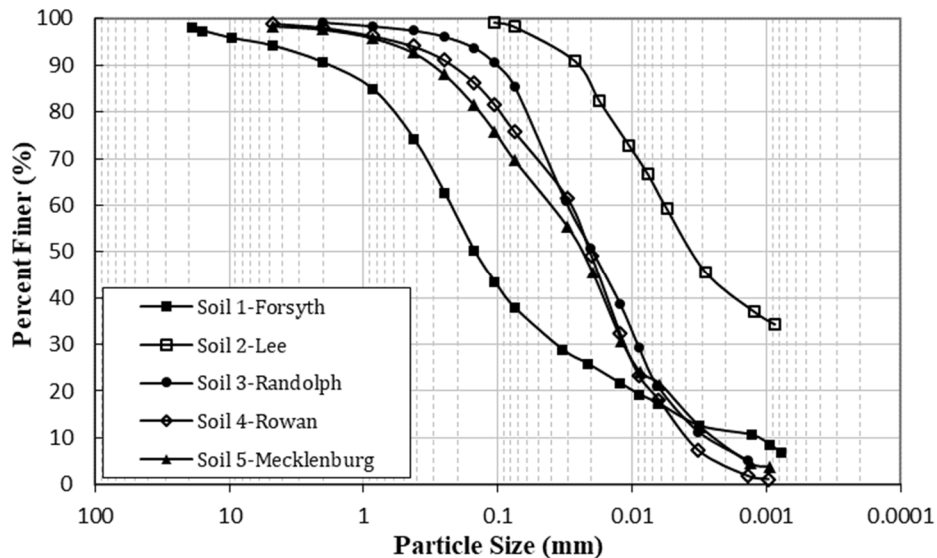
Figure 4.2. Gradation curves of piedmont soil samples received from NCDOT

Table 4.1. Index properties of test soil samples

Soil ID	Classification		Gradation							Atterberg Limits (%)			G_S
	USCS	AASHTO	%G	%S	%Fine	D_{50} (µm)	D_{10} (µm)	C_U	C_C	LL	PL	PI	
Soil 1 - Forsyth	SM	A-4 (0)	5.9	56.3	37.8	148.7	1.2	189.3	5.1	30	28	2	2.75
Soil 2 - Lee	MH	A-7-6 (28)	0.0	1.7	98.3	3.5	0.2	33.6	0.5	58	37	21	2.80
Soil 3 - Randolph	ML	A-4 (1)	0.6	13.9	85.5	19.7	2.4	12.5	1.1	32	35	NP[*]	2.71
Soil 4 - Rowan	ML	A-5 (7)	1.0	23.2	75.8	20.7	3.8	7.6	1.2	48	42	6	2.74
Soil 5 - Mecklenburg	ML	A-5 (5)	1.6	28.8	69.6	24.0	2.4	16.9	1.4	42	37	5	2.80

* NP= nonplastic

Table 4.1 guide:

%G	percent of gravel
%S	percent of sand
%Fine	percent of fines (passing sieve number 200)
µm	micrometer
CU	coefficient of uniformity
CC	coefficient of curvature
GS	specific gravity

5. COMPACTION TESTS RESULTS OF TEST SOIL SAMPLES

In this chapter, compaction curves of the received soil samples are presented. For each soil, compaction tests have been carried out at three energy levels, namely Standard Proctor, Intermediate Proctor and Modified Proctor, following ASTM associated standards. Intermediate energy level is considered to better monitor compaction behavior of the soil samples. In addition to the compaction curve, for each soil a table is also presented which lists compaction curve specifications, namely compaction energy, optimum water content, and maximum dry unit weight.

Moreover, for ease of use of NCDOT engineers, at the end of each section compaction curves are represented in Imperial units (lb & ft) as well.

5.1. Compaction Curves for Soil 1 Forsyth
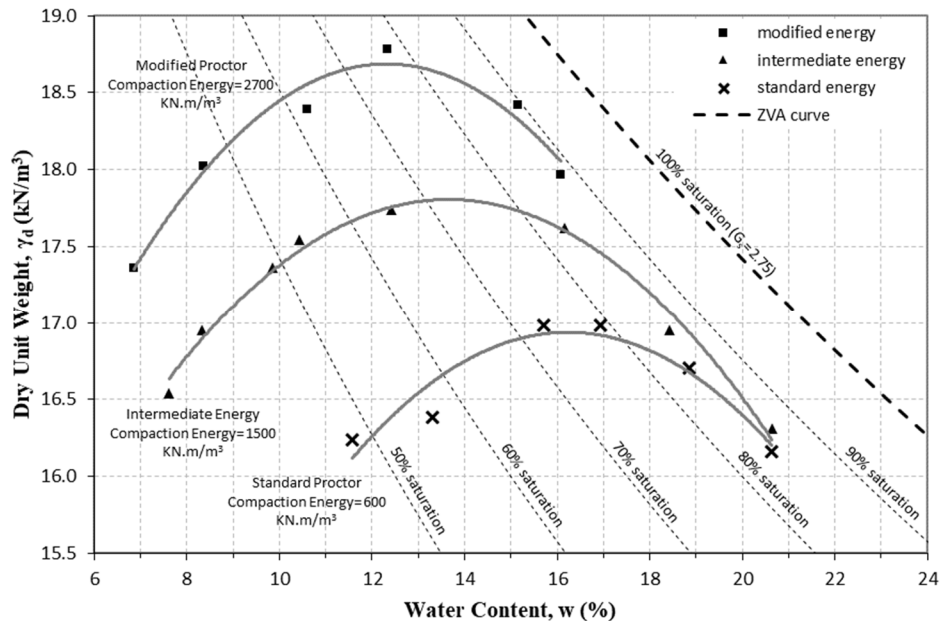
Figure 5.1. Compaction curves for Soil 1 Forsyth at three energy levels

Table 5.1. Summary of compaction test results for Soil 1 Forsyth

Test Series	Compaction Energy	Optimum Water Content	Maximum Dry Unit Weight
	KN-m/m³	%	KN/m³
Modified Proctor	2700	12	18.7
Intermediate Energy	1500	14	17.8
Standard Proctor	600	16	16.9

Interestingly enough, in case of Soil 1 Forsyth optimum point at all energy levels is located relatively exactly on the 75% saturation curve.
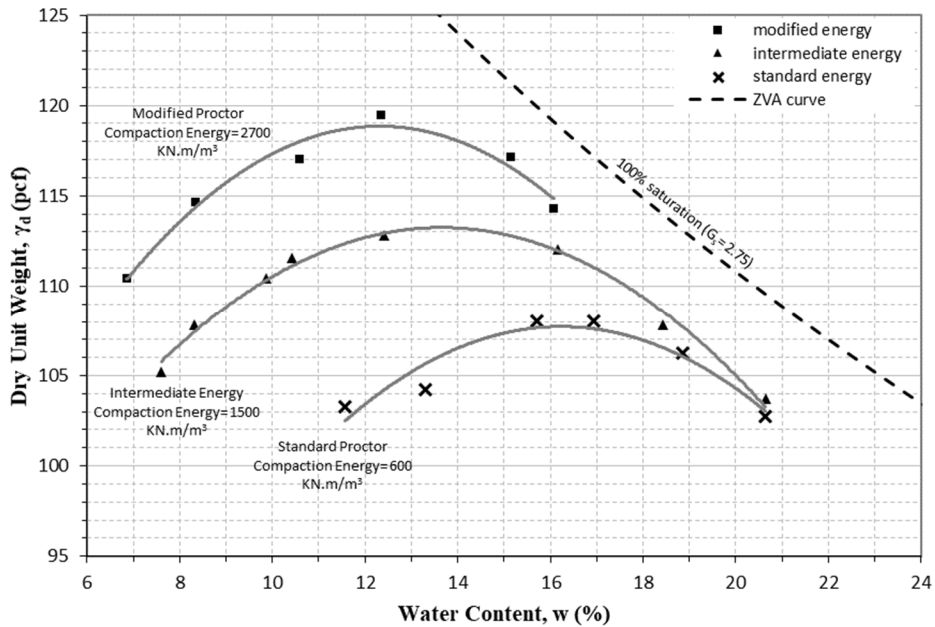
Figure 5.2. Compaction curves in Imperial units for Soil 1 Forsyth at three energy levels

5.2. Compaction Curves for Soil 2 Lee
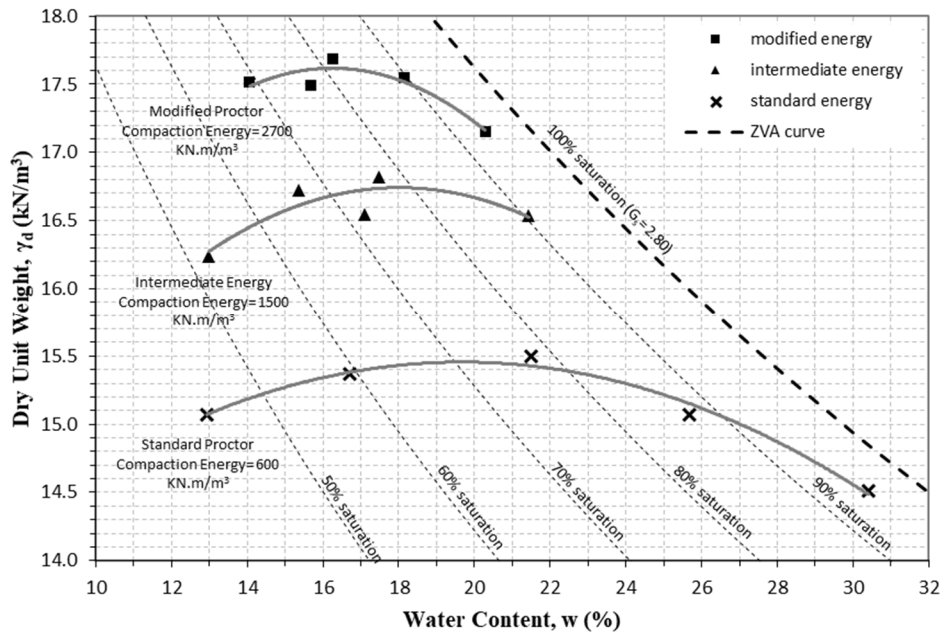
Figure 5.3. Compaction curves for Soil 2 Lee at three energy levels

Table 5.2. Summary of compaction test results for Soil 2 Lee

Test Series	Compaction Energy	Optimum Water Content	Maximum Dry Unit Weight
	KN-m/m^3	%	KN/m^3
Modified Proctor	2700	16	17.7
Intermediate Energy	1500	18	16.7
Standard Proctor	600	20	15.5

It is noted that for Soil 2 Lee, optimum points fall within 70% to 80% of saturation.
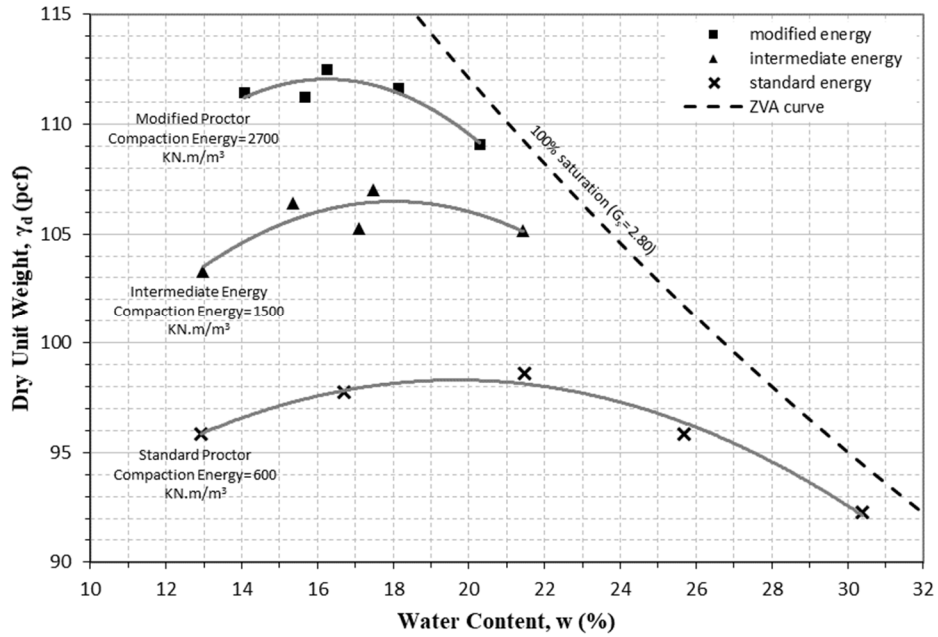
Figure 5.4. Compaction curves in Imperial units for Soil 2 Lee at three energy levels

5.3. Compaction Curves for Soil 3 Randolph
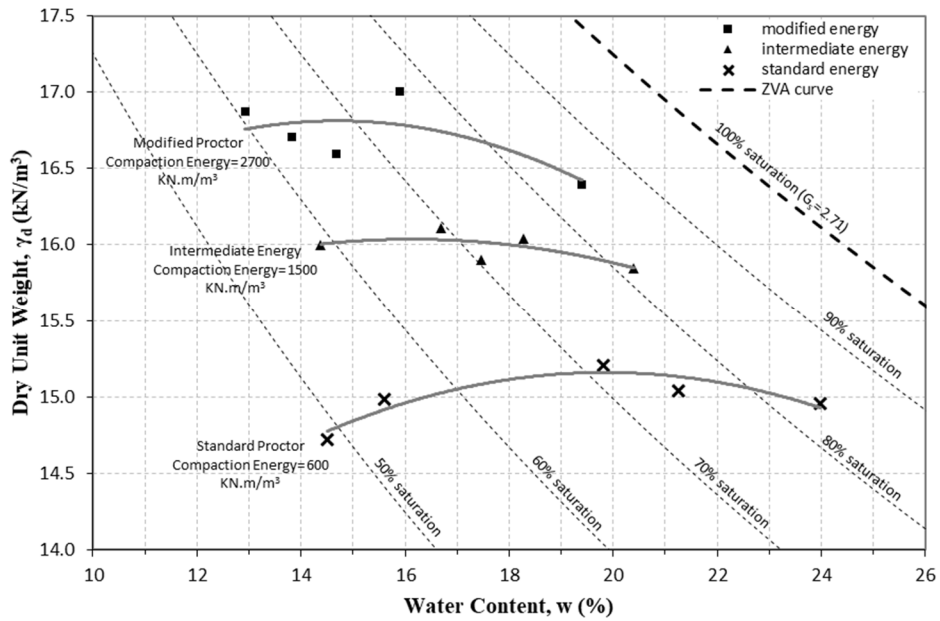
Figure 5.5. Compaction curves for Soil 3 Randolph at three energy levels

Table 5.3. Summary of compaction test results for Soil 3 Randolph

Test Series	Compaction Energy	Optimum Water Content	Maximum Dry Unit Weight
	KN-m/m³	%	KN/m³
Modified Proctor	2700	15	16.8
Intermediate Energy	1500	16	16.0
Standard Proctor	600	20	15.2

For Soil 3 Randolph, all of the optimum points fall between 60% and 80% of saturation while 70% saturation seems to be a rough number for the exact position of optimum points.
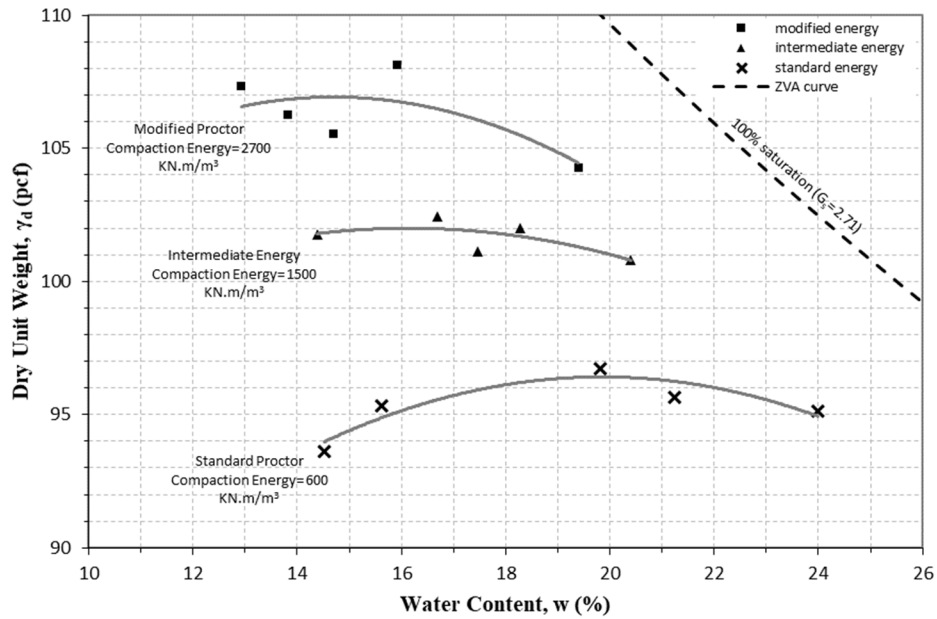
Figure 5.6. Compaction curves in Imperial units for Soil 3 Randolph at three energy levels

5.4. Compaction Curves for Soil 4 Rowan
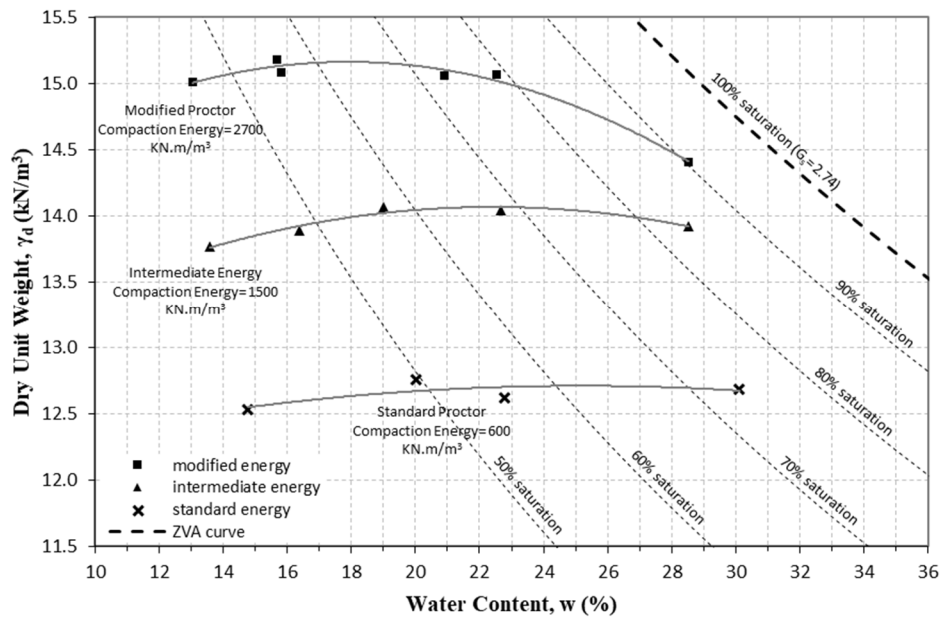
Figure 5.7. Compaction curves for soil 4 Rowan at three energy levels

Table 5.4. Summary of compaction test results for Soil 4 Rowan

Test Series	Compaction Energy	Optimum Water Content	Maximum Dry Unit Weight
	KN-m/m^3	%	KN/m^3
Modified Proctor	2700	18	15.1
Intermediate Energy	1500	23	14.1
Standard Proctor	600	25	12.7

For Soil 4 Rowan, optimum points fall between 60% and 70% of saturation. For soil 4 Rowan, values of dry unit weight are relatively lower than other soil samples.
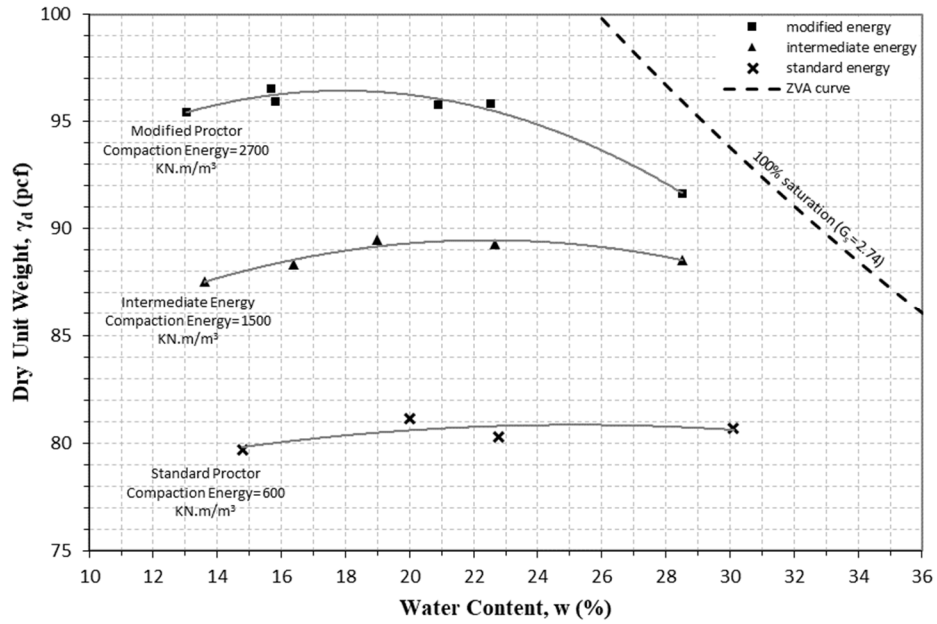
Figure 5.8. Compaction curves in Imperial units for soil 4 Rowan at three energy levels

5.5. Compaction Curves for Soil 5 Mecklenburg
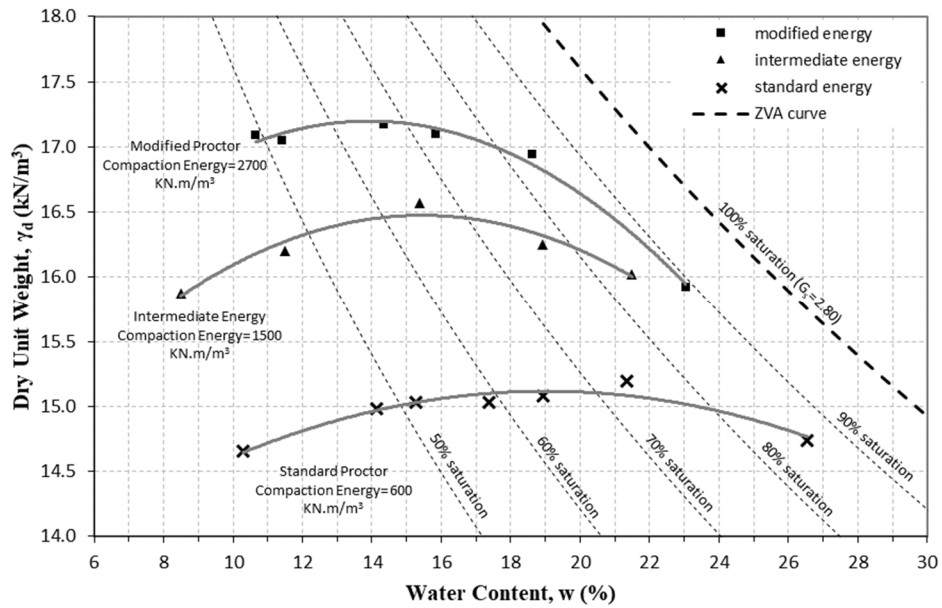
Figure 5.9. Compaction curves for Soil 5 Mecklenburg at three energy levels

Table 5.5. Summary of compaction test results for Soil 5 Mecklenburg

Test Series	Compaction Energy	Optimum Water Content	Maximum Dry Unit Weight
	KN-m/m^3	%	KN/m^3
Modified Proctor	2700	14	17.2
Intermediate Energy	1500	16	16.5
Standard Proctor	600	19	15.2

For Soil 5 Mecklenburg, compaction curves indicate that optimum points tend to be very close to the 65% saturation state, meaning that optimum points may be located very easily within the range of 60% and 70%.
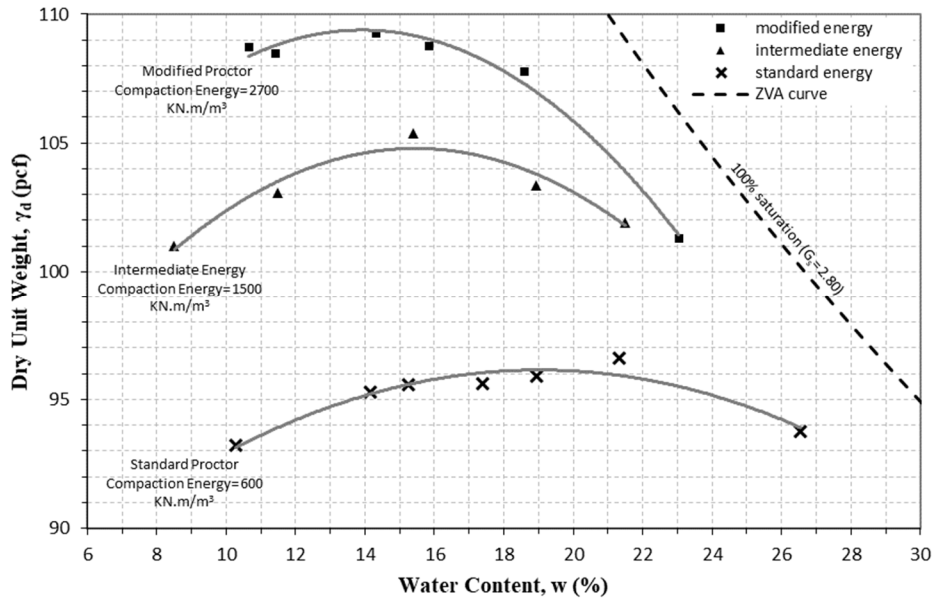
Figure 5.10. Compaction curves in Imperial units for Soil 5 Mecklenburg at three energy levels

5.6. Analysis of Results

Table 5.6 summarizes the location of optimum points of different utilized soils with respect to saturation level. It can be generally claimed that, location of the optimum points may be narrowed to the range between 60% to 80% of saturation.

Table 5.6. Location of optimum points of different utilized soils

soil sample	USCS classification	location of optimum point
Soil 1 Forsyth	SM	roughly on 75% saturation curve
Soil 2 Lee	MH	within 70% to 80% of saturation
Soil 3 Randolph	ML	roughly on 70% saturation curve
Soil 4 Rowan	ML	within 60% and 70% of saturation
Soil 5 Mecklenburg	ML	roughly on 65% saturation curve

Considering maximum dry unit weight ($g_{d\max}$) versus optimum moisture content (OMC) for all soil samples leads to a basic relatively accurate linear regression as shown in Figure 5.11. This regression is the most basic regression that could be developed and is restated in Equation (5-1).

In the second step which seems more rigorous, compaction energy may be entered in regression analysis, making it more complicated but hopefully more accurate. However, this regression is called multivariable linear regression analysis. Result of this regression is presented in Equation (5-2). However, including compaction energy increases coefficient of determination from $R^2 = 0.8905$ to $R^2 = 0.8916$. Further investigations also showed that Equation (5-2) with compaction energy, results in slightly better forecast compared to Equation (5-1). Error of using Equation (5-2) is close to 0.9 kN/m^3 in worst case.
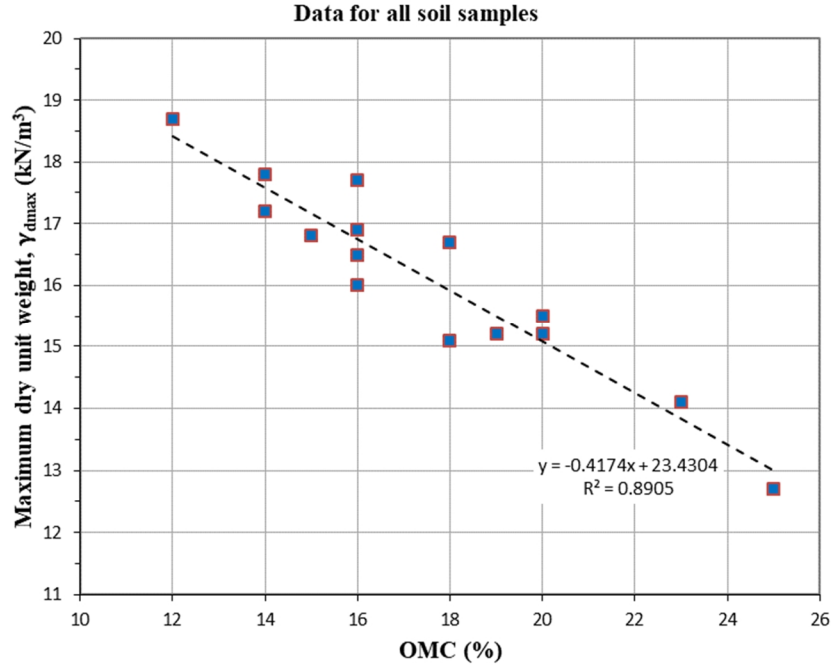
Figure 5.11. Maximum dry unit weight vs OMC for all soil samples

$$g_{d\,max} = 23.4304 - 0.4174 * OMC \tag{5-1}$$

where $g_{d\text{max}}$ is maximum dry unit weight in kN/m³, OMC is optimum moisture content in percent. Coefficient of determination for this equation is $R^2 = 0.8905$.

$$g_{d\,max} = 23.7874 - 0.4271 * OMC - 0.0000698 * E \tag{5-2}$$

where E represents compaction energy and has the unit of kN.m/m³, and rest of parameters are as before. Coefficient of determination for this equation is $R^2 = 0.8916$. it is noted that these two latter equations may be attributed to the silty soils.

6. UNCONSOLIDATED-UNDRAINED TRIAXIAL TESTS RESULTS OF TEST SOIL SAMPLES

In this chapter information related to unconsolidated-undrained triaxial testing program of this project is presented. As mentioned in section 3.2 (Obtaining Strength Parameters), for each point on moisture content - dry unit weight domain three specimens were prepared and three UU triaxial tests were performed at confining cell pressures (S_c) of 25 kPa, 50 kPa and 100 kPa respectively. Rate of the axial strain was equal to 1%/minute for all UU tests. Failure criterion of maximum deviator stress or limiting axial strain of 15%, whichever occurred first was utilized. Then failure points on p-q space were plotted to help obtaining failure line and thereof friction angle and cohesion parameters.

It is noted that during this project, quarterly progress reports have been continuously submitted which include enough information regarding failure lines. Thus for briefness, failure lines are omitted in the current report.

For each soil sample, three plots are presented; values of total stress friction angle f_{uu} in degrees, values of total stress cohesion C_{uu} (kPa), and values of elasticity modulus E_{uu} (MPa). The elasticity modulus which is represented in this chapter belongs to the UU triaxial tests having median confining cell pressure, that is confining pressure equal to $s_c = 50 kPa$.

6.1. Soil 1 Forsyth UU Triaxial Results - Engineering Properties

Engineering properties obtained from UU triaxial tests carried out on Soil 1 Forsyth are presented graphically in this section. Figure 6.1 shows total stress friction angle, Figure 6.2 depicts total stress cohesion, and Figure 6.3 illustrates modulus of elasticity for this soil. As mentioned earlier, the elasticity moduli belong to the UU triaxial tests with confining pressure equal to $s_C = 50kPa$.
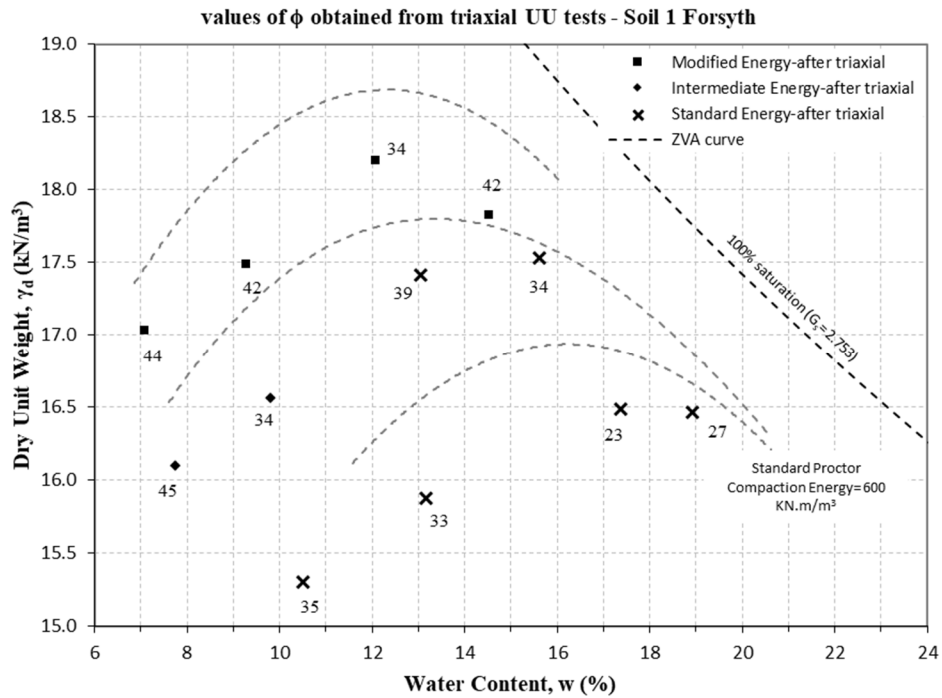
Figure 6.1. Total stress friction angle, f_{uu} (degrees) obtained from UU triaxial tests - Soil 1 Forsyth
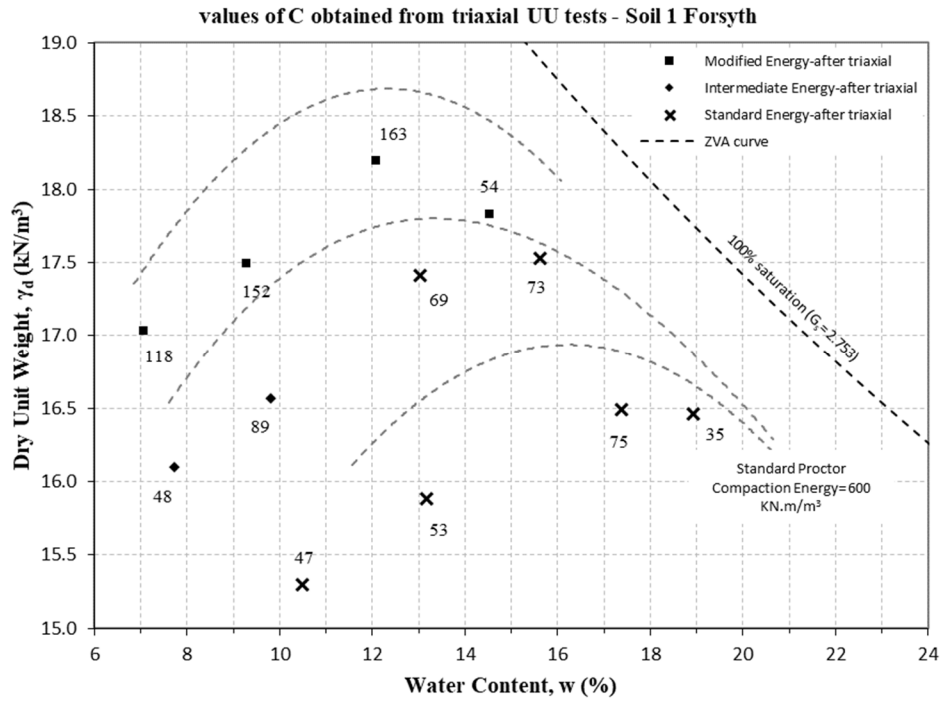
Figure 6.2. Total stress cohesion, C_{uu} (kPa) obtained from UU triaxial tests - Soil 1 Forsyth
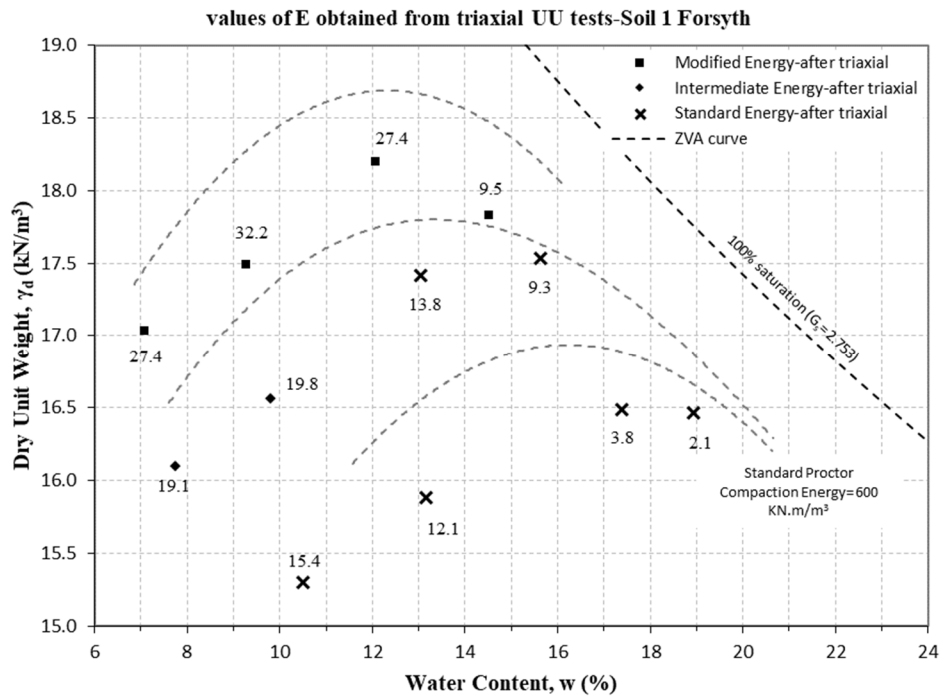
Figure 6.3. Elasticity modulus E_{uu} (MPa) at $s_c = 50\ kPa$ obtained from UU triaxial tests - Soil 1 Forsyth

6.2.   Soil 2 Lee UU Triaxial Results - Engineering Properties

Engineering properties obtained from UU triaxial tests carried out on Soil 2 Lee are presented graphically in this section. Figure 6.4 shows total stress friction angle, Figure 6.5 depicts total stress cohesion, and Figure 6.6 illustrates modulus of elasticity for this soil. As mentioned earlier, the elasticity moduli belong to the UU triaxial tests with confining pressure equal to $s_c = 50kPa$.
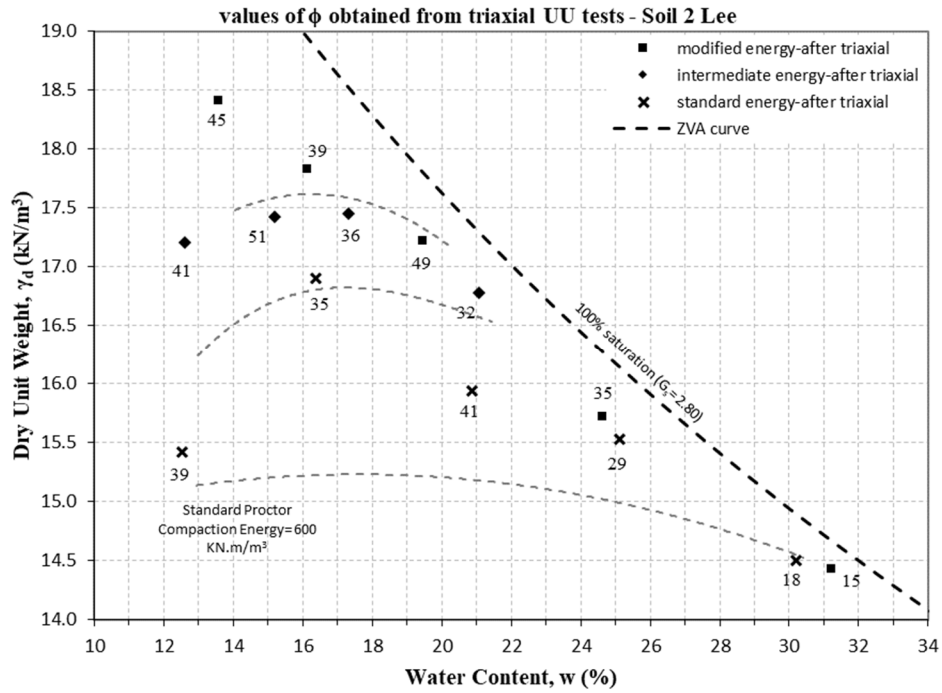
Figure 6.4. Total stress friction angle, f_{uu} (degrees) obtained from UU triaxial tests - Soil 2 Lee
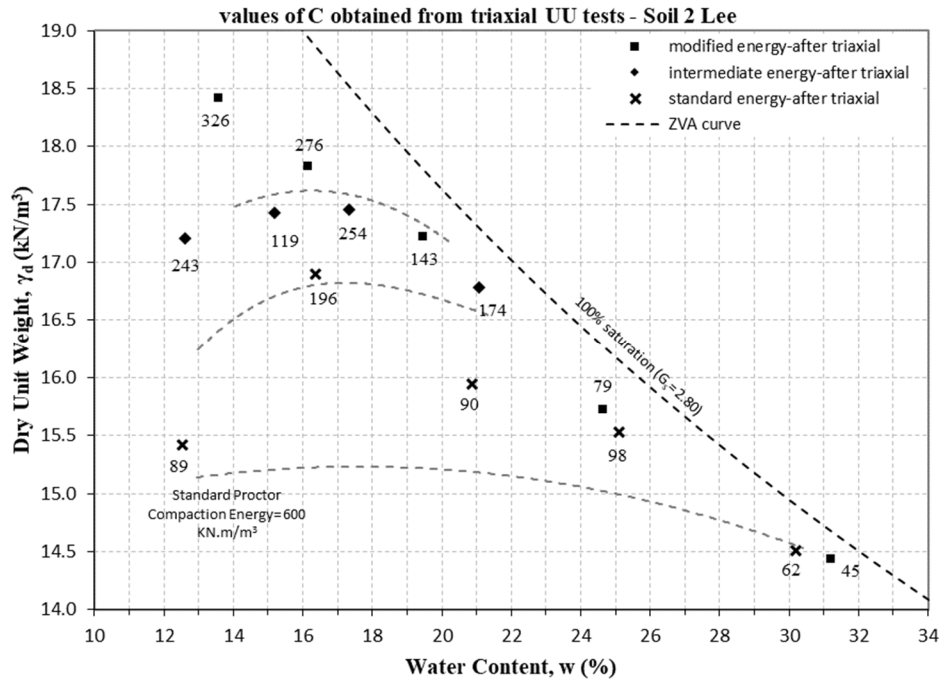
Figure 6.5. Total stress cohesion, C_{UU} (kPa) obtained from UU triaxial tests - Soil 2 Lee
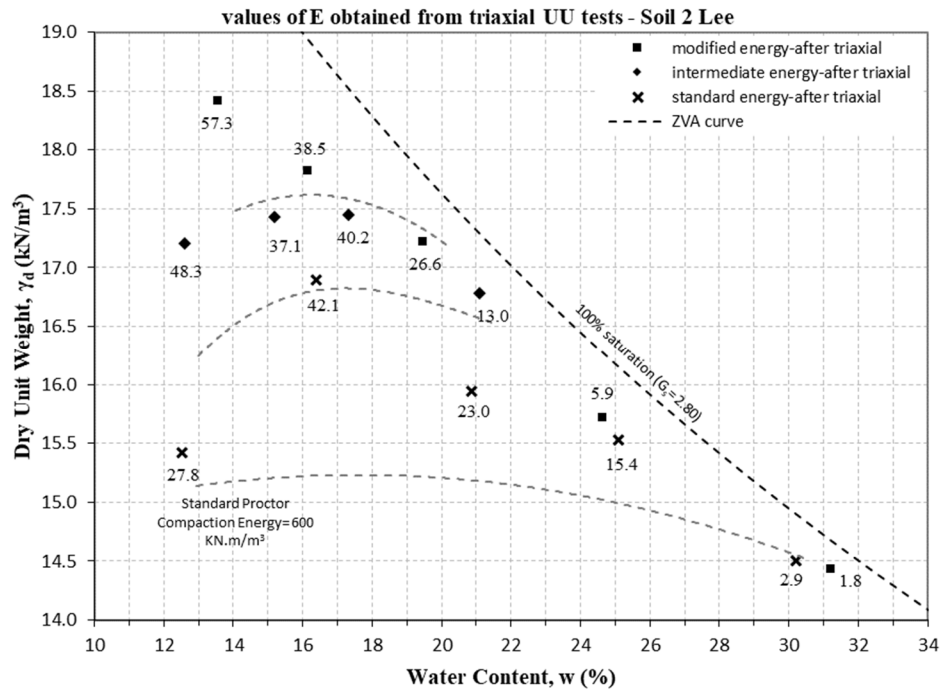
Figure 6.6. Elasticity modulus E_{UU} (MPa) at $s_c = 50\ kPa$ obtained from UU triaxial tests - Soil 2 Lee

6.3. Soil 3 Randolph UU Triaxial Results - Engineering Properties

Engineering properties obtained from UU triaxial tests carried out on Soil 3 Randolph are presented graphically in this section. Figure 6.7 shows total stress friction angle, Figure 6.8 depicts total stress cohesion, and Figure 6.9 illustrates modulus of elasticity for this soil. As mentioned earlier, the elasticity moduli belong to the UU triaxial tests with confining pressure equal to $s_C = 50 kPa$.
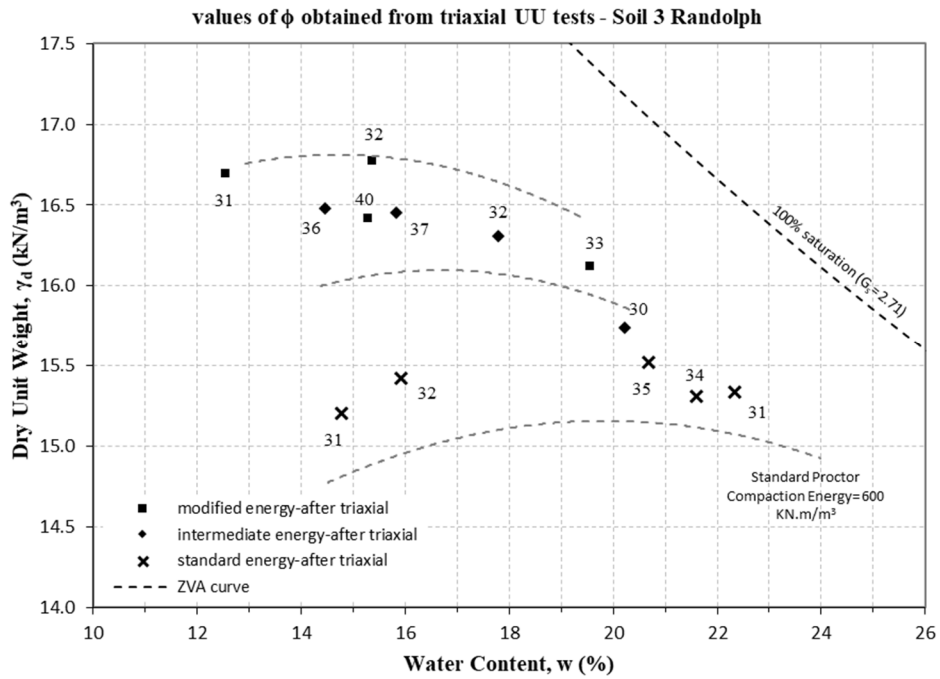
Figure 6.7. Total stress friction angle, f_{UU} (degrees) obtained from UU triaxial tests - Soil 3 Randolph
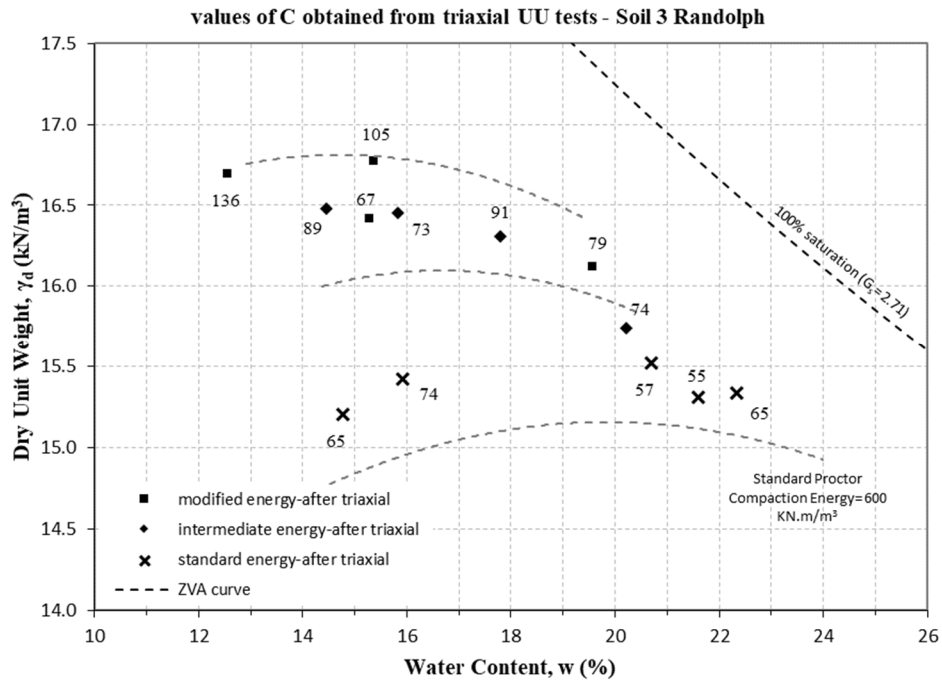
Figure 6.8. Total stress cohesion, C_{uu} (kPa) obtained from UU triaxial tests - Soil 3 Randolph
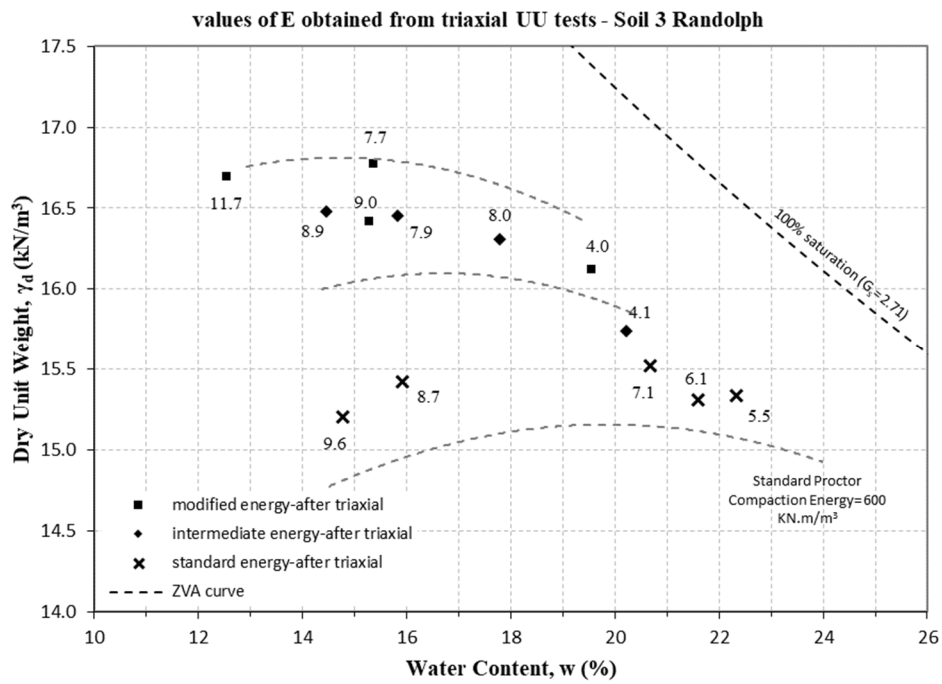
Figure 6.9. Elasticity modulus E_{uu} (MPa) at $s_c = 50\ kPa$ obtained from UU triaxial tests - Soil 3 Randolph

6.4. Soil 4 Rowan UU Triaxial Results - Engineering Properties

Engineering properties obtained from UU triaxial tests carried out on Soil 3 Randolph are presented graphically in this section. Figure 6.10 shows total stress friction angle, Figure 6.11 depicts total stress cohesion, and Figure 6.12 illustrates modulus of elasticity for this soil. As mentioned earlier, the elasticity moduli belong to the UU triaxial tests with confining pressure equal to $s_C = 50kPa$.
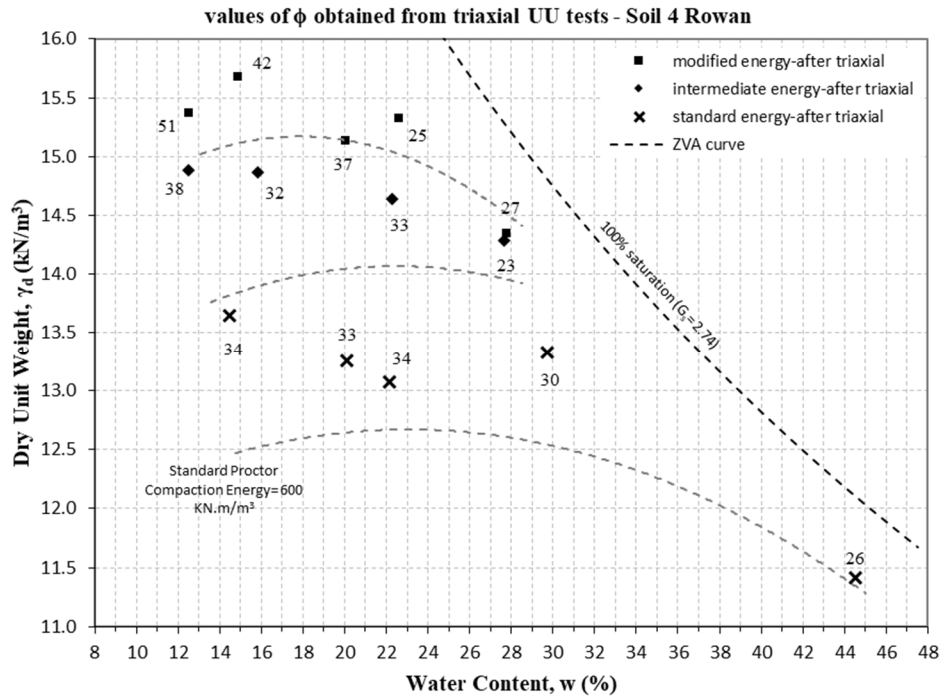
Figure 6.10. Total stress friction angle, f_{UU} (degrees) obtained from UU triaxial tests - Soil 4 Rowan
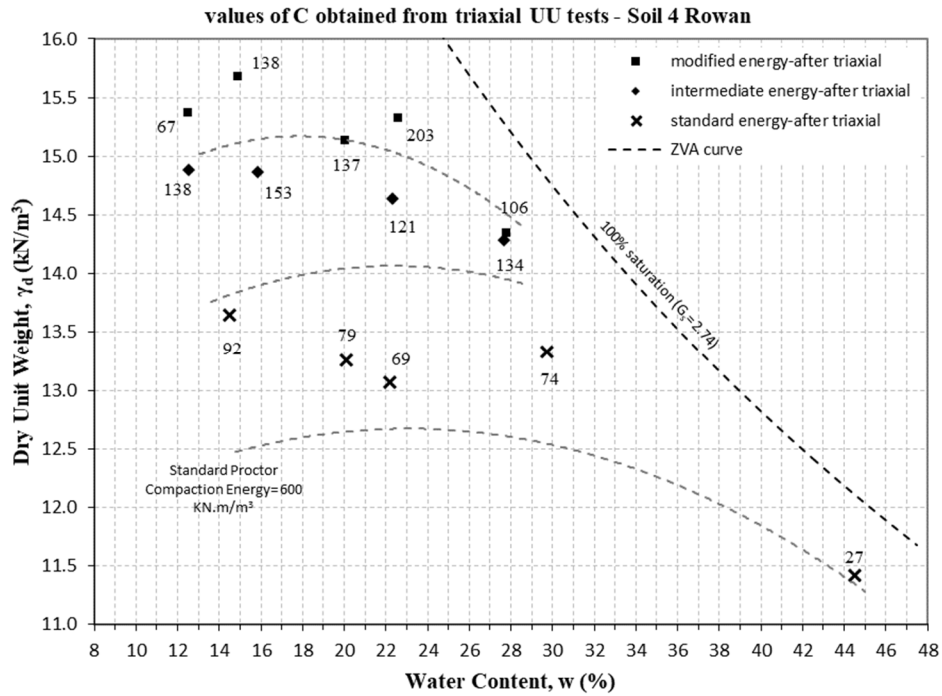
Figure 6.11. Total stress cohesion, C_{UU} (kPa) obtained from UU triaxial tests - Soil 4 Rowan
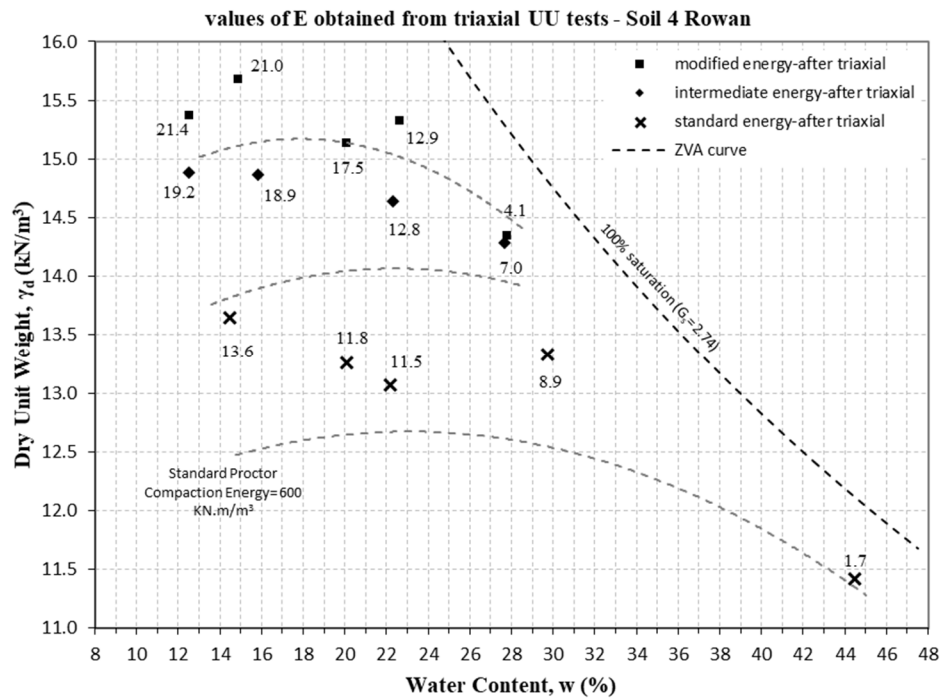
Figure 6.12. Elasticity modulus E_{UU} (MPa) at $s_c = 50\ kPa$ obtained from UU triaxial tests - Soil 4 Rowan

6.5. Soil 5 Mecklenburg UU Triaxial Results - Engineering Properties

Engineering properties obtained from UU triaxial tests carried out on Soil 3 Randolph are presented graphically in this section. Figure 6.13 shows total stress friction angle, Figure 6.14 depicts total stress cohesion, and Figure 6.15 illustrates modulus of elasticity for this soil. As mentioned earlier, the elasticity moduli belong to the UU triaxial tests with confining pressure equal to $s_C = 50kPa$.
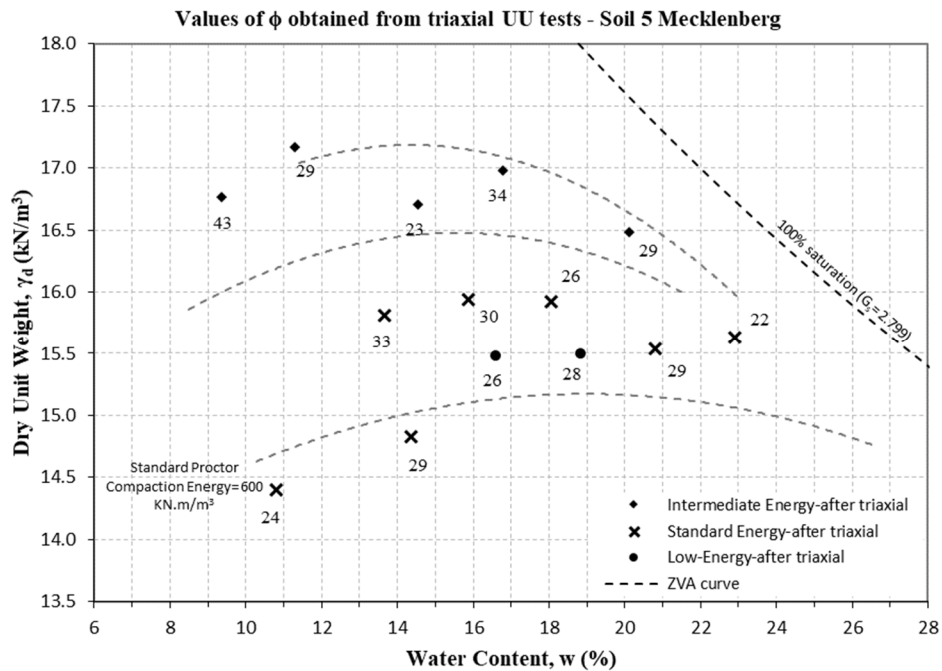
Figure 6.13. Total stress friction angle, f_{UU} (degrees) obtained from UU triaxial tests - Soil 5 Mecklenburg
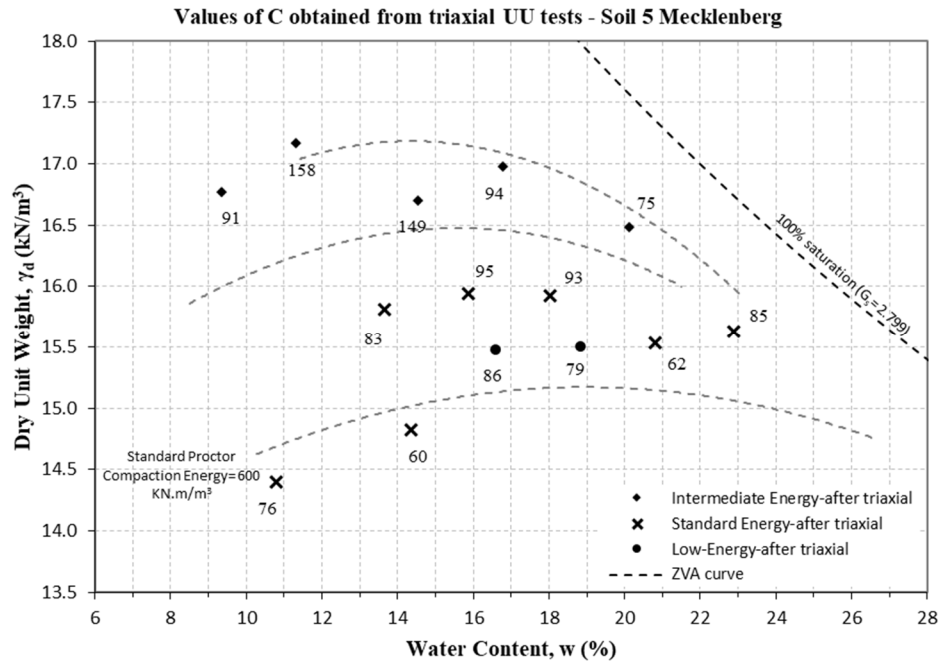
Figure 6.14. Total stress cohesion, C_{uu} (kPa) obtained from UU triaxial tests - Soil 5 Mecklenburg
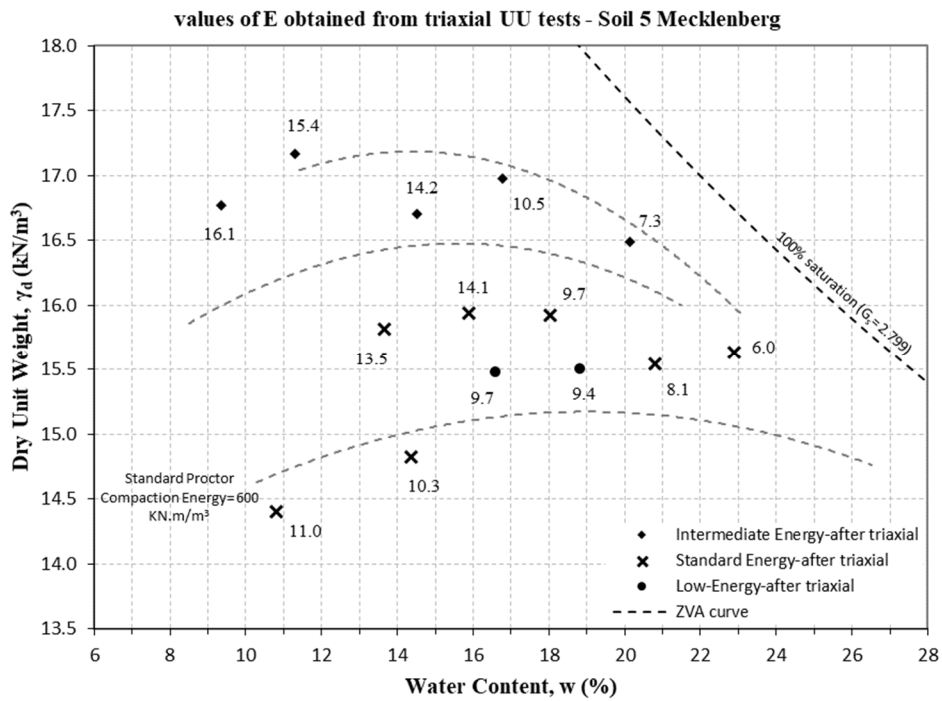
Figure 6.15. Elasticity modulus E_{uu} (MPa) at $s_c = 50\ kPa$ obtained from UU triaxial tests - Soil 5 Mecklenburg

7. CONSOLIDATED-UNDRAINED TRIAXIAL TESTS RESULTS OF TEST SOIL SAMPLES

For the purpose of the current project, failure criterion of generated pore pressure during shear stage equal to zero ($u = 0$) is adopted.

For each CU triaxial test effective stress path is drawn in the $p' - q'$ space. p' and q' at failure point are defined in the Equation (7-1). It is noted that q' is equal to q.

$$p'_f = \frac{s'_{1f} + s'_{3f}}{2}, \quad q'_f = \frac{s'_{1f} - s'_{3f}}{2} \tag{7-1}$$

where s'_{3f} is minor effective principal stress at failure and s'_{1f} is major effective principal stress at failure.

Similar to the UU triaxial tests procedure, three specimens are prepared which are compacted with same energy level, and have more or less same moisture content and dry unit weight.

Having effective stress path of the three consecutive CU triaxial tests, we can determine the point of failure. It is noted that different failure criteria might be used, but in this work generated pore pressure during shear stage equal to zero ($u = 0$) has been selected. After detecting failure points, failure line and thereof effective friction angle and effective cohesion will be known. Figure 7.1 typically shows effective stress paths and failure line for the CU triaxial tests.

It is noted that for briefness purposes, effective stress paths and failure lines associated with CU triaxial tests are presented in appendix C at the end of report.
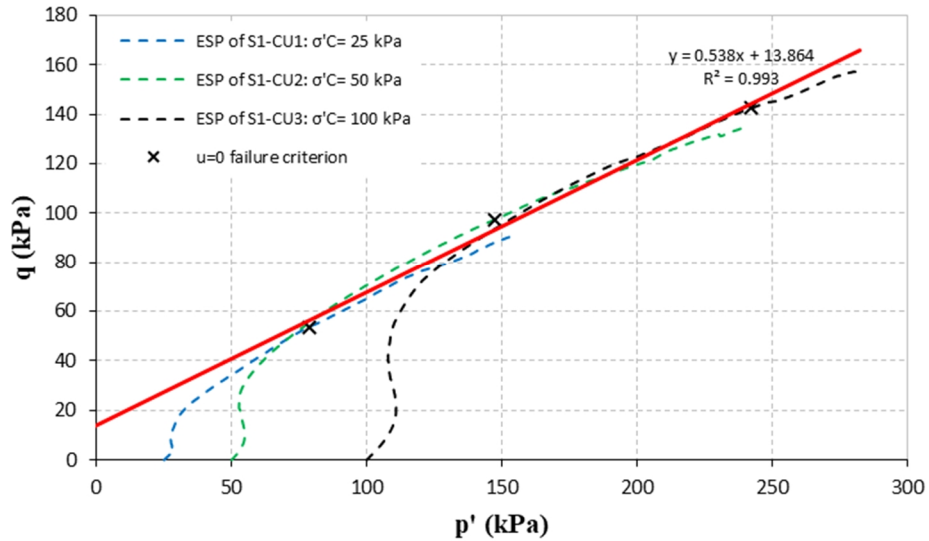
Figure 7.1. Typical effective stress paths and failure line for CU tests - samples of Soil 1 Forsyth compacted at standard energy

Behavior of the samples in a CU triaxial test is quite interesting. A graph on the moisture content-dry unit weight domain might be used to show position of the points during the course of CU triaxial test. This type of graph is shown for all test soils respectively in Figure 7.2 through Figure 7.6. This graph actually shows how samples move toward saturation line during the CU test. Original compaction curves at three energy levels are depicted on this graph as well. Also on this graph value/values of the effective friction angle is written which might be useful for practical purposes.

Downward move of the points on this type of graph which can be seen for all soil samples, is in fact an indication of swelling. It is reminded that dry unit weight is defined as weight of soil solids (w_s) over total volume of sample. Having w_s constant for a sample during CU test, implies that total volume must have increased, due to saturation process. It is also noted that to calculate specimen cross-sectional area after consolidation, Method B of ASTM D4767 is used.

At the end of this chapter a table is presented which summarizes essential information of particular CU tests that were carried out in this project.
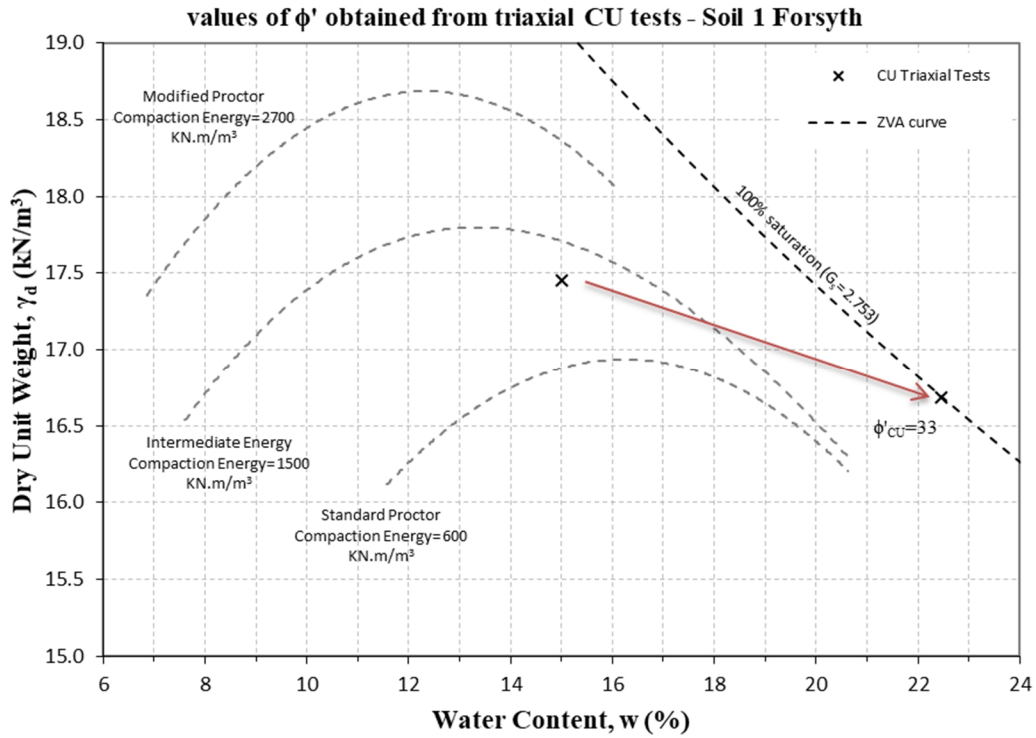
Figure 7.2. Effective stress friction angle, ϕ' obtained from CU triaxial tests - Soil 1 Forsyth
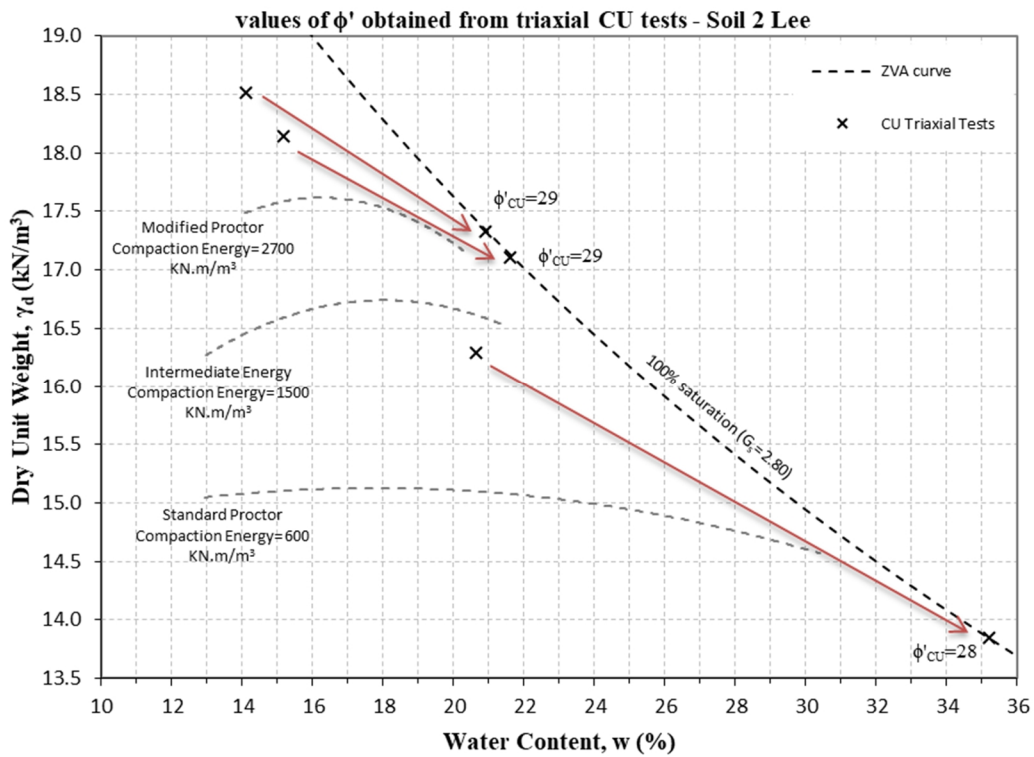
Figure 7.3. Effective stress friction angle, ϕ' obtained from CU triaxial tests - Soil 2 Lee

65
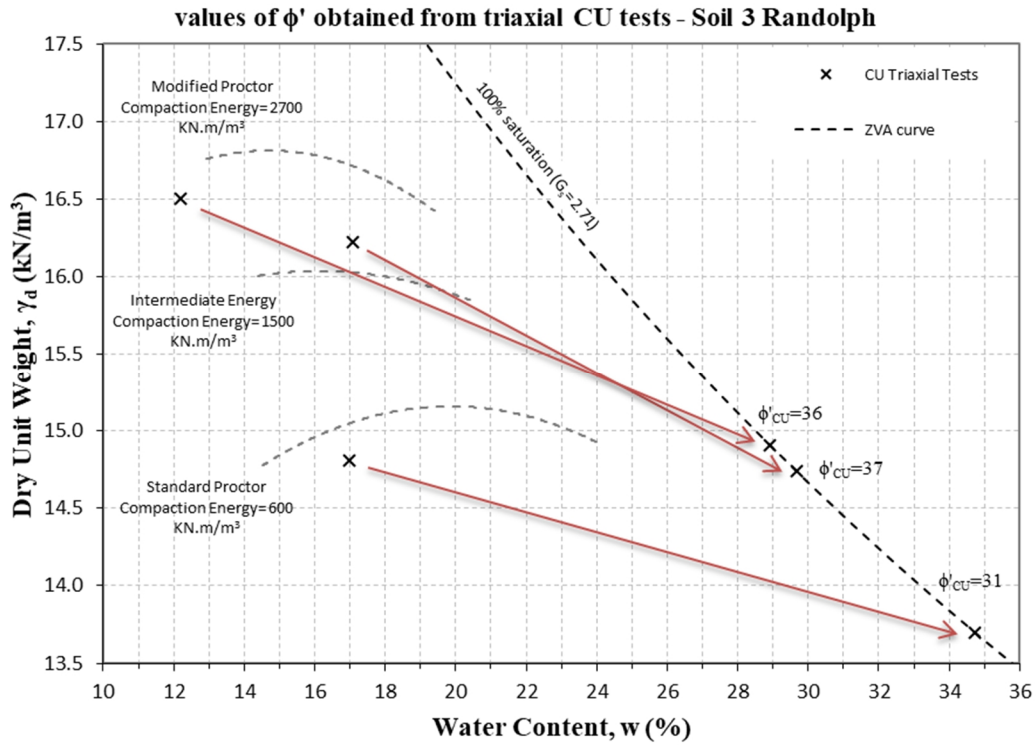
Figure 7.4. Effective stress friction angle, φ' obtained from CU triaxial tests - Soil 3 Randolph
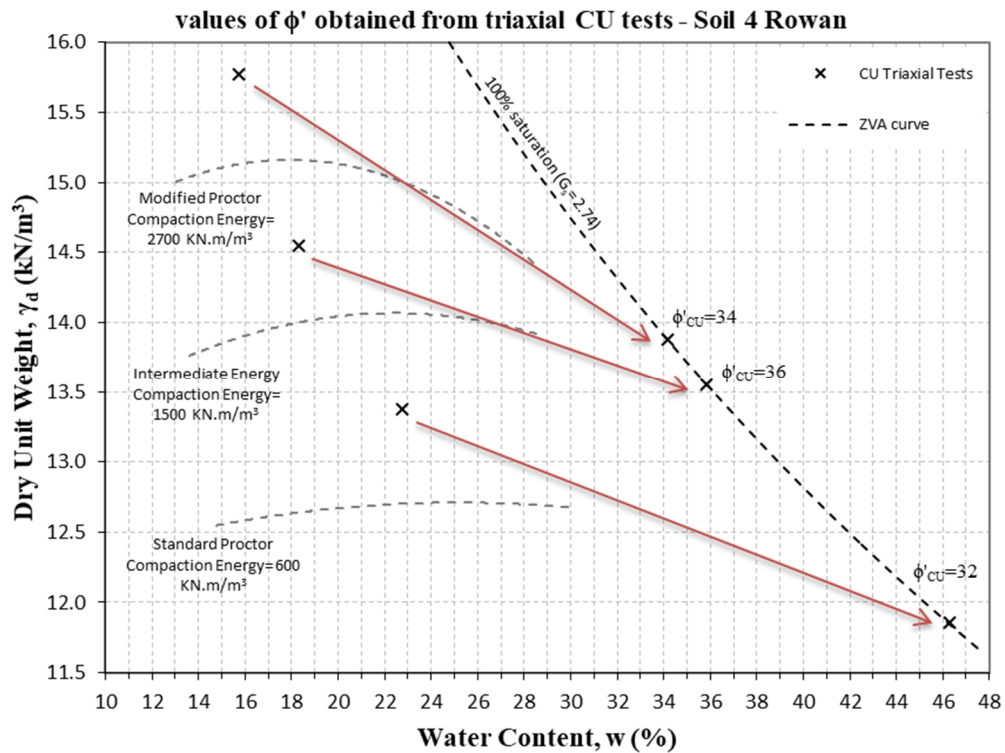
Figure 7.5. Effective stress friction angle, φ' obtained from CU triaxial tests - Soil 4 Rowan
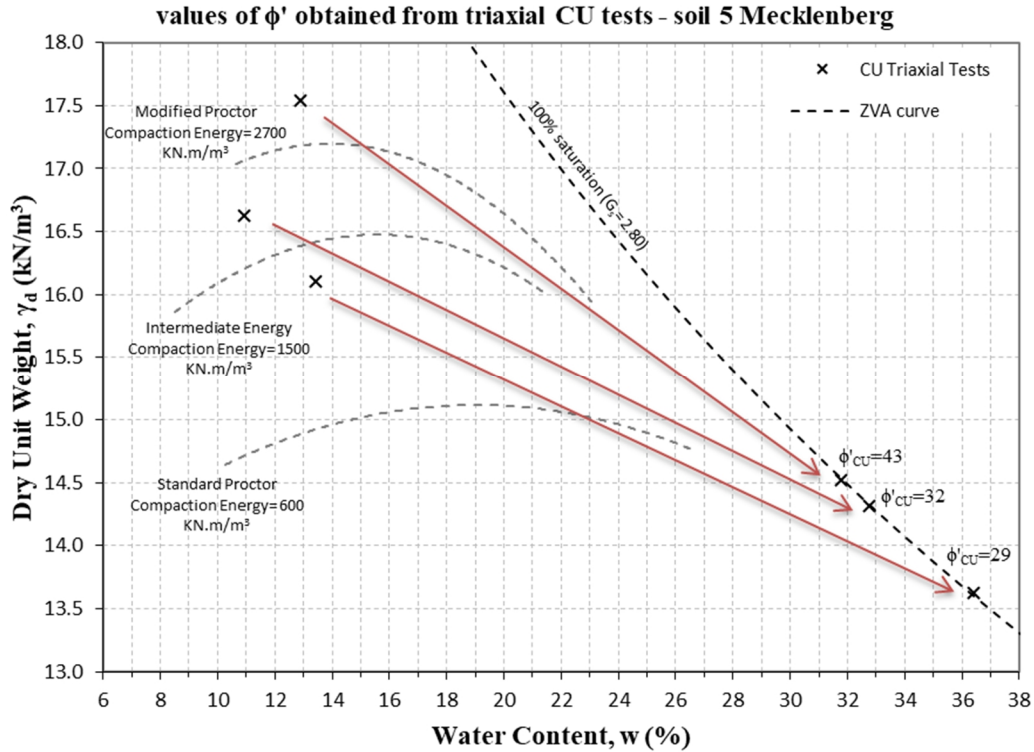
Figure 7.6. Effective stress friction angle, ϕ' obtained from CU triaxial tests - Soil 5 Mecklenburg

7.1. Summary Information and Conclusion of CU Triaxial Tests

It seems effective stress friction angles are same or slightly lower than those of obtained from total stress analysis. But cohesion terms obtained from effective stress analysis are noticeably lower than those of from total stress analysis. This difference is shown in Figure 7.7. This might be due to a concept know as apparent cohesion in the geotechnical literature. In an unsaturated soil specimen with occluded air phase, strong suction exists among water molecules which holds soil particles tightly close to each other. As soil specimen becomes saturated, suction disappears and as a result, cohesion and FS associated with that decrease dramatically.
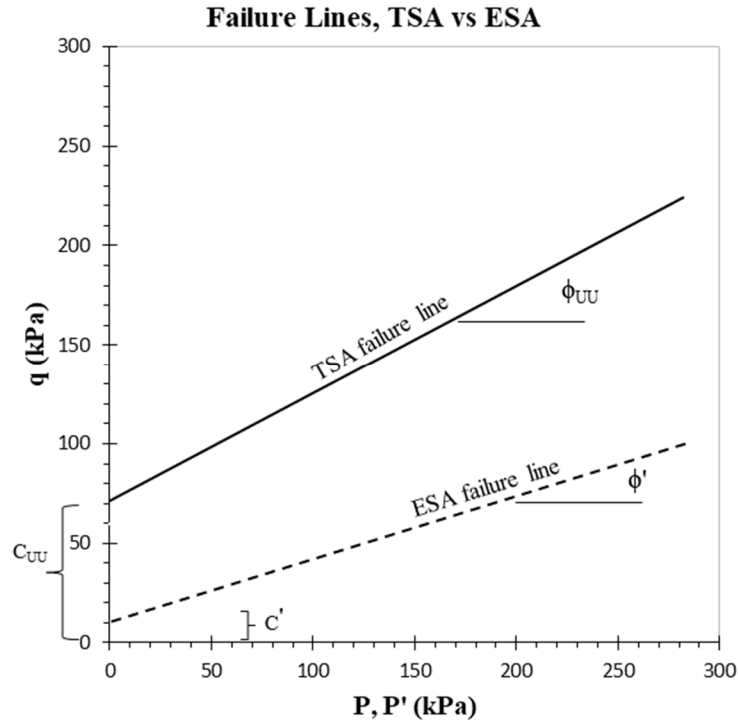
Figure 7.7. TSA failure line vs ESA failure line

Table 7.1 summarizes essential information associated with CU triaxial test. Regarding strength properties (friction angle and cohesion) represented in this table, it is noted that failure criterion of generated pore pressure during shear phase equal to zero (u=0) is picked.

Values of cohesion are also listed in this table. In some few cases where analysis of CU triaxial tests resulted in trivial cohesion value, they are entered zero in this table.

It can be seen that cohesion values are relatively small and negligible, hence one might decide to totally ignore the cohesion component in the effective stress slope stability analysis. It is noted that effective stress slope stability analysis uses CU triaxial results as input. However, in this research cohesion component was not neglected for the slope stability purpose, that is effective stress strength properties are as presented in Table 7.1.

Table 7.1. Summary information of CU triaxial tests

Test No.	Soil ID	molding compactive energy	B$_{value}$	s'_c (kPa)	initial		before shear		u=0 failure criterion	
					w (%)	g_d (kN/m³)	w (%)	g_d (kN/m³)	f	C' (kPa)
S1-CU1	Soil 1 Forsyth	Standard Proctor	0.95	25	15.0	17.5	22.5	16.7	33	16
S1-CU2			0.89	50						
S1-CU3			0.94	100						
S2-CU1	Soil 2 Lee	Standard Proctor	0.96	25	20.6	16.3	35.2	13.8	28	4
S2-CU3			0.95	100						
S2-CU4	Soil 2 Lee	Intermediate Proctor	0.78	25	15.2	18.1	21.6	17.1	29	38
S2-CU5			0.88	50						
S2-CU6			0.82	100						
S2-CU7	Soil 2 Lee	Modified Proctor	0.71	25	14.1	18.5	20.9	17.3	29	46
S2-CU8			-	50						
S2-CU9			0.64	100						
S3-CU1	Soil 3 Randolph	Standard Proctor	0.96	25	17.0	14.8	34.7	13.7	31	5
S3-CU2			0.95	50						
S3-CU3			0.96	100						
S3-CU4	Soil 3 Randolph	Intermediate Proctor	0.99	25	17.1	16.2	29.7	14.7	37	0
S3-CU5			0.95	50						
S3-CU6			0.96	100						
S3-CU7	Soil 3 Randolph	Modified Proctor	0.96	25	12.2	16.5	28.9	14.9	36	2
S3-CU8			0.95	50						
S3-CU9			0.95	100						

Table 7.1. Summary information of CU triaxial tests (continued)

Test No.	Soil ID	molding compactive energy	B_{value}	s'_c (kPa)	initial		before shear		u=0 failure criterion	
					w (%)	g_d (kN/m³)	w (%)	g_d (kN/m³)	f'_{CU}	C'_{CU} (kPa)
S4-CU1	Soil 4 Rowan	Standard Proctor	0.82	25	22.8	13.4	46.3	11.9	32	10
S4-CU2			0.98	50						
S4-CU3			0.97	100						
S4-CU4	Soil 4 Rowan	Intermediate Proctor	0.96	25	18.3	14.5	35.8	13.6	36	5
S4-CU5			0.96	50						
S4-CU6			0.96	100						
S4-CU7	Soil 4 Rowan	Modified Proctor	0.97	25	15.7	15.8	34.2	13.9	34	14
S4-CU9			0.96	100						
S5-CU1	Soil 5 Mecklenburg	Standard Proctor	0.96	25	13.4	16.1	36.4	13.6	29	0
S5-CU3			0.95	100						
S5-CU4	Soil 5 Mecklenburg	Intermediate Proctor	0.95	25	10.9	16.6	32.8	14.3	32	3
S5-CU5			0.96	50						
S5-CU6			0.95	100						
S5-CU7	Soil 5 Mecklenburg	Modified Proctor	0.96	25	12.9	17.5	31.8	14.5	43	0
S5-CU9			0.95	100						

8. SLOPE STABILITY ANALYSIS

8.1. Introduction

Slope stability analysis will be performed in this chapter based on both total stress parameters and effective stress parameters. For TSA strength properties obtained from UU triaxial tests will be used, while for the ESA strength properties obtained from CU triaxial tests (with pore pressure measurements) will be taken as input.

In chapter three where research methodology was discussed, embankment sections/geometries which are considered for slope stability analysis were presented. However, it is noted that there are 16 embankment sections in total which consist of four side slopes and four heights. It is also noted that embankment sections for deformation analysis will be same as the sections which are introduced here. These embankment sections were listed in Table 3.1 and some of them were shown in Figure 3.3.

Regarding slope stability method, it is noted that five methods of ordinary/Fellenius, Bishop simplified, Janbu corrected, Spencer and Morgenstern-Price were considered. Setting aside the old method of ordinary/Fellenius which gives unreasonably low factors of safety, Spencer method, on average, gives the minimum among the other four and hence will be used. FS from Morgenstern-Price method is in most of the cases equal to or very slightly more than that of from Spencer's.

Values of factor of safety need to be investigated and compared for all geometries as well as all soil strength properties. For similarity and comparison purposes, it was decided to keep the slip surface relatively constant. To further investigate the effect of selecting most appropriate slip surface, a section entitled as "investigation of the critical failure surface over the embankment crest" has been defined which is briefed here.

To investigate minimum FS over the crest, intervals of 5 ft have been selected for the offset distance from the crest edge. Slip surfaces have been considered such that start point of each individual slip surface is embankment toe and exit point locates on the crest with offset distance from crest edge. However, this type of analysis is called <u>offset analysis</u> in this research.

Alternatively, the well-known critical slip surface search of "grid and radius" has also been performed.

Conclusion from this section can be stated as following. For each individual geometry, the first step must be running a global grid search via "grid and radius" method. If the critical slip surface starts from the embankment toe and ends at some point on the embankment crest, this slip surface shall be considered critical and the basis for all comparison and formulation purposes. But if the slip surface from grid search does not obey stated geometry rules, an offset analysis seems necessary to find the point on the crest where the critical slip surface, having the minimum FS, will cut the embankment crest. Then, this surface shall be considered as the basis for comparisons.

In other words, all regressed equations that are presented in this chapter for FS, belong to slip surfaces which are relatively consistent with each other in terms of geometry. However, it is noted that this topic particularly applies to the total stress slope stability analysis using UU triaxial parameters.

It should be added that in the process of finding minimum FS, special caution was exercised toward "infinite slope stability" analysis, meaning that FS for the shallow failure was investigated, and in any case where the FS from shallow failure was lower than that of from grid and radius search, the one from shallow failure was reported. However, this means for example for any of the 192 cases run of the Soil 1 Forsyth, the minimum FS is being reported.

Figure 8.1 shows the typical geometry and parameters of an infinite slope. According to Duncan et al. (2014) the required formula to calculate FS for infinite slope stability is proven to be as follows:
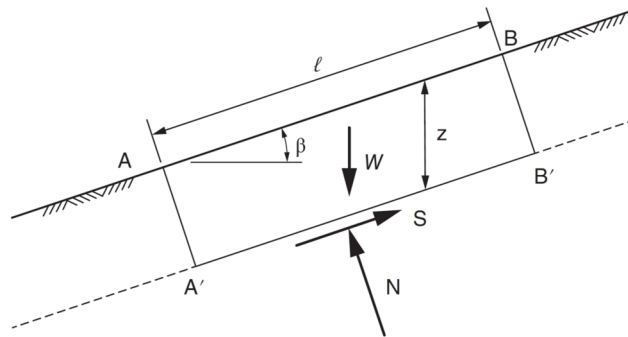
Figure 8.1. Infinite slope stability analysis (adopted from Duncan et al. 2014)

$$FS = \frac{C}{g_m.Z.\sin b.\cos b} + \frac{\tan f}{\tan b} \qquad (8\text{-}1)$$

where C and f are cohesion and friction angle of soil, Z is the slope vertical depth, g_m is the moist unit weight of soil and b is the slope angle. It is noted that Z should not be confused with H, height of embankment. As mentioned in literature review chapter, the depth of the shallow slope failure varies with soil type and slope geometry, but generally ranges between 0.9 and 1.8 m (3-6 ft) (Loehr et al. 2007), or 1.5 to 2 m (Briaud 2013). For the purpose of calculations done as shallow slope failure, Z is assumed equal to 1.5m ($\approx$5ft) which seems to be a conservative choice (relatively high Z) as high values of Z result in lower FS.

8.2. Total Stress Slope Stability Analysis Using UU Triaxial Parameters

As stated earlier, massive number of tries/runs are needed for each of the analyses using total stress parameters and effective stress parameters. For example, total number of analyses done for Soil 1 Forsyth at total stress state was 192. Table 8.1 lists number of slope stability analyses which were done for each soil sample at total stress state, that is using UU triaxial parameters.

Table 8.1. Number of deformation analyses done for each soil sample – TSA

Soil sample	No. of analyses
Soil 1 Forsyth	192
Soil 2 Lee	224
Soil 3 Randolph	208
Soil 4 Rowan	224
Soil 5 Mecklenburg	224

It is noted that in all 1072 cases that were run for five soil samples using TSA parameters, in only one case the infinite slope (shallow) failure was yielding a FS lower than that of from global failure (grid and radius search), and hence was the dominant type of failure. Of course, even for this one case both type of factor of safeties were higher than the minimum. This indicates that, "for the total stress analysis, shallow failure is never dominant".

It is also noted that among all of the 1072 cases not even one case showed TSA factor of safety lower than the minimum value of 1.3. In many of these cases FS is well above the minimum value.

In addition to briefness of this report, this is actually the reason that we are not presenting detailed tables for total stress FS analysis.

This indicates that embankments made from these soil samples are stable right after compaction operation, even if the minimum compactive energy level, that is Standard Proctor is used.

For the TSA state, after obtaining FS values a regression analysis effort was made to find equations which introduce FS based on some basic parameters such as material properties (friction angle, cohesion, unit weight) and embankment geometric properties (side slope, height). Non-linear regression analysis effort resulted in equations with very high coefficients of determination-R^2, which is a sign of good correlation between variables.

It is noted that a set of dimensionless formulae has been generated for ease of use as well. In these equations instead of friction angle tangent of friction angle is used ($f \rightarrow \tan f$) and dimensionless cohesion (C_D) has taken the place of cohesion. Dimensionless cohesion term is defined as follows:

$$C_D = \frac{C}{g_m * H}$$

(8-2)

where C is the cohesion of soil, g_m is total unit weight of soil, and H is embankment height. Dimensioned regressed equations and dimensionless regressed equations are presented separately; however, engineers are expected to decide and carefully use a suitable equation.

Equations are presented for each individual soil and also for all soil samples at the end of each section. Equations (8-8) and (8-14) pertain to regression among data of all soil samples. Equations belonging to all soil samples could somehow be considered for silty soil as silt was the dominant type of soil used in the project.

It is also noted that in these equations, presented factor of safety is under the loading conditions defined earlier in the report; that is traffic and pavement loads were taken equivalent to a uniformly distributed load with a magnitude of 35kPa.

Dimensioned equations for total stress FS analysis

$$FS_{UU} = 0.1849 \frac{f_{UU}^{0.4529} * C_{UU}^{0.6533} * S^{0.5140}}{g_m^{0.2238} * H^{0.3788}}$$

(8-3)

Soil 1 Forsyth, TSA

$$FS_{UU} = 0.2222 \frac{f_{UU}^{0.3579} * C_{UU}^{0.7376} * S^{0.4894}}{g_m^{0.2456} * H^{0.4671}}$$

(8-4)

Soil 2 Lee, TSA

$$FS_{UU} = 0.2774 \frac{f_{UU}^{0.4607} * C_{UU}^{0.7115} * S^{0.5115}}{g_m^{0.4620} * H^{0.3787}}$$

(8-5)

Soil 3 Randolph, TSA

$$FS_{UU} = 0.1531 \frac{f_{UU}^{0.3183} * C_{UU}^{0.7009} * S^{0.4870}}{g_m^{0.0285} * H^{0.4147}}$$

(8-6)

Soil 4 Rowan, TSA

$$FS_{UU} = 0.3127 \frac{f_{UU}^{0.3328} * C_{UU}^{0.7761} * S^{0.4931}}{g_m^{0.4205} * H^{0.4194}}$$

(8-7)

Soil 5 Mecklenburg, TSA

$$FS_{UU} = 0.2584 \frac{f_{UU}^{0.3519} * C_{UU}^{0.7317} * S^{0.4949}}{g_m^{0.3019} * H^{0.4276}}$$

(8-8)

all soil samples, TSA

where FS_{UU} is the factor of safety of the embankment against instability using TSA strength parameters, f_{UU} is total friction angle in degrees, C_{UU} is total cohesion in kPa, and S is embankment side slope, g_m is material total unit weight (kN/m^3), H is embankment height in meters. Coefficients of determination of the above equations are as follows respectively: 0.9974, 0.9984, 0.9986, 0.9969, 0.9984, 0.9973.

Dimensionless equations for total stress FS analysis

$$FS_{UU} = 5.8550 * Tan^{0.4033}(f_{UU}) * C_{D,UU}{}^{0.4888} * S^{0.5126}$$

Soil 1 Forsyth, TSA, dimensionless equation (8-9)

$$FS_{UU} = 6.6618 * Tan^{0.3683}(f_{UU}) * C_{D,UU}{}^{0.5801} * S^{0.4879}$$

Soil 2 Lee, TSA, dimensionless equation (8-10)

$$FS_{UU} = 5.0546 * Tan^{0.1334}(f_{UU}) * C_{D,UU}{}^{0.4267} * S^{0.5108}$$

Soil 3 Randolph, TSA, dimensionless equation (8-11)

$$FS_{UU} = 5.7310 * Tan^{0.1380}(f_{UU}) * C_{D,UU}{}^{0.4982} * S^{0.4856}$$

Soil 4 Rowan, TSA, dimensionless equation (8-12)

$$FS_{UU} = 5.5513 * Tan^{0.2219}(f_{UU}) * C_{D,UU}{}^{0.4856} * S^{0.4920}$$

Soil 5 Mecklenburg, TSA, dimensionless equation (8-13)

$$FS_{UU} = 6.2735 * Tan^{0.3880}(f_{UU}) * C_{D,UU}{}^{0.5645} * S^{0.4929}$$

all soil samples, TSA, dimensionless equation (8-14)

where $C_{D,UU}$ is the dimensionless cohesion based on total stress analysis and rest of parameters are defined as before. Coefficients of determination of the above equations are as follows respectively: 0.9866, 0.9876, 0.9929, 0.9872, 0.9897, 0.9825.

8.3.   Effective Stress Slope Stability Analysis Using CU Triaxial Parameters

It is noted that combination of four embankment heights and four side slopes results in 16 embankment sections as listed in Table 3.1. In fact, specifications of each data point on figures of the type of Figure 7.3 (points on saturation line) are attributed to the embankment sections and then effective stress FS is obtained.

Results of the stability analysis based on ESA parameters were completely different from those of obtained using TSA parameters, as in the effective stress stability analyses many cases were found having FS lower than 1.3.

Strength parameters from CU triaxial tests may be mainly characterized by lower cohesion term compared to those of from UU triaxial tests (concept shown in Figure 7.7). It was also observed that as cohesion of soil material decreases, mode of failure moves from a deep slip surface encompassing all the embankment slope to a shallow, small and local one. In other words, in the effective stress analysis many cases were seen where shallow failure was the dominant mode of failure.

These facts lead us to the following statements: "assuming saturation/inundation for the highway embankments is probable through their service life, effective stress stability may be crucial". Moreover, "for the effective stress slope stability analysis, shallow failure must be checked as it is a case with high possibility".

Moreover, it is noted that height of embankment does not play a considerable role in the FS. This might be because of the fact that in the effective stress stability analysis, mode of failure is dominated by partial failure.

For the effective stress slope stability analysis, as one mode of failure was not dominant and modes of failure were different, no regression analysis was attempted, neither any equation is presented. Instead, reader is referred to wisely using the FS tables presented at the end of this section. However, Table 8.2 also summarizes important information regarding effective stress slope stability analysis in a descriptive way for each project test soil.

Table 8.2. Description of acceptable zones/cases based on effective stress slope stability analyses criterion

Soil sample	Summary points
Soil 1 Forsyth (PI=2) AASHTO class: A-4 (0)	- Even final dry unit weight* is relatively low, numerical values of FS for all embankment sections are higher than 1.3 - However, side slope of 1H:1V cannot be recommended - Non-shallow failure is still the dominant mode of failure **
Soil 2 Lee (PI=21) AASHTO class: A-7-6 (28)	- Side slope of 1H:1V is not recommended - Having high final unit weight/dry unit weight might assure ESA FS even more than 1.3
Soil 3 Randolph (PI=NP) AASHTO class: A-4 (1)	- Side slope 1H:1V shall not be used - Side slope 2H:1V can be tricky and is not recommended - Cohesion term has nearly vanished, and partial failure is almost the dominant mode of failure - Many cases of shallow slope failure were seen to be dominant
Soil 4 Rowan (PI=6) AASHTO class: A-5 (7)	- Side slope 1H:1V seems to be the only problematic section, as other sections yield FS higher than 1.3 even if final dry unit weight is relatively low
Soil 5 Mecklenburg (PI=5) AASHTO class: A-5 (5)	- Side slope 1H:1V shall not be used - Side slope 2H:1V is not very reliable - Cohesion term has nearly vanished, and partial failure is almost the dominant mode of failure - If embankment compacted at low energy levels such as standard energy, it will fail under rain-induced conditions - Has the most cases of instability among tested soils

* Final dry unit weight refers to after saturation and before shear stage, applicable to rain-induced conditions
** Modes of failure will be explained shortly in this section

As mentioned earlier, tables listing effective stress FS values for each data point are presented at the end of this section. Last column of these tables reports mode of failure, which can be one of the three cases of non-shallow, partial, and shallow. Non-shallow failure has a critical slip surface which goes through all the embankment slope and is the result of global grid search (grid and radius search). It is reminded that the scope of this research will consider only issues related to compacted embankment and not due to poor foundation soil conditions. Hence, we avoid calling this mode of failure "global", as global is the terminology usually referring to a critical slip surface which includes embankment and its foundation as well. As stated earlier in this chapter, this critical slip surface (non-shallow) starts more or less from embankment toe and cut the embankment crest at a distance from edge. Partial failure also is a result of global grid search (grid and radius search), but in this case the critical slip surface does not include all the embankment slope. It is noted that FS values in cases partial failure were observed, were very close to the values obtained using shallow failure equation. Finally, shallow failure is the result of Equation (8-1) with Z being 1.5m.

Figure 8.2 schematically illustrates non-shallow slip surface and partial slip surface. Shallow slip surface/failure was already depicted in Figure 8.1.
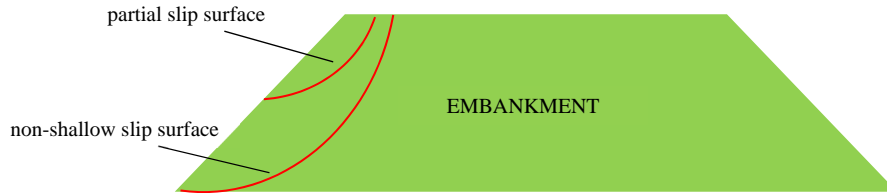
Figure 8.2. Schematic illustration of non-shallow slip surface and partial slip surface

Both dry unit weight (g_d) and moist unit weight (g_m) are listed in these types of tables; of course, the following well-known relationship holds between them:

$$g_d = \frac{g_m}{1+w}$$

(8-15)

where w is moisture content (water content) of soil specimen which is conventionally stated in percent number, but herein regarded as decimal number.

Saturation ratio (Saturation degree)- S, is also presented in these tables. Since all CU tests had high B values, specimens are assumed to be saturated (S ≈ 100%) at the beginning of shear stage.

8.3.1.   FS Tables for Soil 1 Forsyth – Effective Stress Slope Stability Analysis (CU Triaxial Parameters)

Table 8.3. FS for Soil 1 Forsyth - ESA

Tests ID	W (%)	$g_d (kN / m^3)$	$g_m (kN / m^3)$	S (%)	f'(deg)	C'(kPa)	H (m)	slope	Minimum FS	Mode of failure
S1-CU1 S1-CU2 S1-CU3	22.5	16.7	20.4	≈ 100	33	16	12.2	1H:1V	1.3	non-shallow
								2H:1V	2.1	non-shallow
								3H:1V	2.8	non-shallow
								4H:1V	3.6	non-shallow
							9.1	1H:1V	1.4	non-shallow
								2H:1V	2.2	non-shallow
								3H:1V	3.0	non-shallow
								4H:1V	3.7	non-shallow
							6.1	1H:1V	1.6	non-shallow
								2H:1V	2.4	non-shallow
								3H:1V	3.2	non-shallow
								4H:1V	3.9	non-shallow
							3.0	1H:1V	1.7	shallow
								2H:1V	2.6	shallow
								3H:1V	3.5	non-shallow
								4H:1V	3.9	partial

8.3.2. FS Tables for Soil 2 Lee – Effective Stress Slope Stability Analysis (CU Triaxial Parameters)

Table 8.4. FS for Soil 2 Lee - ESA

Tests ID	W (%)	$g_d (kN/m^3)$	$g_m (kN/m^3)$	S (%)	f'(deg)	C'(kPa)	H (m)	slope	Minimum FS	Mode of failure
S2-CU1 S2-CU3	35.2	13.8	18.7	≈ 100	28	4	12.2	1H:1V	0.8	non-shallow
								2H:1V	1.3	non-shallow
								3H:1V	1.9	non-shallow
								4H:1V	2.4	non-shallow
							9.1	1H:1V	0.8	shallow
								2H:1V	1.4	shallow
								3H:1V	1.9	partial
								4H:1V	2.3	partial
							6.1	1H:1V	0.8	shallow
								2H:1V	1.4	shallow
								3H:1V	1.8	partial
								4H:1V	2.1	partial
							3.0	1H:1V	0.8	shallow
								2H:1V	1.4	shallow
								3H:1V	1.7	partial
								4H:1V	1.9	partial

Table 8.4. FS for Soil 2 Lee - ESA (continued)

Tests ID	W (%)	$g_d (kN/m^3)$	$g_m (kN/m^3)$	S (%)	f' (deg)	C' (kPa)	H (m)	slope	Minimum FS	Mode of failure
S2-CU4 S2-CU5 S2-CU6	21.6	17.1	20.8	≈ 100	29	38	12.2	1H:1V	1.7	non-shallow
								2H:1V	2.5	non-shallow
								3H:1V	3.3	non-shallow
								4H:1V	4.1	non-shallow
							9.1	1H:1V	2.0	non-shallow
								2H:1V	2.8	non-shallow
								3H:1V	3.7	non-shallow
								4H:1V	4.5	non-shallow
							6.1	1H:1V	2.3	non-shallow
								2H:1V	3.3	non-shallow
								3H:1V	4.2	non-shallow
								4H:1V	5.0	non-shallow
							3.0	1H:1V	3.0	non-shallow
								2H:1V	4.1	non-shallow
								3H:1V	5.1	non-shallow
								4H:1V	5.9	non-shallow

Table 8.4. FS for Soil 2 Lee - ESA (continued)

Tests ID	W (%)	$g_d (kN/m^3)$	$g_m (kN/m^3)$	S (%)	f'(deg)	C'(kPa)	H (m)	slope	Minimum FS	Mode of failure
S2-CU7 S2-CU8 S2-CU9	20.9	17.3	20.9	≈ 100	29	46	12.2	1H:1V	1.9	non-shallow
								2H:1V	2.8	non-shallow
								3H:1V	3.6	non-shallow
								4H:1V	4.4	non-shallow
							9.1	1H:1V	2.2	non-shallow
								2H:1V	3.1	non-shallow
								3H:1V	4.0	non-shallow
								4H:1V	4.9	non-shallow
							6.1	1H:1V	2.6	non-shallow
								2H:1V	3.6	non-shallow
								3H:1V	4.6	non-shallow
								4H:1V	5.6	non-shallow
							3.0	1H:1V	3.4	shallow
								2H:1V	4.7	shallow
								3H:1V	5.7	non-shallow
								4H:1V	6.7	partial

8.3.3.   FS Tables for Soil 3 Randolph – Effective Stress Slope Stability Analysis (CU Triaxial Parameters)

Table 8.5. FS for Soil 3 Randolph - ESA

Tests ID	W (%)	$g_d (kN/m^3)$	$g_m (kN/m^3)$	S (%)	f'(deg)	C'(kPa)	H (m)	slope	Minimum FS	Mode of failure
S3-CU1 S3-CU2 S3-CU3	34.7	13.7	18.5	≈ 100	31	5	12.2	1H:1V	0.9	non-shallow
								2H:1V	1.5	non-shallow
								3H:1V	2.2	non-shallow
								4H:1V	2.8	partial
							9.1	1H:1V	1.0	non-shallow
								2H:1V	1.6	non-shallow
								3H:1V	2.2	non-shallow
								4H:1V	2.7	partial
							6.1	1H:1V	1.0	shallow
								2H:1V	1.6	shallow
								3H:1V	2.1	partial
								4H:1V	2.5	partial
							3.0	1H:1V	1.0	shallow
								2H:1V	1.6	shallow
								3H:1V	2.0	partial
								4H:1V	2.2	partial

Table 8.5. FS for Soil 3 Randolph - ESA (continued)

Tests ID	W (%)	$g_d (kN / m^3)$	$g_m (kN / m^3)$	S (%)	f'(deg)	C'(kPa)	H (m)	slope	Minimum FS	Mode of failure
S3-CU4 S3-CU5 S3-CU6	29.7	14.7	19.1	≈ 100	37	0	12.2	1H:1V	0.7	partial
								2H:1V	1.4	partial
								3H:1V	2.1	partial
								4H:1V	2.7	partial
							9.1	1H:1V	0.7	partial
								2H:1V	1.4	partial
								3H:1V	2.0	partial
								4H:1V	2.6	partial
							6.1	1H:1V	0.7	partial
								2H:1V	1.3	partial
								3H:1V	1.8	partial
								4H:1V	2.2	partial
							3.0	1H:1V	0.6	partial
								2H:1V	1.1	partial
								3H:1V	1.5	partial
								4H:1V	1.8	partial

Table 8.5. FS for Soil 3 Randolph - ESA (continued)

Tests ID	W (%)	$g_d (kN/m^3)$	$g_m (kN/m^3)$	S (%)	f'(deg)	C'(kPa)	H (m)	slope	Minimum FS	Mode of failure
S3-CU7 S3-CU8 S3-CU9	28.9	14.9	19.2	≈ 100	36	2	12.2	1H:1V	0.8	shallow
								2H:1V	1.6	shallow
								3H:1V	2.3	partial
								4H:1V	2.9	partial
							9.1	1H:1V	0.8	shallow
								2H:1V	1.6	shallow
								3H:1V	2.2	partial
								4H:1V	2.7	partial
							6.1	1H:1V	0.8	shallow
								2H:1V	1.6	partial
								3H:1V	2.0	partial
								4H:1V	2.5	partial
							3.0	1H:1V	0.8	shallow
								2H:1V	1.4	partial
								3H:1V	1.8	partial
								4H:1V	2.0	partial

8.3.4.   FS Tables for Soil 4 Rowan – Effective Stress Slope Stability Analysis (CU Triaxial Parameters)

Table 8.6. FS for Soil 4 Rowan - ESA

Tests ID	W (%)	$g_d (kN/m^3)$	$g_m (kN/m^3)$	S (%)	f'(deg)	C'(kPa)	H (m)	slope	Minimum FS	Mode of failure
S4-CU1 S4-CU2 S4-CU3	46.3	11.9	17.3	≈ 100	32	10	12.2	1H:1V	1.1	non-shallow
								2H:1V	1.8	non-shallow
								3H:1V	2.5	non-shallow
								4H:1V	3.2	non-shallow
							9.1	1H:1V	1.2	non-shallow
								2H:1V	1.9	non-shallow
								3H:1V	2.6	non-shallow
								4H:1V	3.3	non-shallow
							6.1	1H:1V	1.3	non-shallow
								2H:1V	2.1	non-shallow
								3H:1V	2.7	non-shallow
								4H:1V	3.2	partial
							3.0	1H:1V	1.4	shallow
								2H:1V	2.2	shallow
								3H:1V	2.8	partial
								4H:1V	3.0	partial

87

Table 8.6. FS for Soil 4 Rowan - ESA (continued)

Tests ID	W (%)	$g_d(kN/m^3)$	$g_m(kN/m^3)$	S (%)	f'(deg)	C'(kPa)	H (m)	slope	Minimum FS	Mode of failure
S4-CU4 S4-CU5 S4-CU6	35.8	13.6	18.4	≈ 100	36	5	12.2	1H:1V	1.1	non-shallow
								2H:1V	1.8	non-shallow
								3H:1V	2.6	non-shallow
								4H:1V	3.2	partial
							9.1	1H:1V	1.1	shallow
								2H:1V	1.9	non-shallow
								3H:1V	2.6	partial
								4H:1V	3.1	partial
							6.1	1H:1V	1.1	shallow
								2H:1V	1.9	shallow
								3H:1V	2.4	partial
								4H:1V	2.8	partial
							3.0	1H:1V	1.1	shallow
								2H:1V	1.9	shallow
								3H:1V	2.2	partial
								4H:1V	2.5	partial

Table 8.6. FS for Soil 4 Rowan - ESA (continued)

Tests ID	W (%)	$g_d (kN / m^3)$	$g_m (kN / m^3)$	S (%)	f'(deg)	C'(kPa)	H (m)	slope	Minimum FS	Mode of failure
S4-CU7 S4-CU9	34.2	13.9	18.6	≈ 100	34	14	12.2	1H:1V	1.3	non-shallow
								2H:1V	2.1	non-shallow
								3H:1V	2.9	non-shallow
								4H:1V	3.6	non-shallow
							9.1	1H:1V	1.4	non-shallow
								2H:1V	2.2	non-shallow
								3H:1V	3.0	non-shallow
								4H:1V	3.8	non-shallow
							6.1	1H:1V	1.6	non-shallow
								2H:1V	2.4	non-shallow
								3H:1V	3.2	non-shallow
								4H:1V	3.9	partial
							3.0	1H:1V	1.7	shallow
								2H:1V	2.6	shallow
								3H:1V	3.4	non-shallow
								4H:1V	3.7	partial

8.3.5. **FS Tables for Soil 5 Mecklenburg – Effective Stress Slope Stability Analysis (CU Triaxial Parameters)**

Table 8.7. FS for Soil 5 Mecklenburg - ESA

Tests ID	W (%)	$g_d (kN/m^3)$	$g_m (kN/m^3)$	S (%)	f'(deg)	C'(kPa)	H (m)	slope	Minimum FS	Mode of failure
S5-CU1 S5-CU3	36.4	13.6	18.6	≈ 100	29	0	12.2	1H:1V	0.5	partial
								2H:1V	1.1	partial
								3H:1V	1.5	partial
								4H:1V	2.0	partial
							9.1	1H:1V	0.5	partial
								2H:1V	1.0	partial
								3H:1V	1.5	partial
								4H:1V	1.9	partial
							6.1	1H:1V	0.5	partial
								2H:1V	0.9	partial
								3H:1V	1.3	partial
								4H:1V	1.6	partial
							3.0	1H:1V	0.5	partial
								2H:1V	0.8	partial
								3H:1V	1.1	partial
								4H:1V	1.3	partial

Table 8.7. FS for Soil 5 Mecklenburg - ESA (continued)

Tests ID	W (%)	$g_d (kN/m^3)$	$g_m (kN/m^3)$	S (%)	f'(deg)	C'(kPa)	H (m)	slope	Minimum FS	Mode of failure
S5-CU4 S5-CU5 S5-CU6	32.8	14.3	19.0	≈ 100	32	3	12.2	1H:1V	0.8	non-shallow
								2H:1V	1.5	non-shallow
								3H:1V	2.1	partial
								4H:1V	2.6	partial
							9.1	1H:1V	0.9	shallow
								2H:1V	1.5	non-shallow
								3H:1V	2.0	partial
								4H:1V	2.5	partial
							6.1	1H:1V	0.9	shallow
								2H:1V	1.5	partial
								3H:1V	1.9	partial
								4H:1V	2.3	partial
							3.0	1H:1V	0.9	shallow
								2H:1V	1.5	partial
								3H:1V	1.7	partial
								4H:1V	2.0	partial

Table 8.7. FS for Soil 5 Mecklenburg - ESA (continued)

Tests ID	W (%)	$g_d (kN/m^3)$	$g_m (kN/m^3)$	S (%)	f'(deg)	C'(kPa)	H (m)	slope	Minimum FS	Mode of failure
S5-CU7 S5-CU9	31.8	14.5	19.1	≈ 100	43	0	12.2	1H:1V	0.9	partial
								2H:1V	1.8	partial
								3H:1V	2.6	partial
								4H:1V	3.4	partial
							9.1	1H:1V	0.9	partial
								2H:1V	1.7	partial
								3H:1V	2.5	partial
								4H:1V	3.2	partial
							6.1	1H:1V	0.9	partial
								2H:1V	1.6	partial
								3H:1V	2.2	partial
								4H:1V	2.8	partial
							3.0	1H:1V	0.8	partial
								2H:1V	1.4	partial
								3H:1V	1.8	partial
								4H:1V	2.2	partial

9. DEFORMATION ANALYSIS

9.1. Introduction

In this chapter deformation analysis of the highway embankment sections is presented. For this purpose, model properties are first introduced, then general results and regression analyses are presented. In addition, tables including detailed information regarding deformation calculations are presented in two appendices at the end of this report.

In the literature review section it was noted that the amount of initial settlement which is immediate response to the embankment self-weight is compensated during embankment construction. However, deformation in this research refers to the amount of immediate deformation due to external pavement and traffic loading. As mentioned in literature review section, if post-construction settlements are uniform they are considered acceptable.

It is noted that vertical and horizontal stresses increase with depth of embankment. This increase in confining stresses might affect material properties such as elasticity modulus. This fact is reviewed in model properties section and suitable models to capture change in material properties within depth are introduced.

Similar to the slope stability analysis, embankment deformation is investigated under two conditions: total stress parameters using UU triaxial tests results, and effective stress parameters using CU triaxial tests results. Separate sections in this chapter will summarize results obtained under each of these two conditions.

9.2. Model Properties

Finite element based software GeoStudio-SIGMA/W has been used to perform deformation analysis of the embankment. To input material properties, linear elastic model was selected in which stresses are related directly proportional to the strains. Elasticity modulus and unit weight are among input parameters which are coming directly from laboratory results.

For the highway embankment, two-dimensional plane strain conditions were assumed. It is noted that for a two-dimensional plane strain analysis, e_z is zero, thereby having s_z equal to $s_z = n(s_x + s_y)$. In the case of highway embankments the assumption of $e_z = 0$ seems a

reasonable selection, as the third dimension (length of embankment) is very long such that any deformation in z direction would result in zero strain.

Figure 9.1 and Figure 9.2 schematically show deformation of the embankment crest due to traffic loading. It is noted that settlement due to embankment self-weight has been zeroed out, in other words, the maximum deformation is only due to pavement and traffic loading. Also, it can be seen that there is minor heave (upward move) in the sides of embankment which is equal in both sides due to symmetry.
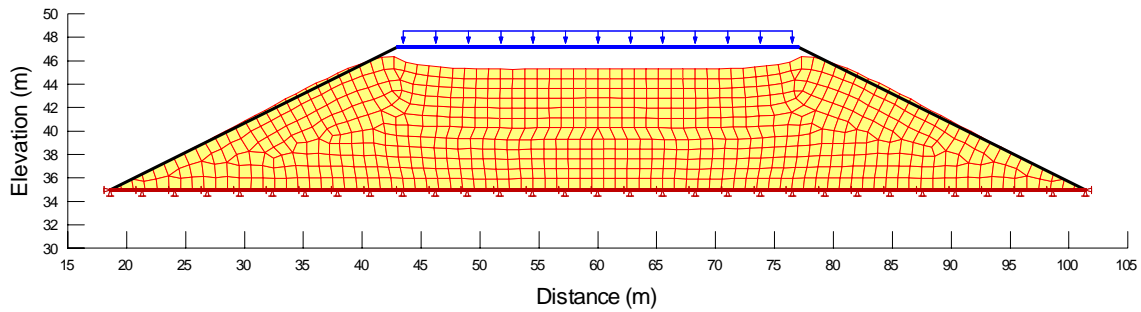
Figure 9.1. Schematic embankment deformed mesh due to traffic loading
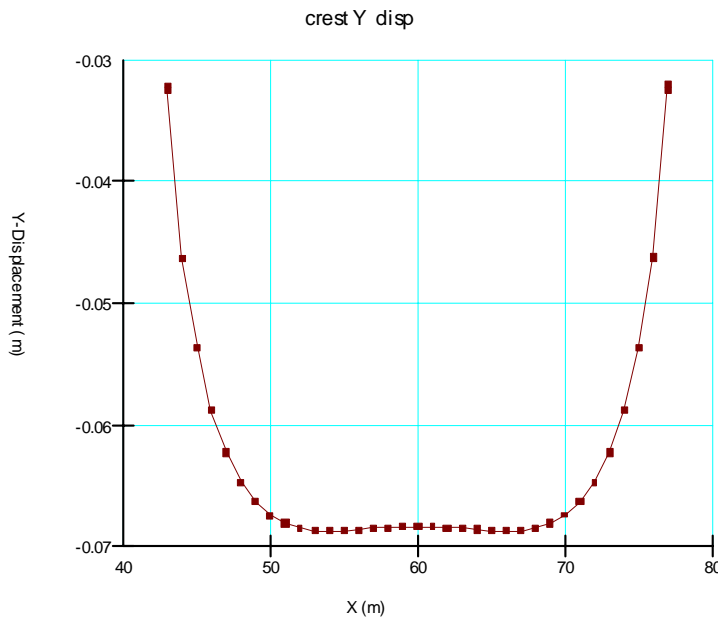
Figure 9.2. Deformation of the embankment crest due to traffic loading

However, elasticity modulus has been selected meticulously; and initial model was improved by the hypothesis of taking into account differences in elasticity modulus within embankment

depth based on average horizontal stresses. Elasticity modulus entered in the model has been synced with output values of $(s_X + s_Z)/2$ obtained from initial run of the software.

However, after rigorous investigations following decision has been made regarding embankment sections. For embankments with H=12.2 m (40 ft) and H=9.1 m (30 ft) three layers with thicknesses of 0.3H, 0.4H, and 0.3H respectively from bottom to top are considered. For embankments with H=6.1 m (20 ft) two layers each with 0.5H thickness seemed to be enough to capture variations of material properties within depth, and for embankments with H=3 m (10 ft) only one layer has been considered. Figure 9.3 shows embankment sections which are considered to capture variations of material properties for four different embankment heights.
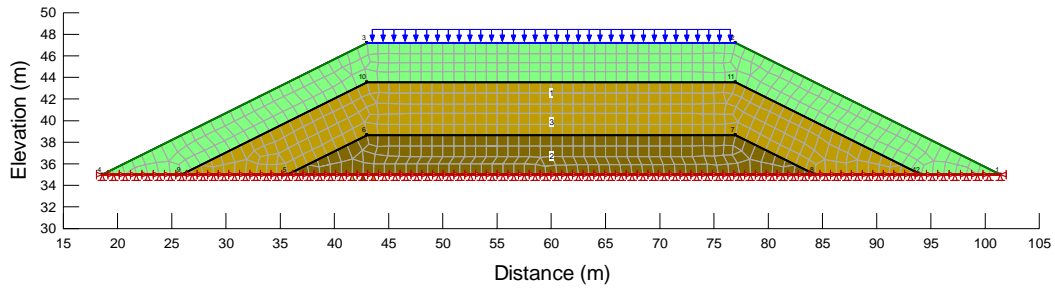
(a) side slope: 2H:1V, height= 12.2 m (40 ft)
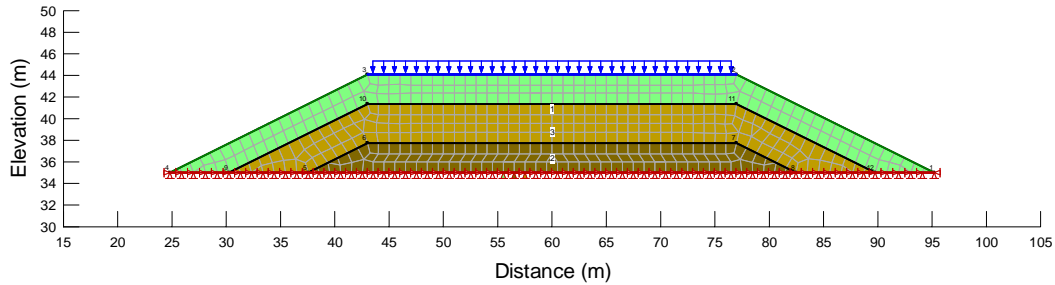
(b) side slope: 2H:1V, height= 9.1 m (30 ft)
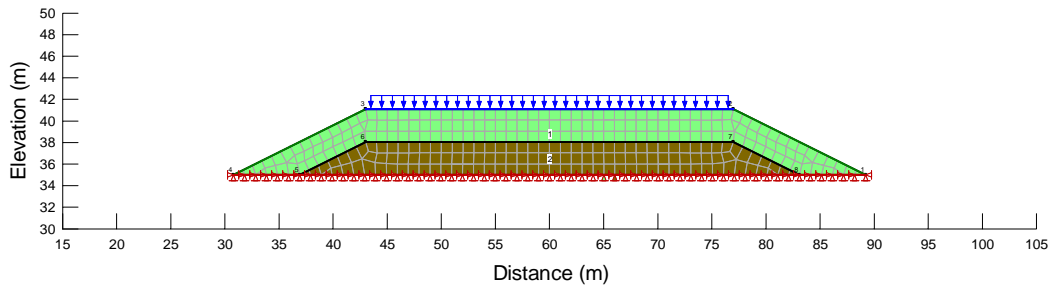
(c) side slope: 2H:1V, height= 6.1 m (20 ft)
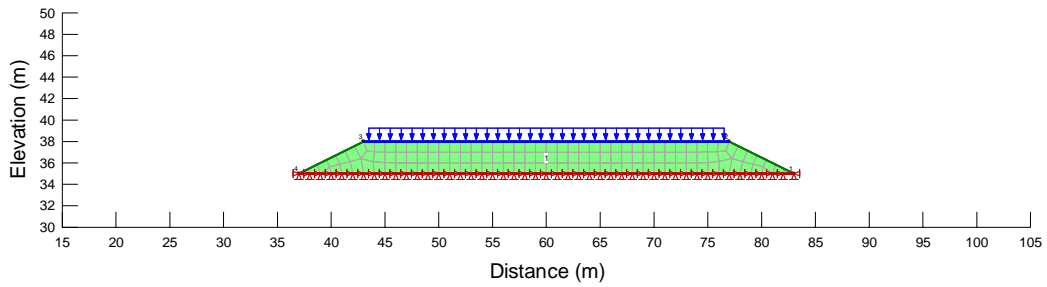
(d) side slope: 2H:1V, height= 3.0 m (10 ft)

Figure 9.3. Typical embankment modified sections for four different heights

9.3. Results and Discussion

In this section, results of deformation analysis are presented. For a clear representation, results of TSA are separated from those of related to ESA. As mentioned earlier in this chapter, for TSA parameters of UU triaxial tests are used and for ESA parameters obtained from CU triaxial tests are utilized.

9.3.1. Total Stress Deformation Analysis Using UU Triaxial Parameters

With the geometric models which take into account differences in elasticity modulus and improving elasticity modulus input based on the average of horizontal stresses obtained from model- $(s_X + s_Z)/2$, embankment crest deformation may be calculated for all soil samples and all test points, that is across moisture content-dry unit weight domain. Figure 9.4 presents results of Soil 1 Forsyth for an embankment with H=40ft and 2H:1V side slope. Red shaded area in this figure shows points that will probably result in crest deformation larger than one inch- the selected maximum allowable settlement for highway embankments. On the other hand, green shaded area shows the acceptable range. It is noted that since total stress stability was not seen to be critical, this area imposed by total stress deformation performance criterion may be accepted as final acceptance zone. As stated, this figure belongs to data for Soil 1 Forsyth applied to the embankment section with H=40ft and side slope of 2H:1V, and of course TSA.

For brevity purposes, this type of figures is not presented for all soil samples and all geometries. Later in this chapter Table 9.2 will provide descriptive information of acceptable cases based on total stress deformation analyses criterion. Also, for other test soils and embankment sections, deformation tables presented in Appendix A of this report will include detailed information.
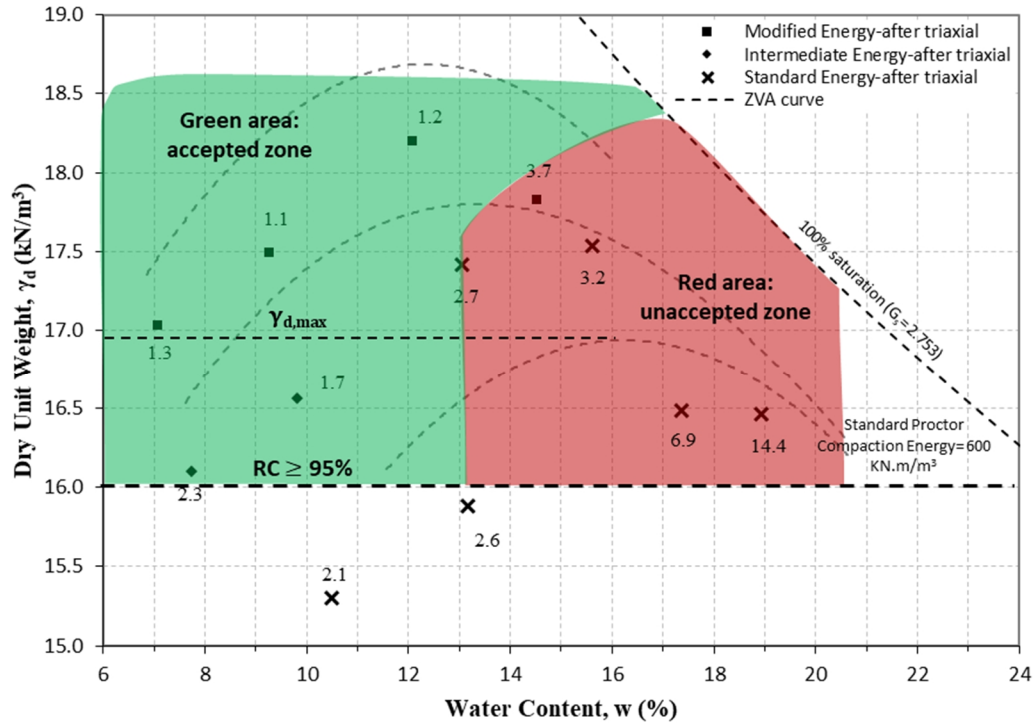
Figure 9.4. Acceptance zone and values of TSA crest deformation for embankment with H=40ft and 2H:1V side slope – Soil 1 Forsyth

Obviously, as embankment height decreases, embankment deformation decreases as well. Result of regression analysis shows that, embankment deformation generally increases with embankment height (H) and friction angle of soil (f_{UU}), and decreases with elasticity modulus of soil (E) and embankment side slope (S). Of course, the effect of side slope was observed to be very subtle, and it becomes even less discernible at lower embankment heights.

Intensive embankment deformation analysis has been carried out. Tables in Appendix A at the end of report provide details of this attempt. Table 9.1 lists number of deformation analyses which were done for each soil sample using total stress parameters, that is using UU triaxial parameters.

Table 9.1. Number of deformation analyses done for each soil sample – TSA

Soil sample	No. of analyses
Soil 1 Forsyth	192
Soil 2 Lee	224
Soil 3 Randolph	208
Soil 4 Rowan	224
Soil 5 Mecklenburg	224

Table 9.2 summarizes huge amount of numerical database and describes acceptable cases based on deformation criterion. It is noted that similar to other information provided in this section, this table reflects embankment behavior associated with total stress parameters or UU triaxial results. It is useful to repeat that in TSA conditions, stability criterion was not seen to be critical. This latter statement means, Table 9.2 may serve as the final acceptance zones/cases.

It might be necessary to remind that we are still on the map of moisture content versus dry unit weight. It was observed that as points move from wet-of-optimum to dry-of-optimum embankment deformation decreases.

Table 9.2. Description of acceptable zones/cases based on total stress deformation analyses criterion
(based on 1" limit for nonuniform immediate deformation)

Soil sample	Acceptable cases
Soil 1 Forsyth (PI=2) AASHTO class: A-4 (0)	- At Standard Proctor for H=40 ft almost all points are not acceptable. - At Standard Proctor points wet-of-optimum, for all sections are not acceptable. - At Standard Proctor points dry-of-optimum, for all sections except H=40 ft are acceptable. - Even at higher energies, points wet-of-optimum could be problematic.
Soil 2 Lee (PI=21) AASHTO class: A-7-6 (28)	- At all energy levels all points ∓ 5% of optimum are acceptable. - Optimum and dry-of-optimum points at all energy levels are acceptable. - Regardless of compactive energy and MC, for H=10 ft all points are acceptable. - Regardless of compactive energy MC more than 8% wet-of-optimum is not recommended.
Soil 3 Randolph (PI=NP) AASHTO class: A-4 (1)	- At Standard Proctor, points wet-of-optimum are not acceptable for almost all sections. - For H=40 ft, regardless of compactive energy and MC, all points are not acceptable. - For H=30 ft, points only drier than 5% of OMC at standard energy and points only drier than 2.5% of OMC at modified energy are acceptable. - For H=10 ft, regardless of compactive energy and MC, all points are acceptable - Many unacceptable cases were observed.
Soil 4 Rowan (PI=6) AASHTO class: A-5 (7)	- At Standard Proctor, wet-of-optimum points are not recommended for H=40 & 30ft; however, for H=40ft dry-of-optimum points are neither recommended. - At Intermediate Proctor and for all sections, points dry-of-optimum are acceptable; however, wet-of-optimum points for H=40 & 30ft are not acceptable. - At Modified Proctor and for all sections, regular points seem to be acceptable. - For H=10 & 20ft regardless of compactive energy and MC all points seem acceptable.
Soil 5 Mecklenburg (PI=5) AASHTO class: A-5 (5)	- At Standard Proctor and for all sections, points dry-of-optimum are acceptable; however, as they get closer to OMC they become unacceptable for H=40ft. Wet-of-optimum points are not accepted for H=40 & 30ft. - At Intermediate Proctor and for all sections, points dry-of-optimum are acceptable; however, for H=40ft points close to optimum are not accepted, neither are points wet-of-optimum for H=40 & 30ft.

However, equations in the following form could be developed which are specific to each soil. Similar to the slope stability analysis chapter, two different sets of equations are separately presented: first set are in the form of dimensioned equations, and second set are in the form of dimensionless equations for ease of use of engineers.

Also, in these equations D is the maximum crest deformation of embankment due to the traffic and pavement loads, which were taken equivalent to the uniformly distributed load of 35kPa. At the end of each section, equations representing all soil samples are also presented.

Dimensioned equations for total stress deformation analysis

$$D = 230.6818 \frac{g_m^{0.0995} * H^{1.0705} * f_{UU}^{0.6643}}{E_{UU}^{1.0340} * S^{0.0185}}$$

(9-1)

Soil 1 Forsyth, TSA

$$D = 374.92 \frac{H^{1.0594} * f_{UU}^{0.5617}}{g_m^{0.0321} * E_{UU}^{1.0034} * S^{0.0280}}$$

(9-2)

Soil 2 Lee, TSA

$$D = 946.893 \frac{g_m^{0.1548} * H^{1.0279} *}{f_{UU}^{0.0068} * E_{UU}^{0.9379} * S^{0.0022}}$$

(9-3)

Soil 3 Randolph, TSA

$$D = 981.1406 \frac{H^{1.0752} * f_{UU}^{0.5354}}{g_m^{0.3008} * E_{UU}^{1.0204} * S^{0.0124}}$$

(9-4)

Soil 4 Rowan, TSA

$$D = 223.4016 \frac{g_m^{0.1405} * H^{1.0367} * f_{UU}^{0.5887}}{E_{UU}^{1.0078} * S^{0.0109}}$$

(9-5)

Soil 5 Mecklenburg, TSA

$$D = 977.0457 \frac{H^{1.0487} * f_{UU}^{0.4247}}{g_m^{0.2405} * E_{UU}^{0.9894} * S^{0.0148}}$$

(9-6)

all soil samples, TSA

where D is the maximum crest deformation of embankment in centimeters, g_m is material total unit weight (kN/m^3), H is the embankment height in meters, f_{UU} is total friction angle in degrees, E_{UU} is elasticity modulus in kPa, and S is embankment side slope. Coefficients of determination of the above equations are as follows respectively: 0.9999, 0.9998, 0.9986, 0.9998, 0.9998, 0.9956.

Cohesion term was not directly an input in the deformation calculation process; however, further investigation showed that including cohesion term in the regression analysis would result in some unpleasant equations with lower coefficient of determination and nasty p-values.

Dimensionless equations for total stress deformation analysis

In dimensionless equations, instead of friction angle tangent of friction angle is used and dimensionless elasticity modulus (E_D) has taken the place of elasticity modulus. Dimensionless elasticity modulus term is defined similar to the dimensionless cohesion and is as follows.

$$E_D = \frac{E}{g_m * H} \tag{9-7}$$

where E is the elasticity modulus of soil, g_m is total unit weight of soil, and H is the embankment height. Dimensionless regression equations are presented as follows.

$$D = 191.1227 \frac{Tan^{0.5181}(f_{UU})}{E_{D,UU}^{1.0283} * S^{0.0187}} \tag{9-8}$$

Soil 1 Forsyth, TSA, dimensionless equation

$$D = 193.0086 \frac{Tan^{0.4997}(f_{UU})}{E_{D,UU}^{1.0347} * S^{0.0280}} \tag{9-9}$$

Soil 2 Lee, TSA, dimensionless equation

$$D = 125.2114 \frac{1}{Tan^{0.0053}(f_{UU}) * E_{D,UU}^{0.9674} * S^{0.0020}} \tag{9-10}$$

Soil 3 Randolph, TSA, dimensionless equation

$$D = 264.0147 \frac{Tan^{0.5460}(f_{UU})}{E_{D,UU}^{1.0793} * S^{0.0117}} \tag{9-11}$$

Soil 4 Rowan, TSA, dimensionless equation

$$D = 160.2522 \frac{Tan^{0.4482}(f_{UU})}{E_{D,UU}^{0.9826} * S^{0.0111}} \tag{9-12}$$

Soil 5 Mecklenburg, TSA, dimensionless equation

$$D = 145.2893 \frac{Tan^{0.2883}(f_{UU})}{E_{D,UU}^{0.9802} * S^{0.0155}}$$

(9-13)

all soil samples, TSA, dimensionless equation

where D is the maximum crest deformation of embankment in centimeters, and other parameters are defined as before. Coefficients of determination of the above equations are as following respectively: 0.9990, 0.9993, 0.9976, 0.9974, 0.9977, 0.9860.

9.3.2.   Effective Stress Deformation Analysis Using CU Triaxial Parameters

Embankment deformation analysis has been carried out with effective stress parameters as well. Tables in Appendix B will provide detailed information of this task. Calculations of the embankment deformation using CU triaxial parameters revealed that, for all test soils (Soil 1 Forsyth through Soil 5 Mecklenburg) and for all embankment sections, deformation is larger than limiting value, except for few cases of Soil 2 Lee where dry unit weight of the soil sample (before shear stage) is high enough. Laboratory results showed that this situation could happen only with the samples initially compacted at compactive energies close to or higher than Modified Proctor. It is noted that for these acceptable cases, FS (associated with ESA) is also higher than the minimum and in the acceptable range. Authors also want to remind that Soil 2 Lee is the soil sample with highest value of plasticity index (PI=21) among the test soils, with A-7-6 (28) as AASHTO classification. This might give grounds to the idea that soils with higher PI perform slightly better under rain-induced inundation conditions. This also may cast doubt on the NCDOT material selection specification of limiting PI to 15% in the North Carolina coastal area.

Moreover, it is noted that since saturated samples in CU triaxial tests provide lower strength parameters than unsaturated samples in UU triaxial tests, deformation incorporated with them is generally higher.

In this type of analysis which incorporates using CU triaxial parameters, since number of analyses for each individual soil were not considerable, regression equations belonging to only all soil samples are presented. Moreover, as in some cases reported value for cohesion (from CU triaxial test) equals zero, it is wise to exclude cohesion parameter from regression process. These equations are presented as Equation (9-14) and Equation (9-15).

$$D = 501.1948 \frac{g_m^{\ 0.2628} * f'^{0.3643} * H^{1.1491}}{E_{CU}^{1.0767} * S^{0.0125}}, \quad R^2 = 0.9993$$

(9-14)

all soil samples, ESA

$$D = 250.5151 \frac{Tan^{1.6628}(f')}{E_{D,CU}^{\ 1.1476} * S^{0.0112}}, \quad R^2 = 0.9980$$

(9-15)

all soil samples, ESA, dimenssionless equation

where f' is effective friction angle and all remaining parameters follow earlier definitions. Coefficients of determination of the above equations are as following respectively: 0.9993, 0.9980.

10. SUMMARY OF FINDINGS AND CONCLUSIONS

Performance of highway embankments was investigated based on two concerns; slope stability and deformation. Each of these concerns was looked at from two perspectives, TSA parameters and ESA parameters. To find total stress soil strength properties a set of unconsolidated-undrained (UU) triaxial tests was designed, and to find out effective stress soil strength properties a set of consolidated-undrained (CU) triaxial tests with pore pressure measurements was considered. Table 10.1 schematically summarizes research workload which has been accomplished for this project. Most important findings and conclusions of this research project are listed in this chapter.

Table 10.1. Research workload performed for NCDOT RP 2015-05

Task #	Test / Task description	Number Done
1	sieve analysis	5
	hydrometer	5
	Atterberg limit, PL	6
	Atterberg limit, LL	6
	specific gravity, Gs	7
2	compaction	121
3	UU triaxial	214
4	CU triaxial	41
5	slope stability analysis	1072 (short-term) + 208 (long-term)
6	deformation analysis	1072 (short-term) + 208 (long-term)
7	regression analysis	done
8	literature review	done

Findings and conclusions drawn from total stress slope stability analyses are as following:

- Among all of the 1072 cases not even one case showed TSA factor of safety lower than the minimum value of 1.3. In many of these cases FS is well above the minimum value.

- In all 1072 cases that were run for five soil samples with total stress strength parameters, in only one case the infinite slope (shallow) failure was yielding a FS lower than that of from non-shallow failure. Of course, even in this case both type of factor of safeties were higher than the minimum. This indicates that, "for the total stress analysis, shallow failure is never dominant".

- This latter indicates that embankments made from these soil samples are stable right after compaction operation, even if the minimum compactive energy level, that is Standard Proctor is used.

Findings and conclusions drawn from total stress deformation analyses are as following:

- Since total stress slope stability was not seen to be critical, acceptance zone imposed by total stress deformation performance criterion may be regarded as final total stress acceptance zone.

- A table (Table 9.2) is presented which provides descriptive information of acceptable cases based on total stress deformation criterion.

- Result of regression analysis shows that, embankment deformation generally increases with embankment height (H) and friction angle of soil (f_{UU}), and decreases with elasticity modulus of soil (E) and embankment side slope (S). Of course, the effect of side slope was observed to be very subtle, and it becomes even less discernible at lower embankment heights.

Conclusions and important findings of the effective stress slope stability analyses could be expressed as following:

- Results of the effective stress slope stability analysis were completely different from those of obtained from total stress slope stability analysis, as in the effective stress stability analysis many cases were found having FS lower than 1.3.

- Strength parameters from CU triaxial tests may be mainly characterized by lower cohesion term compared with those of from UU triaxial tests. As cohesion decreases, mode of failure moves from a deep slip surface encompassing all the slope to a shallow, small and local one. In other words, in the effective stress analysis many cases were seen where shallow failure was the dominant mode of failure.

- This finding leads us to the following statement: "for the effective stress slope stability analysis, shallow failure must be checked as it is a case with high possibility".

- Unlike analyses using total stress parameters, under the effective stress conditions dominant modes of failure were different which consisted of non-shallow, partial, and shallow.

- For the effective stress stability analysis, height of embankment does not play a considerable role in the value of FS.

- A descriptive table (Table 8.2) is presented which may be used as means of acceptance zone/cases based on effective stress slope stability criterion.

And conclusions drawn from the effective stress deformation analyses are as following:

- Calculations of the embankment deformation using CU triaxial parameters revealed that for all test soils (Soil 1 Forsyth through Soil 5 Mecklenburg) and for all embankment sections, deformation was larger than limiting value, except for few cases of Soil 2 Lee (with PI=21 and highest among tested soils) where dry unit weight of the soil sample (before shear stage) was high enough. Laboratory results showed that this situation could happen only with the samples initially compacted at compactive energies close to or higher that Modified Proctor. It is noted that for these acceptable cases, FS (associated with ESA) was also higher than minimum and in the acceptable range.

- This latter finding might give grounds to the idea that soils with higher PI such as Soil 2 Lee perform slightly better under rain-induced inundation conditions. This is in opposition to the criterion of limiting material PI as material selection criteria which is currently used by the NC state standard. Of course, it is noted that Soil 2 Lee has PI=21 which still holds it in the acceptable range of PI ≤ 25 for piedmont area of NC. However, this may cast doubt on the NCDOT material selection specification of limiting PI to 15% in the coastal area. More understanding on this fact needs further research.

- Since saturated samples in CU triaxial tests provide lower strength parameters than unsaturated samples in UU triaxial tests, deformation incorporated with them is generally higher.

General conclusions

- Slope stability failures of the embankment materials (without foundation) is not a high risk design consideration. As among all of the 1072 cases not even one case showed TSA factor of safety lower than the minimum value of 1.3.

- Reported slope stability failures are typically associated with high intensity/duration rainfall events. Results of ESA may explain reported shallow rain-induced failures.

- Under rain-induced conditions, many failures in the form of shallow failure may happen.

- Research project results show that nonuniform deformation service state controls the design, rather than slope stability service sate.

- Providing suitable vegetation cover (to reduce infiltration and promote runoff) as well as drainage measures for the highway embankments could be very helpful to avoid detrimental effects of presence of water in the body of embankment.

- Acceptance zone based on RC $\geq$ 95% with g_{dmax} obtained using Standard Proctor, for the most part satisfies slope stability and deformation performance service states for the geometries of embankments analyzed. However, in segments where embankment is subject to nonuniform settlements, utilizing higher compactive energies may be helpful. Moreover, specifying a range for the placement moisture content may be a possible modification to help keep immediate nonuniform deformations below allowable value (25 mm).

- Among test soils, there are two A-4 soils (one silty sand and one low plasticity silt), two A-5 soils (both low plasticity silt), and one A-7-6 soil (high plasticity silt). Of course according to AASHTO classification all test soils are still rated as "fair to poor" as a subgrade. However, contrary to the traditional trend to avoid using A-7 soil classes (such as South Carolina DOT), results of the current research showed that the A-7 soil sample is performing slightly better than A-4 and A-5 classes.

- Soil 2 Lee with AASHTO class A-7-6 and PI=21 had best performance under rain induced conditions.

- Despite the subtle trend of limiting embankment material PI among the agencies and guidelines, it seems having small amounts of PI will enhance performance of material. This was observed for the silty material; however, authors believe that same outcome might come true regarding granular material.

- Findings of this research may cast doubt on the NCDOT material selection specification of limiting PI to 15% in the North Carolina coastal area.

- Great lessons might be learnt by comparing Soil 1 Forsyth (PI=2) with AASHTO class A-4 as a silty sand (SM), with Soil 3 Randolph (PI=NP) with AASHTO class A-4 as a low plasticity silt. Although AASHTO classes are same, it was observed that the silty sand with PI as little as 2% performed better than the nonplastic silt.

- Analysis process which was performed for this project might be divide into four main categories: TSA FS, TSA deformation, ESA FS, and ESA deformation. Out of these, TSA FS showed very high values, and ESA deformation revealed very weak results, which allows us to ignore these two categories. Table 10.2 provides ranking index for the project test soils. This table is designed based on percentage of failures in the two categories of ESA FS, and TSA deformation. It can be seen that Soil 2 Lee a A-7-6 AASHTO class has the highest rank. Of course, the table has only comparative values and is not designed to provide absolute rating for test soils.

Table 10.2. Test soils ranking index

Test soil sample	Classification		Soil sample rank		
	USCS	AASHTO	ESA FS	TSA deformation	Total rank
Soil 1 Forsyth	SM	A-4 (0)	2	3	2
Soil 2 Lee	MH	A-7-6 (28)	1	1	1
Soil 3 Randolph	ML	A-4 (1)	4	5	5
Soil 4 Rowan	ML	A-5 (7)	3	3	3
Soil 5 Mecklenburg	ML	A-5 (5)	5	2	4

- Results of this study show that side slope 1H:1V must be avoided for highway embankments, and for some weaker soils side slope 2H:1V is neither recommended.

- Moreover, placing moisture content more than 8% wet-of-optimum must be avoided. Also, moisture contents more than 5% wet-of-optimum are not recommended. Regarding placing moisture content, descriptive table provides useful information.

- Creep deformations of compacted soils may be a controlling design factor for high embankments. Specifications limiting PI of material could prove beneficial to decrease likelihood of creep.

REFERENCES

Appalachian Landslide Consultants (2013), "Geological/geotechnical report for Jackson County Planning Department," *Appalachian Landslide Consultants, PLLC.*

ASSHTO (2002), "Standard Specifications for Highway Bridges," *American Association of State Highway and Transportation Officials*, Washington, DC.

AASHTO (2012), "Standard Specification for Materials for Embankments and Subgrades," AASHTO Designation: M 57-80.

AASHTO (2015a), "Standard Method of Test for Moisture-Density Relations of Soils Using a 2.5-kg (5.5-lb) Rammer and a 305-mm (12-in.) Drop," AASHTO T 99.

AASHTO (2015b), "Standard Method of Test for Moisture-Density Relations of Soils Using a 4.54-kg (10-lb) Rammer and a 457-mm (18-in.) Drop," AASHTO T 180.

ASTM (2003), "Unconsolidated-Undrained Triaxial Compression Test on Cohesive Soils," D2850.

ASTM (2007), "Particle-Size Analysis of Soils," D422.

ASTM (2010), "Liquid Limit, Plastic Limit, and Plasticity Index of Soils," D4318.

ASTM (2011), "Consolidated Undrained Triaxial Compression Test for Cohesive Soils," D4767.

ASTM (2012a), "Laboratory Compaction Characteristics of Soil Using Modified Effort," D1557.

ASTM (2012b), "Laboratory Compaction Characteristics of Soil Using Standard Effort," D698.

ASTM (2014), "Specific Gravity of Soil Solids by Water Pycnometer," D854.

Aydilek, A. H., and Ramanathan, R. S. (2013), "Slope failure investigation management system," *Maryland Department of Transportation*, Rep. No.: MD-13-SP009B4N.

Briaud, J. L. (2013), "Geotechnical engineering: unsaturated and saturated soils", *John Wiley & Sons*.

Chen, Y. (2010), "An experimental investigation of the behavior of compacted clay/sand mixtures," M.Sc. Thesis, Adviser: Meehan C. L., University of Delaware.

Das, B. M. (2008), "Advanced Soil Mechanics", Third ed., *Taylor & Francis*.

Duncan, J. M., Byrne, P., Wong, K. S., and Mabry, P. (1980), "Strength, stress-strain, and bulk modulus parameters for finite element analyses of stresses and movements in soil masses," *University of California Berkeley*, Rep. No.: UCB/GT/80-01.

Duncan, J. M., Wright, S. G., and Brandon, T. L. (2014), "Soil strength and slope stability", *John Wiley & Sons*.

FHWA (2006), "Geotechnical Aspects of Pavements", *National Highway Institute*, USDOT, Washington, D.C., Rep. No.: FHWA NHI-05-037.

Hassani, M., Pando, M. A., and Janardhanam, R. (2017), "State of Practice of Highway Embankment Construction in the U.S. - A Literature Review of FHWA and USDOTs Requirements for Embankment Material Selection and Embankment Construction," *UNC Charlotte*, Rep. No.: UNCC-NCDOT RP 2015-05.

Khan, M. S., Hossain, S., and Kibria, G. (2015), "Slope Stabilization Using Recycled Plastic Pins," *Performance of Constructed Facilities, ASCE,* 30 (3), 04015054-(1-10).

Ladd, C. C., and Foott, R. (1977), "Foundation design of embankments constructed on varved clays," *U. S. Department of Transportation*, Rep. No.: FHWA TS-77-214.

Loehr, J. E., Fennessey, T. W., and Bowders, J. J. (2007), "Stabilization of Surficial Slides Using Recycled Plastic Reinforcement," *Transportation Research Record: Journal of the Transportation Research Board,* 1989 (2), 79-87.

Long, J., Olson, S., Stark, T., and Samara, E. (1998), "Differential movement at embankment-bridge structure interface in Illinois," *Transportation Research Record: Journal of the Transportation Research Board,* 1633 53-60.

NAVFAC (1986a), "Foundations and Earth Structures-Design Manual 7.02," *Naval Facilities Engineering Command*.

NCHRP (1971), "NCHRP Synthesis of Highway Practice 8: Construction of Embankments," *Transportation Research Board*, Washington D.C., Rep. No.: Synthesis 8.

NCHRP (1975), "NCHRP Synthesis of Highway Practice 29: Treatment of Soft Foundations for Highway Embankments," *Transportation Research Board, Washington, D.C.*

NCHRP (1983), "Shallow Foundations for Highway Structures," *NCHRP*, Rep. No.: 107.

NCHRP (1989), "NCHRP Synthesis of Highway Practice 147: Treatment of problem foundations for highway embankments," *Transportation Research Board, Washington, D.C.*

NCHRP (1990), "NCHRP Synthesis of Highway Practice 159: Design and Construction of Bridge Approaches," *Transportation Research Board, Washington, D.C.*

NCHRP (2004), "NCHRP Report 529: Guideline and Recommended Standard for Geofoam Applications in Highway Embankments," *Transportation Research Board, Washington, D.C.*

North Carolina DOT (2012), "Pavement Condition Survey Manual," *North Carolina Department of Transportation*.

North Carolina Geological Survey (2006), "August 31, 2006 Embankment Failure - Debris Flow at the Cascades Development Haywood County, North Carolina," *North Carolina Geological Survey*.

Parra, J. R., Loehr, J. E., Hagemeyer, D. J., and Bowders, J. J. (2003), "Field Performance of Embankments Stabilized with Recycled Plastic Reinforcement," *Transportation Research Record: Journal of the Transportation Research Board,* 1849 (1), 31-38.

Samtani, N. C., and Nowatzki, E. A. (2006b), "Soils and Foundations-Reference Manual, Volume II," *Federal Highway Administration*, Rep. No.: FHWA-NHI–06-089.

Soriano, A. (2013), "Embankments and dams, slope stability and landslides: General report", *Proc. of 15th European Conference on Soil Mechanics and Geotechnical Engineering*, Athens, Greece, pp. 171-196.

Stark, T., Arellano, D., Horvath, J., and Leshchinsky, D. (2004), "Geofoam Applications in the Design and Construction of Highway Embankments," *NCHRP*.

Stark, T. D., Olson, S. M., and Long, J. H. (1995), "Differential movement at the embankment/structure interface-mitigation and rehabilitation," *Illinois DOT*, Springfield, Illinois, Rep. No.: LAB-H1 FY93.

Tabrizi, A. A., LaRocque, L. A., Chaudhry, M. H., Viparelli, E., and Imran, J. (2017), "Embankment Failures during the Historic October 2015 Flood in South Carolina: Case Study," *ASCE: Journal of Hydraulic Engineering,* 143 (8), 05017001.

Virginia DOT (2014), "Virginia Manual of Instructions-Chapter 3: Geotechnical Engineering," *Virginia Department of Transportation*.

Wiebe, B., Graham, J., Tang, G. X., and Dixon, D. (1998), "Influence of pressure, saturation, and temperature on the behaviour of unsaturated sand-bentonite," *Canadian Geotechnical Journal,* 35 (2), 194-205.

Wright, S. G. (2005), "Evaluation of soil shear strengths for slope and retaining wall stability analyses with emphasis on high plasticity clays," *Federal Highway Administration*, Rep. No.: FHWA/TX-06/5-1874-01-1.

Zaman, M., Laguros, J., and Jha, R. (1994), "Statistical models for identification of problematic bridge sites and estimation of approach settlements," *Oklahoma Department of Transportation*.

Appendix A - Deformation Tables for Total Stress Analysis (UU Triaxial Parameters)

In this appendix, total stress deformation study of embankments having different sections and constructed with project test soils is presented in the form of tables.

Appendix A1 - Deformation Tables for Soil 1 Forsyth – Total Stress Analysis (UU Triaxial Parameters)

Table A.1. Embankment crest deformation for Soil 1 Forsyth - TSA

Tests ID	W (%)	$g_d (kN/m^3)$	$g_m (kN/m^3)$	S (%)	f_{UU} (deg)	C_{UU} (kPa)	n	E_{50} (MPa)	H (m)	slope	crest deformation (cm)
S1-UU1 S1-UU2 S1-UU3	17.4	16.5	19.4	82.3	23	75	0.3786	2.916 3.816 3.960	12.2	1H:1V	7.11
										2H:1V	6.90
										3H:1V	6.76
										4H:1V	6.78
									9.1	1H:1V	5.35
										2H:1V	5.27
										3H:1V	5.16
										4H:1V	5.15
									6.1	1H:1V	3.66
										2H:1V	3.59
										3H:1V	3.58
										4H:1V	3.56
									3.0	1H:1V	1.89
										2H:1V	1.86
										3H:1V	1.86
										4H:1V	1.86

Table A.1. Embankment crest deformation for Soil 1 Forsyth - TSA (continued)

Tests ID	W (%)	$g_d(kN/m^3)$	$g_m(kN/m^3)$	S (%)	f_{UU} (deg)	C_{UU} (kPa)	n	E_{50} (MPa)	H (m)	slope	crest deformation (cm)
S1-UU4 S1-UU5 S1-UU6	15.6	17.5	20.3	79.7	34	73	0.3056	8.934 9.267 12.348	12.2	1H:1V	3.22
										2H:1V	3.17
										3H:1V	3.15
										4H:1V	3.15
									9.1	1H:1V	2.44
										2H:1V	2.43
										3H:1V	2.42
										4H:1V	2.42
									6.1	1H:1V	1.73
										2H:1V	1.71
										3H:1V	1.71
										4H:1V	1.70
									3.0	1H:1V	0.91
										2H:1V	0.91
										3H:1V	0.90
										4H:1V	0.91

Table A.1. Embankment crest deformation for Soil 1 Forsyth - TSA (continued)

Tests ID	W (%)	$g_d (kN/m^3)$	$g_m (kN/m^3)$	S (%)	f_{UU} (deg)	C_{UU} (kPa)	n	E_{50} (MPa)	H (m)	slope	crest deformation (cm)
S1-UU7 S1-UU8 S1-UU9	13.0	17.4	19.7	65.3	39	69	0.2679	9.290 13.847 17.838	12.2	1H:1V	2.83
										2H:1V	2.70
										3H:1V	2.73
										4H:1V	2.76
									9.1	1H:1V	2.28
										2H:1V	2.28
										3H:1V	2.28
										4H:1V	2.28
									6.1	1H:1V	1.62
										2H:1V	1.62
										3H:1V	1.62
										4H:1V	1.62
									3.0	1H:1V	0.94
										2H:1V	0.94
										3H:1V	0.93
										4H:1V	0.94

Table A.1. Embankment crest deformation for Soil 1 Forsyth - TSA (continued)

Tests ID	W (%)	$g_d (kN / m^3)$	$g_m (kN / m^3)$	S (%)	f_{UU} (deg)	C_{UU} (kPa)	n	E_{50} (MPa)	H (m)	slope	crest deformation (cm)
S1-UU10 S1-UU11 S1-UU12	18.9	16.5	19.6	81.4	27	35	0.3532	1.142 2.139 2.240	12.2	1H:1V	15.22
										2H:1V	14.62
										3H:1V	14.23
										4H:1V	14.24
									9.1	1H:1V	11.91
										2H:1V	11.77
										3H:1V	11.64
										4H:1V	11.53
									6.1	1H:1V	8.43
										2H:1V	8.29
										3H:1V	8.27
										4H:1V	8.26
									3.0	1H:1V	4.76
										2H:1V	4.73
										3H:1V	4.72
										4H:1V	4.73

Table A.1. Embankment crest deformation for Soil 1 Forsyth - TSA (continued)

Tests ID	W (%)	$g_d (kN/m^3)$	$g_m (kN/m^3)$	S (%)	f_{UU} (deg)	C_{UU} (kPa)	n	E_{50} (MPa)	H (m)	slope	crest deformation (cm)
S1-UU13 S1-UU14 S1-UU15	13.2	15.9	18.0	51.6	33	53	0.3141	11.766 12.008 12.288	12.2	1H:1V	2.66
										2H:1V	2.60
										3H:1V	2.64
										4H:1V	2.64
									9.1	1H:1V	1.98
										2H:1V	1.97
										3H:1V	1.96
										4H:1V	1.96
									6.1	1H:1V	1.33
										2H:1V	1.32
										3H:1V	1.32
										4H:1V	1.32
									3.0	1H:1V	0.66
										2H:1V	0.66
										3H:1V	0.65
										4H:1V	0.66

Table A.1. Embankment crest deformation for Soil 1 Forsyth - TSA (continued)

Tests ID	W (%)	$g_d (kN/m^3)$	$g_m (kN/m^3)$	S (%)	f_{UU} (deg)	C_{UU} (kPa)	n	E_{50} (MPa)	H (m)	slope	crest deformation (cm)
S1-UU16 S1-UU17 S1-UU18	10.5	15.3	16.9	37.9	35	47	0.3022	14.539 15.559 16.231	12.2	1H:1V	2.14
										2H:1V	2.10
										3H:1V	2.13
										4H:1V	2.13
									9.1	1H:1V	1.61
										2H:1V	1.60
										3H:1V	1.60
										4H:1V	1.60
									6.1	1H:1V	1.09
										2H:1V	1.09
										3H:1V	1.09
										4H:1V	1.09
									3.0	1H:1V	0.55
										2H:1V	0.55
										3H:1V	0.55
										4H:1V	0.55

Table A.1. Embankment crest deformation for Soil 1 Forsyth - TSA (continued)

Tests ID	W (%)	$g_d (kN/m^3)$	$g_m (kN/m^3)$	S (%)	f_{UU} (deg)	C_{UU} (kPa)	n	E_{50} (MPa)	H (m)	slope	crest deformation (cm)
S1-UU19 S1-UU20 S1-UU21	9.8	16.6	18.2	42.6	34	89	0.3059	17.034 19.776 21.565	12.2	1H:1V	1.69
										2H:1V	1.70
										3H:1V	1.66
										4H:1V	1.66
									9.1	1H:1V	1.29
										2H:1V	1.29
										3H:1V	1.28
										4H:1V	1.28
									6.1	1H:1V	0.89
										2H:1V	0.89
										3H:1V	0.89
										4H:1V	0.89
									3.0	1H:1V	0.46
										2H:1V	0.46
										3H:1V	0.46
										4H:1V	0.46

Table A.1. Embankment crest deformation for Soil 1 Forsyth - TSA (continued)

Tests ID	W (%)	$g_d (kN/m^3)$	$g_m (kN/m^3)$	S (%)	f_{UU} (deg)	C_{UU} (kPa)	n	E_{50} (MPa)	H (m)	slope	crest deformation (cm)
S1-UU22 S1-UU23 S1-UU24	7.7	16.1	17.3	31.4	45	48	0.2265	14.296 19.440 22.473	12.2	1H:1V	2.33
										2H:1V	2.30
										3H:1V	2.32
										4H:1V	2.32
									9.1	1H:1V	1.83
										2H:1V	1.83
										3H:1V	1.83
										4H:1V	1.83
									6.1	1H:1V	1.32
										2H:1V	1.32
										3H:1V	1.32
										4H:1V	1.32
									3.0	1H:1V	0.72
										2H:1V	0.72
										3H:1V	0.72
										4H:1V	0.72

Table A.1. Embankment crest deformation for Soil 1 Forsyth - TSA (continued)

Tests ID	W (%)	$g_d (kN/m^3)$	$g_m (kN/m^3)$	S (%)	f_{UU} (deg)	C_{UU} (kPa)	n	E_{50} (MPa)	H (m)	slope	crest deformation (cm)
S1-UU25 S1-UU26 S1-UU27	9.3	17.5	19.1	47.0	42	152	0.2486	27.529 32.222 37.121	12.2	1H:1V	1.17
										2H:1V	1.10
										3H:1V	1.16
										4H:1V	1.17
									9.1	1H:1V	0.91
										2H:1V	0.91
										3H:1V	0.91
										4H:1V	0.91
									6.1	1H:1V	0.64
										2H:1V	0.64
										3H:1V	0.64
										4H:1V	0.64
									3.0	1H:1V	0.34
										2H:1V	0.34
										3H:1V	0.34
										4H:1V	0.34

Table A.1. Embankment crest deformation for Soil 1 Forsyth - TSA (continued)

Tests ID	W (%)	$g_d(kN/m^3)$	$g_m(kN/m^3)$	S (%)	f_{UU} (deg)	C_{UU} (kPa)	n	E_{50}(MPa)	H (m)	slope	crest deformation (cm)
S1-UU28 S1-UU29 S1-UU30	7.1	17.0	18.2	33.2	44	118	0.2339	26.436 27.388 36.450	12.2	1H:1V	1.33
										2H:1V	1.30
										3H:1V	1.33
										4H:1V	1.33
									9.1	1H:1V	1.02
										2H:1V	1.02
										3H:1V	1.02
										4H:1V	1.02
									6.1	1H:1V	0.72
										2H:1V	0.72
										3H:1V	0.72
										4H:1V	0.72
									3.0	1H:1V	0.39
										2H:1V	0.39
										3H:1V	0.39
										4H:1V	0.39

Table A.1. Embankment crest deformation for Soil 1 Forsyth - TSA (continued)

Tests ID	W (%)	$g_d (kN/m^3)$	$g_m (kN/m^3)$	S (%)	f_{UU} (deg)	C_{UU} (kPa)	n	E_{50} (MPa)	H (m)	slope	crest deformation (cm)
S1-UU31 S1-UU32 S1-UU33	12.1	18.2	20.4	68.7	34	163	0.3059	22.110 27.449 32.073	12.2	1H:1V	1.19
										2H:1V	1.17
										3H:1V	1.17
										4H:1V	1.17
									9.1	1H:1V	0.91
										2H:1V	0.91
										3H:1V	0.91
										4H:1V	0.91
									6.1	1H:1V	0.64
										2H:1V	0.64
										3H:1V	0.64
										4H:1V	0.64
									3.0	1H:1V	0.34
										2H:1V	0.34
										3H:1V	0.34
										4H:1V	0.34

Table A.1. Embankment crest deformation for Soil 1 Forsyth - TSA (continued)

Tests ID	W (%)	$g_d (kN/m^3)$	$g_m (kN/m^3)$	S (%)	f_{UU} (deg)	C_{UU} (kPa)	n	E_{50} (MPa)	H (m)	slope	crest deformation (cm)
S1-UU34 S1-UU35 S1-UU36	14.5	17.8	20.4	77.7	42	54	0.2486	7.549 9.513 16.503	12.2	1H:1V	3.73
										2H:1V	3.69
										3H:1V	3.69
										4H:1V	3.69
									9.1	1H:1V	3.12
										2H:1V	3.12
										3H:1V	3.12
										4H:1V	3.12
									6.1	1H:1V	2.36
										2H:1V	2.36
										3H:1V	2.36
										4H:1V	2.34
									3.0	1H:1V	1.41
										2H:1V	1.41
										3H:1V	1.41
										4H:1V	1.41

Appendix A2 - Deformation Tables for Soil 2 Lee – Total Stress Analysis (UU Triaxial Parameters)

Table A.2. Embankment crest deformation for Soil 2 Lee - TSA

Tests ID	W (%)	$g_d (kN/m^3)$	$g_m (kN/m^3)$	S (%)	f_{UU} (deg)	C_{UU} (kPa)	n	E_{50} (MPa)	H (m)	slope	crest deformation (cm)
S2-UU10 S2-UU11 S2-UU12	30.2	14.5	18.9	95.7	18	62	0.4086	2.010 2.868 2.979	12.2	1H:1V	8.33
										2H:1V	7.92
										3H:1V	7.78
										4H:1V	7.74
									9.1	1H:1V	6.20
										2H:1V	6.04
										3H:1V	5.95
										4H:1V	5.92
									6.1	1H:1V	4.29
										2H:1V	4.15
										3H:1V	4.12
										4H:1V	4.06
									3.0	1H:1V	2.21
										2H:1V	2.19
										3H:1V	2.15
										4H:1V	2.15

Table A.2. Embankment crest deformation for Soil 2 Lee - TSA (continued)

Tests ID	W (%)	$g_d (kN/m^3)$	$g_m (kN/m^3)$	S (%)	f_{UU} (deg)	C_{UU} (kPa)	n	E_{50} (MPa)	H (m)	slope	crest deformation (cm)
S2-UU16 S2-UU17 S2-UU18	25.1	15.5	19.4	91.6	29	98	0.3400	6.977 9.430 12.774	12.2	1H:1V	3.07
										2H:1V	2.93
										3H:1V	2.90
										4H:1V	2.89
									9.1	1H:1V	2.32
										2H:1V	2.30
										3H:1V	2.42
										4H:1V	2.30
									6.1	1H:1V	1.69
										2H:1V	1.68
										3H:1V	1.68
										4H:1V	1.68
									3.0	1H:1V	0.94
										2H:1V	0.93
										3H:1V	0.93
										4H:1V	0.93

Table A.2. Embankment crest deformation for Soil 2 Lee - TSA (continued)

Tests ID	W (%)	$g_d (kN / m^3)$	$g_m (kN / m^3)$	S (%)	f_{UU} (deg)	C_{UU} (kPa)	n	E_{50} (MPa)	H (m)	slope	crest deformation (cm)
S2-UU19 S2-UU20 S2-UU21	20.9	15.9	19.3	81.0	41	90	0.2559	22.751 22.989 23.225	12.2	1H:1V	1.57
										2H:1V	1.57
										3H:1V	1.57
										4H:1V	1.57
									9.1	1H:1V	1.16
										2H:1V	1.16
										3H:1V	1.16
										4H:1V	1.16
									6.1	1H:1V	0.78
										2H:1V	0.78
										3H:1V	0.78
										4H:1V	0.78
									3.0	1H:1V	0.39
										2H:1V	0.39
										3H:1V	0.39
										4H:1V	0.39

Table A.2. Embankment crest deformation for Soil 2 Lee - TSA (continued)

Tests ID	W (%)	$g_d (kN/m^3)$	$g_m (kN/m^3)$	S (%)	f_{UU} (deg)	C_{UU} (kPa)	n	E_{50} (MPa)	H (m)	slope	crest deformation (cm)
S2-UU25 S2-UU26 S2-UU27	12.5	15.4	17.4	45.0	39	89	0.2704	22.931 27.799 33.744	12.2	1H:1V	1.30
										2H:1V	1.30
										3H:1V	1.30
										4H:1V	1.30
									9.1	1H:1V	1.02
										2H:1V	1.02
										3H:1V	1.02
										4H:1V	1.02
									6.1	1H:1V	0.73
										2H:1V	0.73
										3H:1V	0.73
										4H:1V	0.73
									3.0	1H:1V	0.39
										2H:1V	0.38
										3H:1V	0.38
										4H:1V	0.38

Table A.2. Embankment crest deformation for Soil 2 Lee - TSA (continued)

Tests ID	W (%)	$g_d (kN/m^3)$	$g_m (kN/m^3)$	S (%)	f_{UU} (deg)	C_{UU} (kPa)	n	E_{50} (MPa)	H (m)	slope	crest deformation (cm)
S2-UU50 S2-UU51 S2-UU52	16.4	16.9	19.7	73.5	35	196	0.2989	40.535 42.094 44.409	12.2	1H:1V	0.78
										2H:1V	0.78
										3H:1V	0.78
										4H:1V	0.78
									9.1	1H:1V	0.58
										2H:1V	0.58
										3H:1V	0.58
										4H:1V	0.58
									6.1	1H:1V	0.40
										2H:1V	0.39
										3H:1V	0.39
										4H:1V	0.39
									3.0	1H:1V	0.20
										2H:1V	0.20
										3H:1V	0.20
										4H:1V	0.20

Table A.2. Embankment crest deformation for Soil 2 Lee - TSA (continued)

Tests ID	W (%)	$g_d (kN/m^3)$	$g_m (kN/m^3)$	S (%)	f_{UU} (deg)	C_{UU} (kPa)	n	E_{50} (MPa)	H (m)	slope	crest deformation (cm)
S2-UU28 S2-UU29 S2-UU30	15.2	17.4	20.1	73.9	51	119	0.1822	35.660 37.086 50.641	12.2	1H:1V	1.09
										2H:1V	1.09
										3H:1V	1.09
										4H:1V	1.09
									9.1	1H:1V	0.86
										2H:1V	0.86
										3H:1V	0.86
										4H:1V	0.86
									6.1	1H:1V	0.61
										2H:1V	0.61
										3H:1V	0.61
										4H:1V	0.61
									3.0	1H:1V	0.33
										2H:1V	0.33
										3H:1V	0.33
										4H:1V	0.33

Table A.2. Embankment crest deformation for Soil 2 Lee - TSA (continued)

Tests ID	W (%)	$g_d (kN / m^3)$	$g_m (kN / m^3)$	S (%)	f_{UU} (deg)	C_{UU} (kPa)	n	E_{50} (MPa)	H (m)	slope	crest deformation (cm)
S2-UU31 S2-UU32 S2-UU33	21.1	16.8	20.3	92.9	32	174	0.3198	13.507 15.390 17.468	12.2	1H:1V	2.01
										2H:1V	1.98
										3H:1V	1.97
										4H:1V	1.97
									9.1	1H:1V	1.53
										2H:1V	1.51
										3H:1V	1.51
										4H:1V	1.51
									6.1	1H:1V	1.05
										2H:1V	1.04
										3H:1V	1.04
										4H:1V	1.04
									3.0	1H:1V	0.55
										2H:1V	0.55
										3H:1V	0.55
										4H:1V	0.55

Table A.2. Embankment crest deformation for Soil 2 Lee - TSA (continued)

Tests ID	W (%)	$g_d (kN / m^3)$	$g_m (kN / m^3)$	S (%)	f_{UU} (deg)	C_{UU} (kPa)	n	E_{50} (MPa)	H (m)	slope	crest deformation (cm)
S2-UU34 S2-UU35 S2-UU36	17.3	17.5	20.5	84.8	36	254	0.2919	28.781 40.247 45.274	12.2	1H:1V	0.88
										2H:1V	0.88
										3H:1V	0.88
										4H:1V	0.88
									9.1	1H:1V	0.69
										2H:1V	0.69
										3H:1V	0.69
										4H:1V	0.69
									6.1	1H:1V	0.50
										2H:1V	0.50
										3H:1V	0.50
										4H:1V	0.50
									3.0	1H:1V	0.27
										2H:1V	0.27
										3H:1V	0.27
										4H:1V	0.27

Table A.2. Embankment crest deformation for Soil 2 Lee - TSA (continued)

Tests ID	W (%)	$g_d(kN/m^3)$	$g_m(kN/m^3)$	S (%)	f_{UU} (deg)	C_{UU} (kPa)	n	E_{50}(MPa)	H (m)	slope	crest deformation (cm)
S2-UU37 S2-UU38 S2-UU39	12.6	17.2	19.4	59.3	41	243	0.2559	50.072 59.010 69.549	12.2	1H:1V	0.63
										2H:1V	0.63
										3H:1V	0.63
										4H:1V	0.63
									9.1	1H:1V	0.49
										2H:1V	0.49
										3H:1V	0.49
										4H:1V	0.49
									6.1	1H:1V	0.35
										2H:1V	0.35
										3H:1V	0.35
										4H:1V	0.35
									3.0	1H:1V	0.18
										2H:1V	0.18
										3H:1V	0.18
										4H:1V	0.18

Table A.2. Embankment crest deformation for Soil 2 Lee - TSA (continued)

Tests ID	W (%)	$g_d(kN/m^3)$	$g_m(kN/m^3)$	S (%)	f_{UU} (deg)	C_{UU} (kPa)	n	E_{50} (MPa)	H (m)	slope	crest deformation (cm)
S2-UU4 S2-UU5 S2-UU6	24.6	15.7	19.6	92.5	35	79	0.2989	4.756 5.928 7.132	12.2	1H:1V	5.58
										2H:1V	5.56
										3H:1V	5.55
										4H:1V	5.55
									9.1	1H:1V	4.34
										2H:1V	4.33
										3H:1V	4.33
										4H:1V	4.33
									6.1	1H:1V	3.11
										2H:1V	3.10
										3H:1V	3.10
										4H:1V	3.09
									3.0	1H:1V	1.68
										2H:1V	1.68
										3H:1V	1.68
										4H:1V	1.68

Table A.2. Embankment crest deformation for Soil 2 Lee - TSA (continued)

Tests ID	W (%)	$g_d (kN/m^3)$	$g_m (kN/m^3)$	S (%)	f_{UU} (deg)	C_{UU} (kPa)	n	E_{50} (MPa)	H (m)	slope	crest deformation (cm)
S2-UU7 S2-UU8 S2-UU9	31.2	14.4	18.9	93.1	15	45	0.4257	1.338 1.515 1.715	12.2	1H:1V	13.50
										2H:1V	12.83
										3H:1V	12.61
										4H:1V	12.50
									9.1	1H:1V	9.84
										2H:1V	9.51
										3H:1V	9.42
										4H:1V	9.33
									6.1	1H:1V	6.60
										2H:1V	6.40
										3H:1V	6.33
										4H:1V	6.30
									3.0	1H:1V	3.33
										2H:1V	3.23
										3H:1V	3.19
										4H:1V	3.19

Table A.2. Embankment crest deformation for Soil 2 Lee - TSA (continued)

Tests ID	W (%)	$g_d (kN/m^3)$	$g_m (kN/m^3)$	S (%)	f_{UU} (deg)	C_{UU} (kPa)	n	E_{50} (MPa)	H (m)	slope	crest deformation (cm)
S2-UU22 S2-UU23 S2-UU24	19.4	17.2	20.6	91.7	49	143	0.1970	23.699 26.555 32.595	12.2	1H:1V	1.52
										2H:1V	1.52
										3H:1V	1.52
										4H:1V	1.52
									9.1	1H:1V	1.20
										2H:1V	1.20
										3H:1V	1.20
										4H:1V	1.20
									6.1	1H:1V	0.87
										2H:1V	0.87
										3H:1V	0.87
										4H:1V	0.87
									3.0	1H:1V	0.46
										2H:1V	0.46
										3H:1V	0.46
										4H:1V	0.46

Table A.2. Embankment crest deformation for Soil 2 Lee - TSA (continued)

Tests ID	W (%)	$g_d (kN/m^3)$	$g_m (kN/m^3)$	S (%)	f_{UU} (deg)	C_{UU} (kPa)	n	E_{50} (MPa)	H (m)	slope	crest deformation (cm)
S2-UU47 S2-UU48 S2-UU49	16.1	17.8	20.7	83.8	39	276	0.2704	34.719 38.456 51.274	12.2	1H:1V	0.87
										2H:1V	0.87
										3H:1V	0.87
										4H:1V	0.87
									9.1	1H:1V	0.67
										2H:1V	0.67
										3H:1V	0.67
										4H:1V	0.67
									6.1	1H:1V	0.48
										2H:1V	0.48
										3H:1V	0.48
										4H:1V	0.48
									3.0	1H:1V	0.26
										2H:1V	0.26
										3H:1V	0.26
										4H:1V	0.26

Table A.2. Embankment crest deformation for Soil 2 Lee - TSA (continued)

Tests ID	W (%)	$g_d (kN/m^3)$	$g_m (kN/m^3)$	S (%)	f_{UU} (deg)	C_{UU} (kPa)	n	E_{50} (MPa)	H (m)	slope	crest deformation (cm)
S2-UU53 S2-UU54 S2-UU55	13.6	18.4	20.9	77.4	45	326	0.2265	48.763 57.319 71.676	12.2	1H:1V	0.67
										2H:1V	0.67
										3H:1V	0.67
										4H:1V	0.67
									9.1	1H:1V	0.53
										2H:1V	0.53
										3H:1V	0.53
										4H:1V	0.53
									6.1	1H:1V	0.38
										2H:1V	0.38
										3H:1V	0.38
										4H:1V	0.38
									3.0	1H:1V	0.21
										2H:1V	0.21
										3H:1V	0.21
										4H:1V	0.21

Appendix A3 - Deformation Tables for Soil 3 Randolph – Total Stress Analysis (UU Triaxial Parameters)

Table A.3. Embankment crest deformation for Soil 3 Randolph - TSA

Tests ID	W (%)	$g_d (kN/m^3)$	$g_m (kN/m^3)$	S (%)	f_{UU} (deg)	C_{UU} (kPa)	n	E_{50} (MPa)	H (m)	slope	crest deformation (cm)
S3-UU1 S3-UU2 S3-UU3	20.7	15.5	18.7	78.6	35	57	0.3022	5.601 7.118 9.387	12.2	1H:1V	4.65
										2H:1V	4.50
										3H:1V	4.50
										4H:1V	4.50
									9.1	1H:1V	3.61
										2H:1V	3.59
										3H:1V	3.59
										4H:1V	3.59
									6.1	1H:1V	2.59
										2H:1V	2.58
										3H:1V	2.58
										4H:1V	2.58
									3.0	1H:1V	1.41
										2H:1V	1.41
										3H:1V	1.41
										4H:1V	1.41

Table A.3. Embankment crest deformation for Soil 3 Randolph - TSA (continued)

Tests ID	W (%)	$g_d (kN/m^3)$	$g_m (kN/m^3)$	S (%)	f_{UU} (deg)	C_{UU} (kPa)	n	E_{50} (MPa)	H (m)	slope	crest deformation (cm)
S3-UU4 S3-UU5 S3-UU6	21.6	15.3	18.6	79.5	34	55	0.3084	4.844 6.113 8.535	12.2	1H:1V	5.17
										2H:1V	5.10
										3H:1V	5.09
										4H:1V	5.08
									9.1	1H:1V	4.07
										2H:1V	4.05
										3H:1V	4.05
										4H:1V	4.05
									6.1	1H:1V	2.94
										2H:1V	2.86
										3H:1V	2.86
										4H:1V	2.86
									3.0	1H:1V	1.62
										2H:1V	1.62
										3H:1V	1.62
										4H:1V	1.62

Table A.3. Embankment crest deformation for Soil 3 Randolph - TSA (continued)

Tests ID	W (%)	$g_d (kN/m^3)$	$g_m (kN/m^3)$	S (%)	f_{UU} (deg)	C_{UU} (kPa)	n	E_{50} (MPa)	H (m)	slope	crest deformation (cm)
S3-UU7 S3-UU8 S3-UU9	22.3	15.3	18.8	82.6	31	65	0.3298	4.187 5.483 7.180	12.2	1H:1V	5.42
										2H:1V	5.34
										3H:1V	5.33
										4H:1V	5.32
									9.1	1H:1V	4.25
										2H:1V	4.19
										3H:1V	4.19
										4H:1V	4.18
									6.1	1H:1V	3.01
										2H:1V	2.99
										3H:1V	2.99
										4H:1V	2.99
									3.0	1H:1V	1.67
										2H:1V	1.66
										3H:1V	1.66
										4H:1V	1.66

Table A.3. Embankment crest deformation for Soil 3 Randolph - TSA (continued)

Tests ID	W (%)	$g_d(kN/m^3)$	$g_m(kN/m^3)$	S (%)	f_{UU} (deg)	C_{UU} (kPa)	n	E_{50}(MPa)	H (m)	slope	crest deformation (cm)
S3-UU10 S3-UU11 S3-UU12	15.9	15.4	17.9	59.7	32	74	0.3197	7.186 8.652 11.326	12.2	1H:1V	3.54
										2H:1V	3.52
										3H:1V	3.45
										4H:1V	3.45
									9.1	1H:1V	2.76
										2H:1V	2.75
										3H:1V	2.75
										4H:1V	2.75
									6.1	1H:1V	1.94
										2H:1V	1.92
										3H:1V	1.92
										4H:1V	1.92
									3.0	1H:1V	1.05
										2H:1V	1.05
										3H:1V	1.05
										4H:1V	1.05

Table A.3. Embankment crest deformation for Soil 3 Randolph - TSA (continued)

Tests ID	W (%)	$g_d(kN/m^3)$	$g_m(kN/m^3)$	S (%)	f_{UU} (deg)	C_{UU} (kPa)	n	E_{50}(MPa)	H (m)	slope	crest deformation (cm)
S3-UU13 S3-UU14 S3-UU15	14.8	15.2	17.5	53.5	31	65	0.3280	7.041 9.597 19.639	12.2	1H:1V	2.82
										2H:1V	2.80
										3H:1V	2.72
										4H:1V	2.72
									9.1	1H:1V	2.30
										2H:1V	2.28
										3H:1V	2.28
										4H:1V	2.28
									6.1	1H:1V	1.72
										2H:1V	1.71
										3H:1V	1.64
										4H:1V	1.64
									3.0	1H:1V	1.04
										2H:1V	1.04
										3H:1V	1.04
										4H:1V	1.04

Table A.3. Embankment crest deformation for Soil 3 Randolph - TSA (continued)

Tests ID	W (%)	$g_d (kN/m^3)$	$g_m (kN/m^3)$	S (%)	f_{UU} (deg)	C_{UU} (kPa)	n	E_{50} (MPa)	H (m)	slope	crest deformation (cm)
S3-UU22 S3-UU23 S3-UU24	14.5	16.5	18.9	67.5	36	89	0.2903	8.210 8.947 12.162	12.2	1H:1V	3.59
										2H:1V	3.57
										3H:1V	3.57
										4H:1V	3.57
									9.1	1H:1V	2.73
										2H:1V	2.73
										3H:1V	2.72
										4H:1V	2.72
									6.1	1H:1V	1.94
										2H:1V	1.93
										3H:1V	1.93
										4H:1V	1.93
									3.0	1H:1V	1.04
										2H:1V	1.04
										3H:1V	1.04
										4H:1V	1.04

Table A.3. Embankment crest deformation for Soil 3 Randolph - TSA (continued)

Tests ID	W (%)	$g_d (kN/m^3)$	$g_m (kN/m^3)$	S (%)	f_{UU} (deg)	C_{UU} (kPa)	n	E_{50} (MPa)	H (m)	slope	crest deformation (cm)
S3-UU25 S3-UU26 S3-UU27	15.8	16.5	19.1	69.6	37	73	0.2826	7.335 7.853 12.289	12.2	1H:1V	3.93
										2H:1V	3.92
										3H:1V	3.92
										4H:1V	3.91
									9.1	1H:1V	3.11
										2H:1V	3.07
										3H:1V	3.07
										4H:1V	3.07
									6.1	1H:1V	2.22
										2H:1V	2.22
										3H:1V	2.21
										4H:1V	2.21
									3.0	1H:1V	1.23
										2H:1V	1.23
										3H:1V	1.23
										4H:1V	1.23

Table A.3. Embankment crest deformation for Soil 3 Randolph - TSA (continued)

Tests ID	W (%)	$g_d (kN/m^3)$	$g_m (kN/m^3)$	S (%)	f_{UU} (deg)	C_{UU} (kPa)	n	E_{50} (MPa)	H (m)	slope	crest deformation (cm)
S3-UU31 S3-UU33	17.8	16.3	19.2	76.5	32	91	0.3174	6.623 9.816	12.2	1H:1V	3.83
										2H:1V	3.81
										3H:1V	3.80
										4H:1V	3.80
									9.1	1H:1V	2.96
										2H:1V	2.94
										3H:1V	2.94
										4H:1V	2.94
									6.1	1H:1V	2.09
										2H:1V	2.08
										3H:1V	2.05
										4H:1V	2.05
									3.0	1H:1V	1.12
										2H:1V	1.12
										3H:1V	1.12
										4H:1V	1.12

Table A.3. Embankment crest deformation for Soil 3 Randolph - TSA (continued)

Tests ID	W (%)	$g_d(kN/m^3)$	$g_m(kN/m^3)$	S (%)	f_{UU} (deg)	C_{UU} (kPa)	n	E_{50}(MPa)	H (m)	slope	crest deformation (cm)
S3-UU37 S3-UU38 S3-UU39	20.2	15.7	18.9	79.5	30	74	0.3311	3.044 4.081 5.062	12.2	1H:1V	7.53
										2H:1V	7.48
										3H:1V	7.29
										4H:1V	7.28
									9.1	1H:1V	5.75
										2H:1V	5.71
										3H:1V	5.66
										4H:1V	5.66
									6.1	1H:1V	4.11
										2H:1V	4.09
										3H:1V	4.06
										4H:1V	4.06
									3.0	1H:1V	2.24
										2H:1V	2.23
										3H:1V	2.23
										4H:1V	2.23

Table A.3. Embankment crest deformation for Soil 3 Randolph - TSA (continued)

Tests ID	W (%)	$g_d (kN/m^3)$	$g_m (kN/m^3)$	S (%)	f_{UU} (deg)	C_{UU} (kPa)	n	E_{50}(MPa)	H (m)	slope	crest deformation (cm)
S3-UU16 S3-UU17 S3-UU18	12.5	16.7	18.8	57.5	31	136	0.3261	10.697 11.727 12.684	12.2	1H:1V	2.63
										2H:1V	2.60
										3H:1V	2.60
										4H:1V	2.60
									9.1	1H:1V	1.97
										2H:1V	1.96
										3H:1V	1.96
										4H:1V	1.96
									6.1	1H:1V	1.35
										2H:1V	1.34
										3H:1V	1.33
										4H:1V	1.33
									3.0	1H:1V	0.69
										2H:1V	0.68
										3H:1V	0.68
										4H:1V	0.68

Table A.3. Embankment crest deformation for Soil 3 Randolph - TSA (continued)

Tests ID	W (%)	$g_d (kN/m^3)$	$g_m (kN/m^3)$	S (%)	f_{UU} (deg)	C_{UU} (kPa)	n	E_{50} (MPa)	H (m)	slope	crest deformation (cm)
S3-UU19 S3-UU20 S3-UU21	15.3	16.4	18.9	66.9	40	67	0.2658	7.153 8.988 11.322	12.2	1H:1V	4.06
										2H:1V	4.05
										3H:1V	4.05
										4H:1V	4.05
									9.1	1H:1V	3.24
										2H:1V	3.23
										3H:1V	3.23
										4H:1V	3.23
									6.1	1H:1V	2.35
										2H:1V	2.29
										3H:1V	2.29
										4H:1V	2.29
									3.0	1H:1V	1.26
										2H:1V	1.26
										3H:1V	1.26
										4H:1V	1.26

Table A.3. Embankment crest deformation for Soil 3 Randolph - TSA (continued)

Tests ID	W (%)	$g_d(kN/m^3)$	$g_m(kN/m^3)$	S (%)	f_{UU} (deg)	C_{UU} (kPa)	n	E_{50}(MPa)	H (m)	slope	crest deformation (cm)
S3-UU28 S3-UU30	15.4	16.8	19.4	71.2	32	105	0.3202	6.4821 9.0404	12.2	1H:1V	4.02
										2H:1V	4.00
										3H:1V	3.98
										4H:1V	3.98
									9.1	1H:1V	3.08
										2H:1V	3.06
										3H:1V	3.06
										4H:1V	3.06
									6.1	1H:1V	2.16
										2H:1V	2.15
										3H:1V	2.12
										4H:1V	2.12
									3.0	1H:1V	1.14
										2H:1V	1.14
										3H:1V	1.14
										4H:1V	1.14

Table A.3. Embankment crest deformation for Soil 3 Randolph - TSA (continued)

Tests ID	W (%)	$g_d (kN/m^3)$	$g_m (kN/m^3)$	S (%)	f_{UU} (deg)	C_{UU} (kPa)	n	E_{50} (MPa)	H (m)	slope	crest deformation (cm)
S3-UU34 S3-UU35 S3-UU36	19.6	16.1	19.3	81.7	33	79	0.3160	3.073 3.962 5.021	12.2	1H:1V	7.84
										2H:1V	7.80
										3H:1V	7.79
										4H:1V	7.78
									9.1	1H:1V	6.35
										2H:1V	6.16
										3H:1V	6.09
										4H:1V	6.08
									6.1	1H:1V	4.42
										2H:1V	4.37
										3H:1V	4.32
										4H:1V	4.32
									3.0	1H:1V	2.40
										2H:1V	2.39
										3H:1V	2.39
										4H:1V	2.39

Appendix A4 - Deformation Tables for Soil 4 Rowan – Total Stress Analysis (UU Triaxial Parameters)

Table A.4. Embankment crest deformation for Soil 4 Rowan - TSA

Tests ID	W (%)	$g_d (kN/m^3)$	$g_m (kN/m^3)$	S (%)	f_{UU} (deg)	C_{UU} (kPa)	n	E_{50}(MPa)	H (m)	slope	crest deformation (cm)
S4-UU1 S4-UU2 S4-UU3	44.5	11.4	16.5	90.3	26	27	0.3590	1.143 1.667 2.514	12.2	1H:1V	16.54
										2H:1V	15.68
										3H:1V	15.61
										4H:1V	15.58
									9.1	1H:1V	12.68
										2H:1V	12.27
										3H:1V	12.22
										4H:1V	12.22
									6.1	1H:1V	9.19
										2H:1V	9.17
										3H:1V	9.15
										4H:1V	9.04
									3.0	1H:1V	5.15
										2H:1V	5.11
										3H:1V	5.10
										4H:1V	5.11

Table A.4. Embankment crest deformation for Soil 4 Rowan - TSA (continued)

Tests ID	W (%)	$g_d(kN/m^3)$	$g_m(kN/m^3)$	S (%)	f_{UU} (deg)	C_{UU} (kPa)	n	E_{50}(MPa)	H (m)	slope	crest deformation (cm)
S4-UU4 S4-UU5 S4-UU6	22.2	13.1	16.0	57.6	34	69	0.3046	8.553 11.466 13.944	12.2	1H:1V	3.08
										2H:1V	3.04
										3H:1V	3.04
										4H:1V	3.04
									9.1	1H:1V	2.37
										2H:1V	2.36
										3H:1V	2.36
										4H:1V	2.36
									6.1	1H:1V	1.68
										2H:1V	1.67
										3H:1V	1.67
										4H:1V	1.67
									3.0	1H:1V	0.91
										2H:1V	0.91
										3H:1V	0.91
										4H:1V	0.91

Table A.4. Embankment crest deformation for Soil 4 Rowan - TSA (continued)

Tests ID	W (%)	$g_d(kN/m^3)$	$g_m(kN/m^3)$	S (%)	f_{UU} (deg)	C_{UU} (kPa)	n	E_{50}(MPa)	H (m)	slope	crest deformation (cm)
S4-UU10 S4-UU11 S4-UU12	20.1	13.3	15.9	53.7	33	79	0.3151	8.333 11.786 14.513	12.2	1H:1V	2.95
										2H:1V	2.94
										3H:1V	2.93
										4H:1V	2.93
									9.1	1H:1V	2.31
										2H:1V	2.27
										3H:1V	2.27
										4H:1V	2.27
									6.1	1H:1V	1.65
										2H:1V	1.64
										3H:1V	1.63
										4H:1V	1.63
									3.0	1H:1V	0.91
										2H:1V	0.90
										3H:1V	0.90
										4H:1V	0.90

Table A.4. Embankment crest deformation for Soil 4 Rowan - TSA (continued)

Tests ID	W (%)	$g_d (kN/m^3)$	$g_m (kN/m^3)$	S (%)	f_{UU} (deg)	C_{UU} (kPa)	n	E_{50} (MPa)	H (m)	slope	crest deformation (cm)
S4-UU19 S4-UU20 S4-UU21	29.7	13.3	17.3	80.2	30	74	0.3324	6.773 8.872 11.852	12.2	1H:1V	3.39
										2H:1V	3.32
										3H:1V	3.27
										4H:1V	3.27
									9.1	1H:1V	2.65
										2H:1V	2.59
										3H:1V	2.55
										4H:1V	2.55
									6.1	1H:1V	1.89
										2H:1V	1.84
										3H:1V	1.82
										4H:1V	1.82
									3.0	1H:1V	1.04
										2H:1V	1.03
										3H:1V	1.03
										4H:1V	1.03

Table A.4. Embankment crest deformation for Soil 4 Rowan - TSA (continued)

Tests ID	W (%)	$g_d (kN/m^3)$	$g_m (kN/m^3)$	S (%)	f_{UU} (deg)	C_{UU} (kPa)	n	E_{50} (MPa)	H (m)	slope	crest deformation (cm)
S4-UU28 S4-UU29 S4-UU30	14.5	13.6	15.6	41.0	34	92	0.3094	12.448 13.614 18.113	12.2	1H:1V	2.29
										2H:1V	2.27
										3H:1V	2.27
										4H:1V	2.27
									9.1	1H:1V	1.75
										2H:1V	1.74
										3H:1V	1.74
										4H:1V	1.74
									6.1	1H:1V	1.22
										2H:1V	1.22
										3H:1V	1.22
										4H:1V	1.22
									3.0	1H:1V	0.65
										2H:1V	0.65
										3H:1V	0.65
										4H:1V	0.65

Table A.4. Embankment crest deformation for Soil 4 Rowan - TSA (continued)

Tests ID	W (%)	$g_d (kN/m^3)$	$g_m (kN/m^3)$	S (%)	f_{UU} (deg)	C_{UU} (kPa)	n	E_{50} (MPa)	H (m)	slope	crest deformation (cm)
S4-UU13 S4-UU14 S4-UU15	22.3	14.6	17.9	73.1	33	121	0.3141	11.752 12.805 15.386	12.2	1H:1V	2.43
										2H:1V	2.42
										3H:1V	2.38
										4H:1V	2.38
									9.1	1H:1V	1.84
										2H:1V	1.83
										3H:1V	1.83
										4H:1V	1.83
									6.1	1H:1V	1.28
										2H:1V	1.27
										3H:1V	1.27
										4H:1V	1.27
									3.0	1H:1V	0.67
										2H:1V	0.66
										3H:1V	0.66
										4H:1V	0.66

Table A.4. Embankment crest deformation for Soil 4 Rowan - TSA (continued)

Tests ID	W (%)	$g_d (kN/m^3)$	$g_m (kN/m^3)$	S (%)	f_{UU} (deg)	C_{UU} (kPa)	n	E_{50} (MPa)	H (m)	slope	crest deformation (cm)
S4-UU22 S4-UU23 S4-UU24	27.7	14.3	18.2	86.1	23	134	0.3777	5.924 6.956 7.919	12.2	1H:1V	3.72
										2H:1V	3.60
										3H:1V	3.58
										4H:1V	3.58
									9.1	1H:1V	2.78
										2H:1V	2.74
										3H:1V	2.74
										4H:1V	2.74
									6.1	1H:1V	1.91
										2H:1V	1.88
										3H:1V	1.88
										4H:1V	1.86
									3.0	1H:1V	0.98
										2H:1V	0.97
										3H:1V	0.97
										4H:1V	0.97

Table A.4. Embankment crest deformation for Soil 4 Rowan - TSA (continued)

Tests ID	W (%)	$g_d (kN/m^3)$	$g_m (kN/m^3)$	S (%)	f_{UU} (deg)	C_{UU} (kPa)	n	E_{50} (MPa)	H (m)	slope	crest deformation (cm)
S4-UU31 S4-UU32 S4-UU33	15.8	14.9	17.2	53.7	32	153	0.3211	17.377 18.872 19.793	12.2	1H:1V	1.68
										2H:1V	1.67
										3H:1V	1.66
										4H:1V	1.66
									9.1	1H:1V	1.26
										2H:1V	1.25
										3H:1V	1.25
										4H:1V	1.25
									6.1	1H:1V	0.86
										2H:1V	0.85
										3H:1V	0.85
										4H:1V	0.85
									3.0	1H:1V	0.43
										2H:1V	0.43
										3H:1V	0.43
										4H:1V	0.43

Table A.4. Embankment crest deformation for Soil 4 Rowan - TSA (continued)

Tests ID	W (%)	$g_d(kN/m^3)$	$g_m(kN/m^3)$	S (%)	f_{UU} (deg)	C_{UU} (kPa)	n	E_{50}(MPa)	H (m)	slope	crest deformation (cm)
S4-UU37 S4-UU38 S4-UU39	12.5	14.9	16.8	42.6	38	138	0.2785	16.877 19.181 22.201	12.2	1H:1V	1.84
										2H:1V	1.84
										3H:1V	1.83
										4H:1V	1.83
									9.1	1H:1V	1.41
										2H:1V	1.41
										3H:1V	1.41
										4H:1V	1.41
									6.1	1H:1V	0.99
										2H:1V	0.99
										3H:1V	0.99
										4H:1V	0.98
									3.0	1H:1V	0.51
										2H:1V	0.51
										3H:1V	0.51
										4H:1V	0.51

Table A.4. Embankment crest deformation for Soil 4 Rowan - TSA (continued)

Tests ID	W (%)	$g_d (kN / m^3)$	$g_m (kN / m^3)$	S (%)	f_{UU} (deg)	C_{UU} (kPa)	n	E_{50}(MPa)	H (m)	slope	crest deformation (cm)
S4-UU7 S4-UU8 S4-UU9	20.0	15.1	18.2	70.9	37	137	0.2883	13.624 15.364 17.314	12.2	1H:1V	2.22
										2H:1V	2.21
										3H:1V	2.21
										4H:1V	2.21
									9.1	1H:1V	1.69
										2H:1V	1.68
										3H:1V	1.68
										4H:1V	1.68
									6.1	1H:1V	1.17
										2H:1V	1.17
										3H:1V	1.17
										4H:1V	1.17
									3.0	1H:1V	0.61
										2H:1V	0.61
										3H:1V	0.61
										4H:1V	0.61

Table A.4. Embankment crest deformation for Soil 4 Rowan - TSA (continued)

Tests ID	W (%)	$g_d (kN/m^3)$	$g_m (kN/m^3)$	S (%)	f_{UU} (deg)	C_{UU} (kPa)	n	E_{50} (MPa)	H (m)	slope	crest deformation (cm)
S4-UU16 S4-UU17 S4-UU18	22.6	15.3	18.8	82.2	25	203	0.3691	10.808 12.888 13.969	12.2	1H:1V	2.11
										2H:1V	2.06
										3H:1V	2.05
										4H:1V	2.05
									9.1	1H:1V	1.58
										2H:1V	1.56
										3H:1V	1.56
										4H:1V	1.56
									6.1	1H:1V	1.09
										2H:1V	1.08
										3H:1V	1.08
										4H:1V	1.07
									3.0	1H:1V	0.56
										2H:1V	0.55
										3H:1V	0.55
										4H:1V	0.55

Table A.4. Embankment crest deformation for Soil 4 Rowan - TSA (continued)

Tests ID	W (%)	$g_d(kN/m^3)$	$g_m(kN/m^3)$	S (%)	f_{UU} (deg)	C_{UU} (kPa)	n	E_{50}(MPa)	H (m)	slope	crest deformation (cm)
S4-UU25 S4-UU26 S4-UU27	27.8	14.4	18.3	87.4	27	106	0.3540	3.638 4.114 5.121	12.2	1H:1V	6.52
										2H:1V	6.40
										3H:1V	6.38
										4H:1V	6.38
									9.1	1H:1V	4.92
										2H:1V	4.87
										3H:1V	4.86
										4H:1V	4.86
									6.1	1H:1V	3.46
										2H:1V	3.39
										3H:1V	3.38
										4H:1V	3.38
									3.0	1H:1V	1.80
										2H:1V	1.79
										3H:1V	1.79
										4H:1V	1.79

Table A.4. Embankment crest deformation for Soil 4 Rowan - TSA (continued)

Tests ID	W (%)	$g_d(kN/m^3)$	$g_m(kN/m^3)$	S (%)	f_{UU} (deg)	C_{UU} (kPa)	n	E_{50}(MPa)	H (m)	slope	crest deformation (cm)
S4-UU34 S4-UU35 S4-UU36	14.9	15.7	18.0	57.2	42	138	0.2515	19.875 20.985 22.335	12.2	1H:1V	1.75
										2H:1V	1.75
										3H:1V	1.75
										4H:1V	1.75
									9.1	1H:1V	1.32
										2H:1V	1.31
										3H:1V	1.31
										4H:1V	1.31
									6.1	1H:1V	0.90
										2H:1V	0.90
										3H:1V	0.90
										4H:1V	0.90
									3.0	1H:1V	0.45
										2H:1V	0.45
										3H:1V	0.45
										4H:1V	0.45

Table A.4. Embankment crest deformation for Soil 4 Rowan - TSA (continued)

Tests ID	W (%)	$g_d (kN/m^3)$	$g_m (kN/m^3)$	S (%)	f_{UU} (deg)	C_{UU} (kPa)	n	E_{50} (MPa)	H (m)	slope	crest deformation (cm)
S4-UU40 S4-UU41 S4-UU42	12.5	15.4	17.3	45.8	51	67	0.1790	12.388 21.370 22.998	12.2	1H:1V	2.82
										2H:1V	2.82
										3H:1V	2.82
										4H:1V	2.82
									9.1	1H:1V	2.28
										2H:1V	2.28
										3H:1V	2.28
										4H:1V	2.28
									6.1	1H:1V	1.67
										2H:1V	1.67
										3H:1V	1.67
										4H:1V	1.67
									3.0	1H:1V	0.97
										2H:1V	0.97
										3H:1V	0.97
										4H:1V	0.97

Appendix A5 - Deformation Tables for Soil 5 Mecklenburg – Total Stress Analysis (UU Triaxial Parameters)

Table A.5. Embankment crest deformation for Soil 5 Mecklenburg - TSA

Tests ID	W (%)	$g_d (kN/m^3)$	$g_m (kN/m^3)$	S (%)	f_{UU} (deg)	C_{UU} (kPa)	n	E_{50} (MPa)	H (m)	slope	crest deformation (cm)
S5-UU31 S5-UU32 S5-UU33	18.8	15.5	18.4	68.3	28	79	0.3498	8.553 9.908 10.210	12.2	1H:1V	3.04
										2H:1V	2.99
										3H:1V	2.98
										4H:1V	2.98
									9.1	1H:1V	2.26
										2H:1V	2.24
										3H:1V	2.23
										4H:1V	2.23
									6.1	1H:1V	1.55
										2H:1V	1.54
										3H:1V	1.53
										4H:1V	1.53
									3.0	1H:1V	0.78
										2H:1V	0.78
										3H:1V	0.78
										4H:1V	0.78

Table A.5. Embankment crest deformation for Soil 5 Mecklenburg - TSA (continued)

Tests ID	W (%)	$g_d(kN/m^3)$	$g_m(kN/m^3)$	S (%)	f_{UU} (deg)	C_{UU} (kPa)	n	E_{50}(MPa)	H (m)	slope	crest deformation (cm)
S5-UU34 S5-UU35 S5-UU36	16.6	15.5	18.0	60.0	26	86	0.3614	8.560 9.969 10.982	12.2	1H:1V	2.84
										2H:1V	2.78
										3H:1V	2.76
										4H:1V	2.76
									9.1	1H:1V	2.13
										2H:1V	2.09
										3H:1V	2.08
										4H:1V	2.08
									6.1	1H:1V	1.46
										2H:1V	1.44
										3H:1V	1.43
										4H:1V	1.43
									3.0	1H:1V	0.75
										2H:1V	0.74
										3H:1V	0.74
										4H:1V	0.74

Table A.5. Embankment crest deformation for Soil 5 Mecklenburg - TSA (continued)

Tests ID	W (%)	$g_d(kN/m^3)$	$g_m(kN/m^3)$	S (%)	f_{UU} (deg)	C_{UU} (kPa)	n	E_{50}(MPa)	H (m)	slope	crest deformation (cm)
S5-UU1 S5-UU2 S5-UU3	18.0	15.9	18.8	69.8	26	93	0.3602	9.316 9.691 11.566	12.2	1H:1V	2.71
										2H:1V	2.64
										3H:1V	2.64
										4H:1V	2.63
									9.1	1H:1V	2.02
										2H:1V	1.99
										3H:1V	1.98
										4H:1V	1.98
									6.1	1H:1V	1.38
										2H:1V	1.36
										3H:1V	1.36
										4H:1V	1.36
									3.0	1H:1V	0.70
										2H:1V	0.70
										3H:1V	0.70
										4H:1V	0.70

Table A.5. Embankment crest deformation for Soil 5 Mecklenburg - TSA (continued)

Tests ID	W (%)	$g_d (kN/m^3)$	$g_m (kN/m^3)$	S (%)	f_{UU} (deg)	C_{UU} (kPa)	n	E_{50}(MPa)	H (m)	slope	crest deformation (cm)
S5-UU4 S5-UU5 S5-UU6	20.8	15.5	18.8	76.0	29	62	0.3399	6.089 8.112 9.580	12.2	1H:1V	3.73
										2H:1V	3.63
										3H:1V	3.62
										4H:1V	3.62
									9.1	1H:1V	2.89
										2H:1V	2.79
										3H:1V	2.79
										4H:1V	2.79
									6.1	1H:1V	2.00
										2H:1V	1.99
										3H:1V	1.98
										4H:1V	1.98
									3.0	1H:1V	1.09
										2H:1V	1.08
										3H:1V	1.08
										4H:1V	1.08

Table A.5. Embankment crest deformation for Soil 5 Mecklenburg - TSA (continued)

Tests ID	W (%)	$g_d (kN/m^3)$	$g_m (kN/m^3)$	S (%)	f_{UU} (deg)	C_{UU} (kPa)	n	E_{50} (MPa)	H (m)	slope	crest deformation (cm)
S5-UU7 S5-UU8 S5-UU9	15.9	15.9	18.5	61.6	30	95	0.3320	9.815 14.077 15.843	12.2	1H:1V	2.31
										2H:1V	2.26
										3H:1V	2.26
										4H:1V	2.26
									9.1	1H:1V	1.80
										2H:1V	1.75
										3H:1V	1.74
										4H:1V	1.74
									6.1	1H:1V	1.27
										2H:1V	1.24
										3H:1V	1.24
										4H:1V	1.24
									3.0	1H:1V	0.69
										2H:1V	0.68
										3H:1V	0.68
										4H:1V	0.68

Table A.5. Embankment crest deformation for Soil 5 Mecklenburg - TSA (continued)

Tests ID	W (%)	$g_d (kN / m^3)$	$g_m (kN / m^3)$	S (%)	f_{UU} (deg)	C_{UU} (kPa)	n	E_{50} (MPa)	H (m)	slope	crest deformation (cm)
S5-UU19 S5-UU20 S5-UU21	22.9	15.6	19.2	84.8	22	85	0.3850	4.654 6.931 7.156	12.2	1H:1V	4.03
									12.2	2H:1V	3.85
									12.2	3H:1V	3.78
									12.2	4H:1V	3.77
									9.1	1H:1V	3.04
									9.1	2H:1V	2.90
									9.1	3H:1V	2.89
									9.1	4H:1V	2.88
									6.1	1H:1V	2.11
									6.1	2H:1V	2.05
									6.1	3H:1V	2.05
									6.1	4H:1V	2.05
									3.0	1H:1V	1.12
									3.0	2H:1V	1.10
									3.0	3H:1V	1.09
									3.0	4H:1V	1.09

Table A.5. Embankment crest deformation for Soil 5 Mecklenburg - TSA (continued)

Tests ID	W (%)	$g_d(kN/m^3)$	$g_m(kN/m^3)$	S (%)	f_{UU} (deg)	C_{UU} (kPa)	n	E_{50}(MPa)	H (m)	slope	crest deformation (cm)
S5-UU22 S5-UU23 S5-UU24	13.7	15.8	18.0	52.0	33	83	0.3155	12.097 14.106 14.186	12.2	1H:1V	2.38
										2H:1V	2.35
										3H:1V	2.35
										4H:1V	2.35
									9.1	1H:1V	1.78
										2H:1V	1.77
										3H:1V	1.77
										4H:1V	1.77
									6.1	1H:1V	1.22
										2H:1V	1.21
										3H:1V	1.21
										4H:1V	1.21
									3.0	1H:1V	0.62
										2H:1V	0.62
										3H:1V	0.62
										4H:1V	0.62

Table A.5. Embankment crest deformation for Soil 5 Mecklenburg - TSA (continued)

Tests ID	W (%)	$g_d(kN/m^3)$	$g_m(kN/m^3)$	S (%)	f_{UU} (deg)	C_{UU} (kPa)	n	E_{50}(MPa)	H (m)	slope	crest deformation (cm)
S5-UU37 S5-UU38 S5-UU39	14.4	14.8	17.0	47.2	29	60	0.3395	9.438 10.357 12.200	12.2	1H:1V	2.89
										2H:1V	2.85
										3H:1V	2.83
										4H:1V	2.82
									9.1	1H:1V	2.16
										2H:1V	2.14
										3H:1V	2.13
										4H:1V	2.12
									6.1	1H:1V	1.48
										2H:1V	1.46
										3H:1V	1.46
										4H:1V	1.46
									3.0	1H:1V	0.75
										2H:1V	0.75
										3H:1V	0.75
										4H:1V	0.75

Table A.5. Embankment crest deformation for Soil 5 Mecklenburg - TSA (continued)

Tests ID	W (%)	$g_d (kN / m^3)$	$g_m (kN / m^3)$	S (%)	f_{UU} (deg)	C_{UU} (kPa)	n	E_{50} (MPa)	H (m)	slope	crest deformation (cm)
S5-UU40 S5-UU41 S5-UU42	10.8	14.4	16.0	33.4	24	76	0.3754	10.308 11.942 13.011	12.2	1H:1V	2.27
										2H:1V	2.22
										3H:1V	2.21
										4H:1V	2.20
									9.1	1H:1V	1.68
										2H:1V	1.67
										3H:1V	1.66
										4H:1V	1.65
									6.1	1H:1V	1.15
										2H:1V	1.13
										3H:1V	1.13
										4H:1V	1.13
									3.0	1H:1V	0.58
										2H:1V	0.58
										3H:1V	0.58
										4H:1V	0.58

Table A.5. Embankment crest deformation for Soil 5 Mecklenburg - TSA (continued)

Tests ID	W (%)	$g_d(kN/m^3)$	$g_m(kN/m^3)$	S (%)	f_{UU} (deg)	C_{UU} (kPa)	n	E_{50}(MPa)	H (m)	slope	crest deformation (cm)
S5-UU10 S5-UU11 S5-UU12	14.5	16.7	19.1	63.2	23	149	0.3785	13.260 14.241 15.150	12.2	1H:1V	1.82
										2H:1V	1.79
										3H:1V	1.78
										4H:1V	1.77
									9.1	1H:1V	1.35
										2H:1V	1.33
										3H:1V	1.32
										4H:1V	1.32
									6.1	1H:1V	0.91
										2H:1V	0.90
										3H:1V	0.89
										4H:1V	0.89
									3.0	1H:1V	0.45
										2H:1V	0.45
										3H:1V	0.45
										4H:1V	0.45

Table A.5. Embankment crest deformation for Soil 5 Mecklenburg - TSA (continued)

Tests ID	W (%)	$g_d (kN/m^3)$	$g_m (kN/m^3)$	S (%)	f_{UU} (deg)	C_{UU} (kPa)	n	E_{50}(MPa)	H (m)	slope	crest deformation (cm)
S5-UU13 S5-UU14	16.8	17.0	19.8	76.2	34	94	0.3031	7.933 13.119	12.2	1H:1V	3.26
										2H:1V	3.15
										3H:1V	3.11
										4H:1V	3.11
									9.1	1H:1V	2.51
										2H:1V	2.49
										3H:1V	2.49
										4H:1V	2.45
									6.1	1H:1V	1.81
										2H:1V	1.79
										3H:1V	1.79
										4H:1V	1.79
									3.0	1H:1V	0.99
										2H:1V	0.99
										3H:1V	0.99
										4H:1V	0.99

Table A.5. Embankment crest deformation for Soil 5 Mecklenburg - TSA (continued)

Tests ID	W (%)	$g_d (kN/m^3)$	$g_m (kN/m^3)$	S (%)	f_{UU} (deg)	C_{UU} (kPa)	n	E_{50} (MPa)	H (m)	slope	crest deformation (cm)
S5-UU16 S5-UU17 S5-UU18	20.1	16.5	19.8	84.7	29	75	0.3421	6.005 7.555 9.158	12.2	1H:1V	3.90
										2H:1V	3.79
										3H:1V	3.78
										4H:1V	3.77
									9.1	1H:1V	2.96
										2H:1V	2.94
										3H:1V	2.93
										4H:1V	2.93
									6.1	1H:1V	2.10
										2H:1V	2.08
										3H:1V	2.07
										4H:1V	2.07
									3.0	1H:1V	1.12
										2H:1V	1.12
										3H:1V	1.12
										4H:1V	1.12

Table A.5. Embankment crest deformation for Soil 5 Mecklenburg - TSA (continued)

Tests ID	W (%)	$g_d (kN/m^3)$	$g_m (kN/m^3)$	S (%)	f_{UU} (deg)	C_{UU} (kPa)	n	E_{50} (MPa)	H (m)	slope	crest deformation (cm)
S5-UU25 S5-UU27	11.3	17.2	19.1	52.8	29	158	0.3369	12.869 18.531	12.2	1H:1V	1.91
										2H:1V	1.87
										3H:1V	1.86
										4H:1V	1.86
									9.1	1H:1V	1.45
										2H:1V	1.42
										3H:1V	1.42
										4H:1V	1.42
									6.1	1H:1V	1.01
										2H:1V	1.00
										3H:1V	1.00
										4H:1V	1.00
									3.0	1H:1V	0.54
										2H:1V	0.53
										3H:1V	0.53
										4H:1V	0.53

Table A.5. Embankment crest deformation for Soil 5 Mecklenburg - TSA (continued)

Tests ID	W (%)	$g_d (kN/m^3)$	$g_m (kN/m^3)$	S (%)	f_{UU} (deg)	C_{UU} (kPa)	n	E_{50} (MPa)	H (m)	slope	crest deformation (cm)
S5-UU28 S5-UU29 S5-UU30	9.4	16.8	18.3	41.3	43	91	0.2430	12.045 16.050 20.479	12.2	1H:1V	2.58
										2H:1V	2.56
										3H:1V	2.55
										4H:1V	2.55
									9.1	1H:1V	2.02
										2H:1V	2.01
										3H:1V	2.01
										4H:1V	2.01
									6.1	1H:1V	1.48
										2H:1V	1.48
										3H:1V	1.46
										4H:1V	1.46
									3.0	1H:1V	0.80
										2H:1V	0.80
										3H:1V	0.80
										4H:1V	0.80

Appendix B - Deformation Tables for Effective Stress Analysis (CU Triaxial Parameters)

Appendix B1 - Deformation Tables for Soil 1 Forsyth – Effective Stress Analysis (CU Triaxial Parameters)

Table B.1. Embankment crest deformation for Soil 1 Forsyth - ESA

Tests ID	W (%)	$g_d(kN/m^3)$	$g_m(kN/m^3)$	S (%)	f'(deg)	C'(kPa)	n	E_{50}(MPa)	H (m)	slope	crest deformation (cm)
S1-CU1 S1-CU2 S1-CU3	22.5	16.7	20.4	≈ 100	33	16	0.3160	1.399 2.663 4.213	12.2	1H:1V	12.92
										2H:1V	12.37
										3H:1V	12.08
										4H:1V	12.07
									9.1	1H:1V	10.80
										2H:1V	10.27
										3H:1V	10.12
										4H:1V	10.11
									6.1	1H:1V	7.89
										2H:1V	7.51
										3H:1V	7.51
										4H:1V	7.50
									3.0	1H:1V	4.91
										2H:1V	4.89
										3H:1V	4.89
										4H:1V	4.89

Appendix B2 - Deformation Tables for Soil 2 Lee – Effective Stress Analysis (CU Triaxial Parameters)

Table B.2. Embankment crest deformation for Soil 2 Lee - ESA

Tests ID	W (%)	$g_d (kN/m^3)$	$g_m (kN/m^3)$	S (%)	f'(deg)	C'(kPa)	n	E_{50}(MPa)	H (m)	slope	crest deformation (cm)
S2-CU1 S2-CU3	35.2	13.8	18.7	≈ 100	28	4	0.3490	1.843 6.246	12.2	1H:1V	8.68
										2H:1V	8.09
										3H:1V	7.97
										4H:1V	7.65
									9.1	1H:1V	6.59
										2H:1V	6.48
										3H:1V	6.48
										4H:1V	6.45
									6.1	1H:1V	5.07
										2H:1V	5.01
										3H:1V	5.01
										4H:1V	4.98
									3.0	1H:1V	3.15
										2H:1V	3.04
										3H:1V	3.04
										4H:1V	3.04

Table B.2. Embankment crest deformation for Soil 2 Lee - ESA (continued)

Tests ID	W (%)	$g_d (kN/m^3)$	$g_m (kN/m^3)$	S (%)	f'(deg)	C'(kPa)	n	E_{50}(MPa)	H (m)	slope	crest deformation (cm)
S2-CU4 S2-CU5 S2-CU6	21.6	17.1	20.8	≈ 100	29	38	0.3377	3.677 5.279 7.585	12.2	1H:1V	5.47
										2H:1V	5.22
										3H:1V	5.20
										4H:1V	5.03
									9.1	1H:1V	4.18
										2H:1V	4.11
										3H:1V	4.10
										4H:1V	4.09
									6.1	1H:1V	3.08
										2H:1V	3.02
										3H:1V	3.02
										4H:1V	3.01
									3.0	1H:1V	1.76
										2H:1V	1.75
										3H:1V	1.75
										4H:1V	1.75

Table B.2. Embankment crest deformation for Soil 2 Lee - ESA (continued)

Tests ID	W (%)	$g_d (kN/m^3)$	$g_m (kN/m^3)$	S (%)	f'(deg)	C'(kPa)	n	E_{50}(MPa)	H (m)	slope	crest deformation (cm)
S2-CU7 S2-CU8 S2-CU9	20.9	17.3	20.9	≈ 100	29	46	0.3430	5.378 10.174 12.972	12.2	1H:1V	3.16
										2H:1V	2.94
										3H:1V	2.93
										4H:1V	2.93
									9.1	1H:1V	2.40
										2H:1V	2.37
										3H:1V	2.37
										4H:1V	2.36
									6.1	1H:1V	1.82
										2H:1V	1.78
										3H:1V	1.78
										4H:1V	1.77
									3.0	1H:1V	1.06
										2H:1V	1.05
										3H:1V	1.05
										4H:1V	1.05

Appendix B3 - Deformation Tables for Soil 3 Randolph – Effective Stress Analysis (CU Triaxial Parameters)

Table B.3. Embankment crest deformation for Soil 3 Randolph - ESA

Tests ID	W (%)	$g_d (kN/m^3)$	$g_m (kN/m^3)$	S (%)	f'(deg)	C'(kPa)	n	E_{50}(MPa)	H (m)	slope	crest deformation (cm)
S3-CU1 S3-CU2 S3-CU3	34.7	13.7	18.5	≈ 100	31	5	0.3284	1.440 2.207 4.823	12.2	1H:1V	12.77
										2H:1V	12.11
										3H:1V	12.11
										4H:1V	12.10
									9.1	1H:1V	10.75
										2H:1V	10.15
										3H:1V	10.13
										4H:1V	9.97
									6.1	1H:1V	7.96
										2H:1V	7.48
										3H:1V	7.47
										4H:1V	7.46
									3.0	1H:1V	4.82
										2H:1V	4.80
										3H:1V	4.80
										4H:1V	4.80

Table B.3. Embankment crest deformation for Soil 3 Randolph - ESA (continued)

Tests ID	W (%)	$g_d (kN/m^3)$	$g_m (kN/m^3)$	S (%)	f'(deg)	C'(kPa)	n	E_{50}(MPa)	H (m)	slope	crest deformation (cm)
S3-CU4 S3-CU5 S3-CU6	29.7	14.7	19.1	≈ 100	37	0	0.2821	1.591 1.632 4.590	12.2	1H:1V	16.89
										2H:1V	16.83
										3H:1V	16.20
										4H:1V	15.99
									9.1	1H:1V	14.27
										2H:1V	13.72
										3H:1V	13.70
										4H:1V	13.43
									6.1	1H:1V	10.85
										2H:1V	10.21
										3H:1V	10.21
										4H:1V	10.21
									3.0	1H:1V	6.40
										2H:1V	6.39
										3H:1V	6.39
										4H:1V	6.39

Hassani et al. (2019) – Final Report for NCDOT RP 2015-05

Table B.3. Embankment crest deformation for Soil 3 Randolph - ESA (continued)

Tests ID	W (%)	$g_d(kN/m^3)$	$g_m(kN/m^3)$	S (%)	f'(deg)	C'(kPa)	n	E_{50}(MPa)	H (m)	slope	crest deformation (cm)
S3-CU7 S3-CU8 S3-CU9	28.9	14.9	19.2	≈ 100	36	2	0.2928	1.627 2.625 4.203	12.2	1H:1V	13.88
										2H:1V	13.33
										3H:1V	13.17
										4H:1V	13.17
									9.1	1H:1V	11.09
										2H:1V	10.89
										3H:1V	10.88
										4H:1V	10.54
									6.1	1H:1V	8.34
										2H:1V	8.20
										3H:1V	8.20
										4H:1V	8.19
									3.0	1H:1V	5.13
										2H:1V	5.12
										3H:1V	5.12
										4H:1V	5.12

187

Appendix B4 - Deformation Tables for Soil 4 Rowan – Effective Stress Analysis (CU Triaxial Parameters)

Table B.4. Embankment crest deformation for Soil 4 Rowan - ESA

Tests ID	W (%)	$g_d (kN/m^3)$	$g_m (kN/m^3)$	S (%)	f'(deg)	C'(kPa)	n	E_{50}(MPa)	H (m)	slope	crest deformation (cm)
S4-CU1 S4-CU2 S4-CU3	46.3	11.9	17.3	≈ 100	32	10	0.3169	2.482 3.154 5.018	12.2	1H:1V	9.77
										2H:1V	9.42
										3H:1V	9.40
										4H:1V	9.39
									9.1	1H:1V	7.61
										2H:1V	7.41
										3H:1V	7.40
										4H:1V	7.32
									6.1	1H:1V	5.58
										2H:1V	5.52
										3H:1V	5.52
										4H:1V	5.51
									3.0	1H:1V	3.15
										2H:1V	3.14
										3H:1V	3.14
										4H:1V	3.14

Table B.4. Embankment crest deformation for Soil 4 Rowan - ESA (continued)

Tests ID	W (%)	$g_d(kN/m^3)$	$g_m(kN/m^3)$	S (%)	f'(deg)	C'(kPa)	n	E_{50}(MPa)	H (m)	slope	crest deformation (cm)
S4-CU4 S4-CU5 S4-CU6	35.8	13.6	18.4	≈ 100	36	5	0.2908	2.433 3.493 5.994	12.2	1H:1V	9.95
										2H:1V	9.88
										3H:1V	9.87
										4H:1V	9.61
									9.1	1H:1V	8.00
										2H:1V	7.86
										3H:1V	7.85
										4H:1V	7.85
									6.1	1H:1V	5.85
										2H:1V	5.83
										3H:1V	5.83
										4H:1V	5.83
									3.0	1H:1V	3.57
										2H:1V	3.56
										3H:1V	3.56
										4H:1V	3.56

Table B.4. Embankment crest deformation for Soil 4 Rowan - ESA (continued)

Tests ID	W (%)	$g_d(kN/m^3)$	$g_m(kN/m^3)$	S (%)	f'(deg)	C'(kPa)	n	E_{50}(MPa)	H (m)	slope	crest deformation (cm)
S4-CU7 S4-CU9	34.2	13.9	18.6	≈ 100	34	14	0.3056	2.306 5.322	12.2	1H:1V	9.81
										2H:1V	9.46
										3H:1V	9.45
										4H:1V	9.44
									9.1	1H:1V	7.78
										2H:1V	7.74
										3H:1V	7.53
										4H:1V	7.44
									6.1	1H:1V	5.79
										2H:1V	5.76
										3H:1V	5.72
										4H:1V	5.72
									3.0	1H:1V	3.35
										2H:1V	3.34
										3H:1V	3.34
										4H:1V	3.34

Appendix B5 - Deformation Tables for Soil 5 Mecklenburg – Effective Stress Analysis (CU Triaxial Parameters)

Table B.5. Embankment crest deformation for Soil 5 Mecklenburg - ESA

Tests ID	W (%)	$g_d(kN/m^3)$	$g_m(kN/m^3)$	S (%)	f'(deg)	C'(kPa)	n	E_{50}(MPa)	H (m)	slope	crest deformation (cm)
S5-CU1 S5-CU3	36.4	13.6	18.6	≈ 100	29	0	0.3412	1.632 4.056	12.2	1H:1V	11.36
										2H:1V	10.93
										3H:1V	10.77
										4H:1V	10.78
									9.1	1H:1V	8.83
										2H:1V	8.59
										3H:1V	8.56
										4H:1V	8.50
									6.1	1H:1V	6.50
										2H:1V	6.45
										3H:1V	6.43
										4H:1V	6.43
									3.0	1H:1V	3.89
										2H:1V	3.87
										3H:1V	3.87
										4H:1V	3.87

Table B.5. Embankment crest deformation for Soil 5 Mecklenburg - ESA (continued)

Tests ID	W (%)	$g_d(kN/m^3)$	$g_m(kN/m^3)$	S (%)	f'(deg)	C'(kPa)	n	E_{50}(MPa)	H (m)	slope	crest deformation (cm)
S5-CU4 S5-CU5 S5-CU6	32.8	14.3	19.0	≈ 100	32	3	0.3174	1.422 2.466 4.437	12.2	1H:1V	13.68
										2H:1V	12.48
										3H:1V	12.31
										4H:1V	12.30
									9.1	1H:1V	11.00
										2H:1V	10.32
										3H:1V	10.32
										4H:1V	10.27
									6.1	1H:1V	7.98
										2H:1V	7.93
										3H:1V	7.92
										4H:1V	7.91
									3.0	1H:1V	4.93
										2H:1V	4.92
										3H:1V	4.92
										4H:1V	4.92

Table B.5. Embankment crest deformation for Soil 5 Mecklenburg - ESA (continued)

Tests ID	W (%)	$g_d(kN/m^3)$	$g_m(kN/m^3)$	S (%)	f'(deg)	C'(kPa)	n	E_{50}(MPa)	H (m)	slope	crest deformation (cm)
S5-CU7 S5-CU9	31.8	14.5	19.1	≈ 100	43	0	0.2395	1.447 4.007	12.2	1H:1V	19.37
										2H:1V	19.07
										3H:1V	19.07
										4H:1V	19.06
									9.1	1H:1V	15.71
										2H:1V	15.41
										3H:1V	15.41
										4H:1V	15.40
									6.1	1H:1V	12.12
										2H:1V	12.11
										3H:1V	12.11
										4H:1V	12.11
									3.0	1H:1V	7.61
										2H:1V	7.61
										3H:1V	7.61
										4H:1V	7.61

Appendix C - Failure Lines for CU Tests
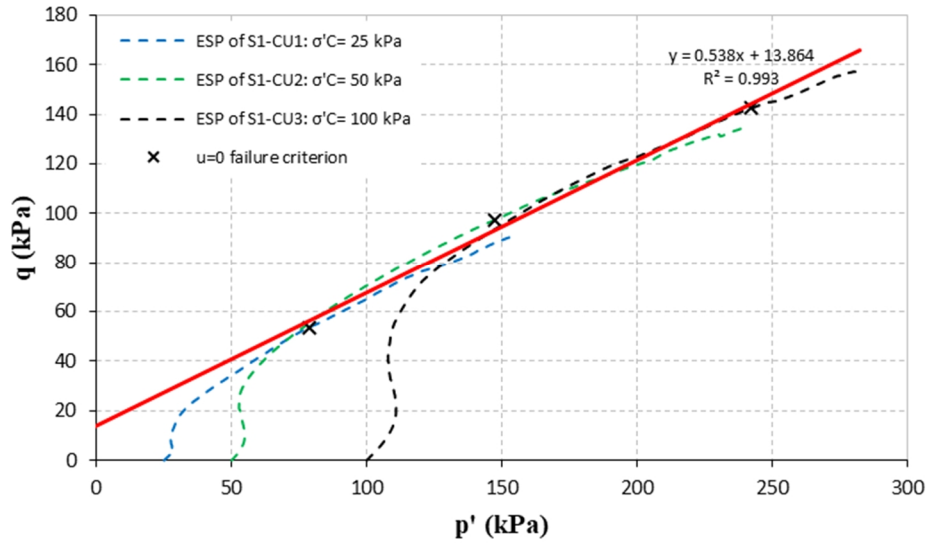
Figure C.1. Effective stress paths and failure line for CU tests on Soil 1 Forsyth - samples compacted at standard energy
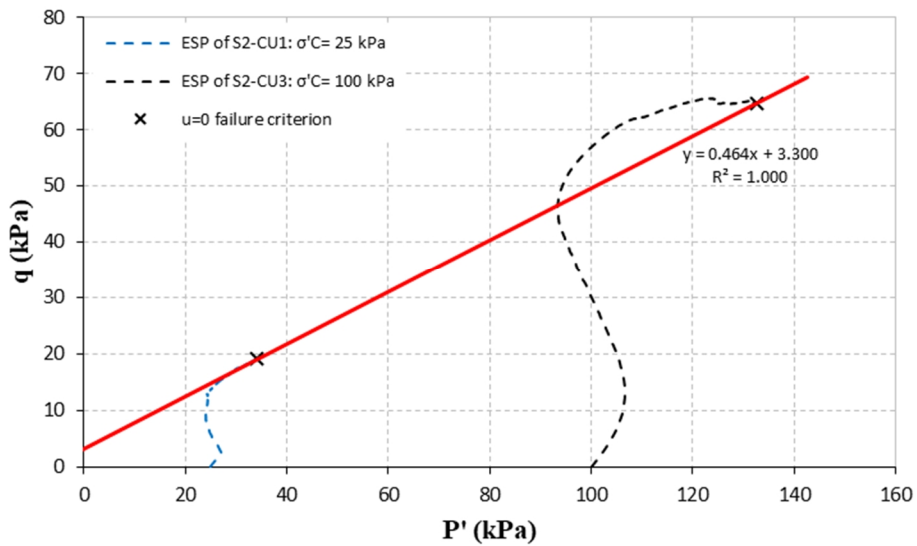
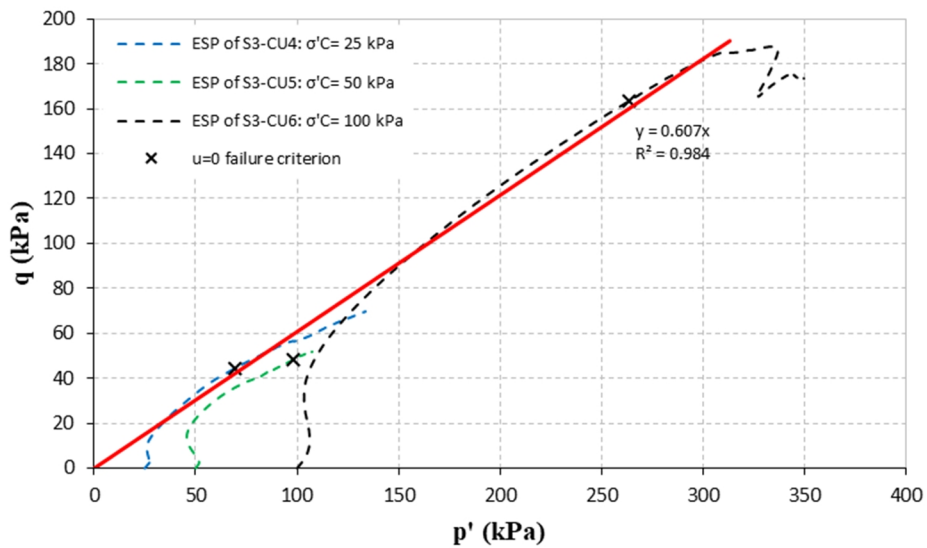Figure C.2. Effective stress path and failure line for CU tests on Soil 2 Lee - samples compacted at standard energy
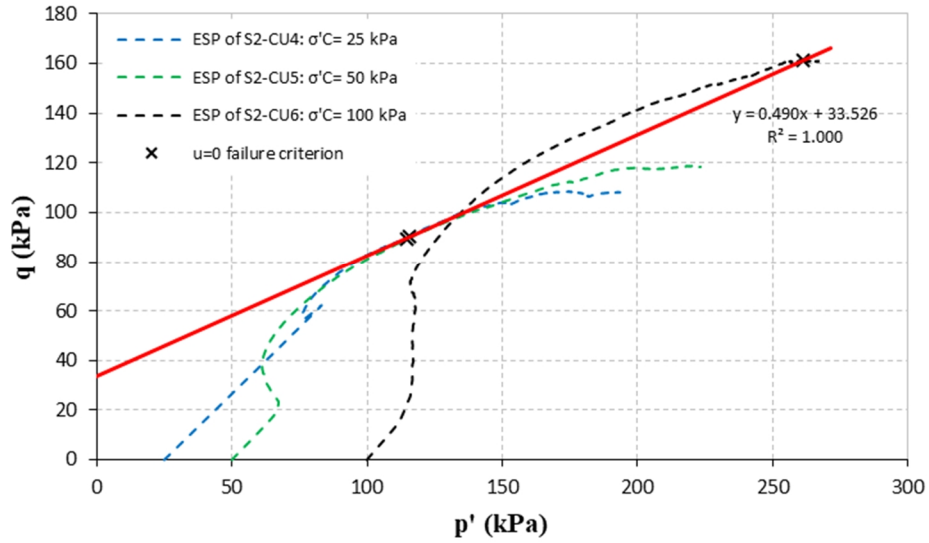
Figure C.3. Effective stress path and failure line for CU tests on Soil 2 Lee - samples compacted at intermediate energy
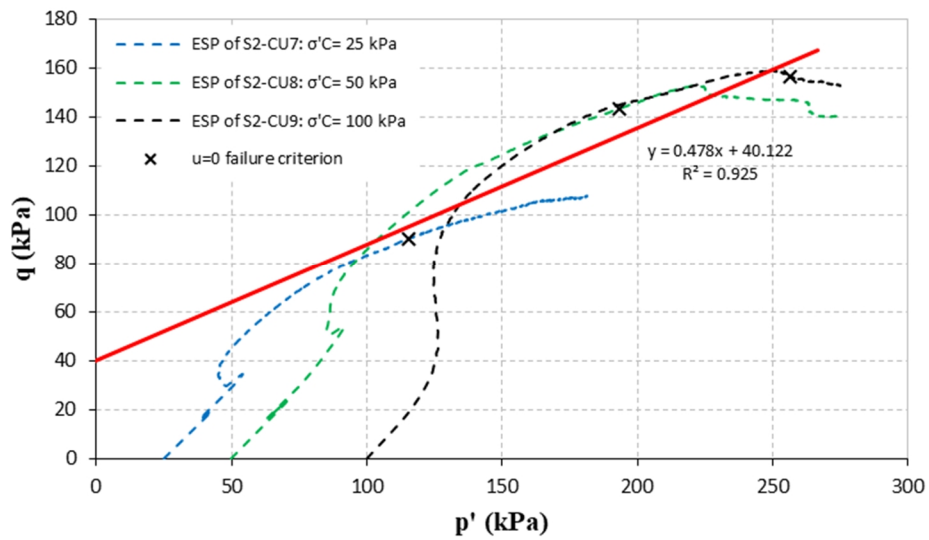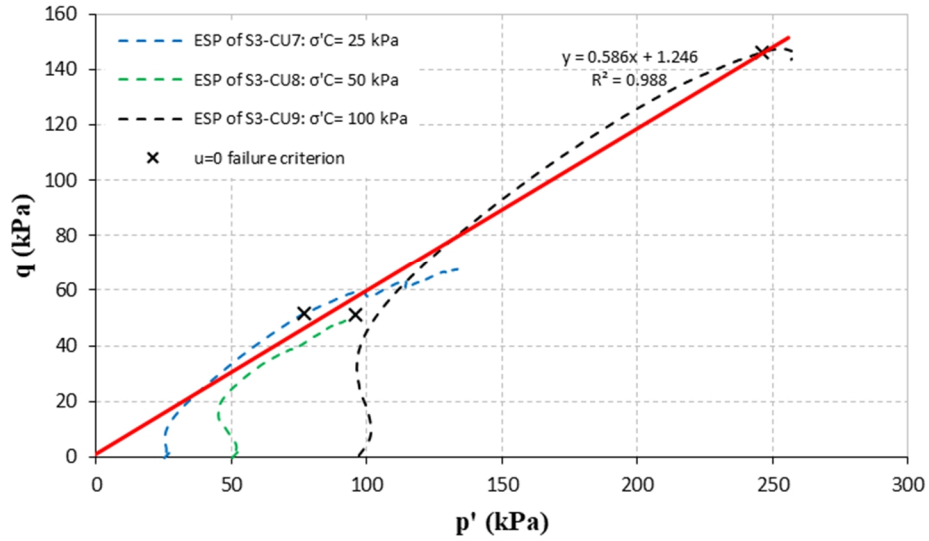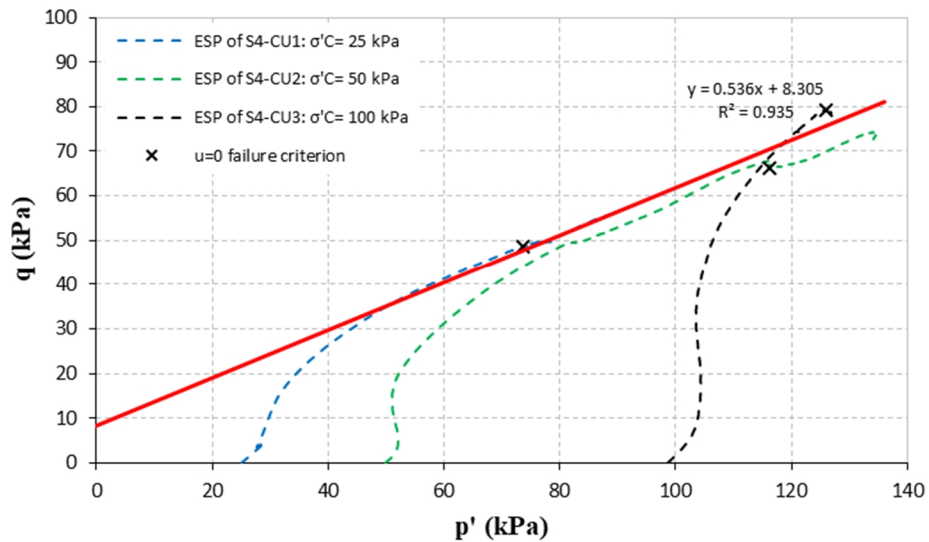

Figure C.4. Effective stress path and failure line for CU tests on Soil 2 Lee - samples compacted at modified energy
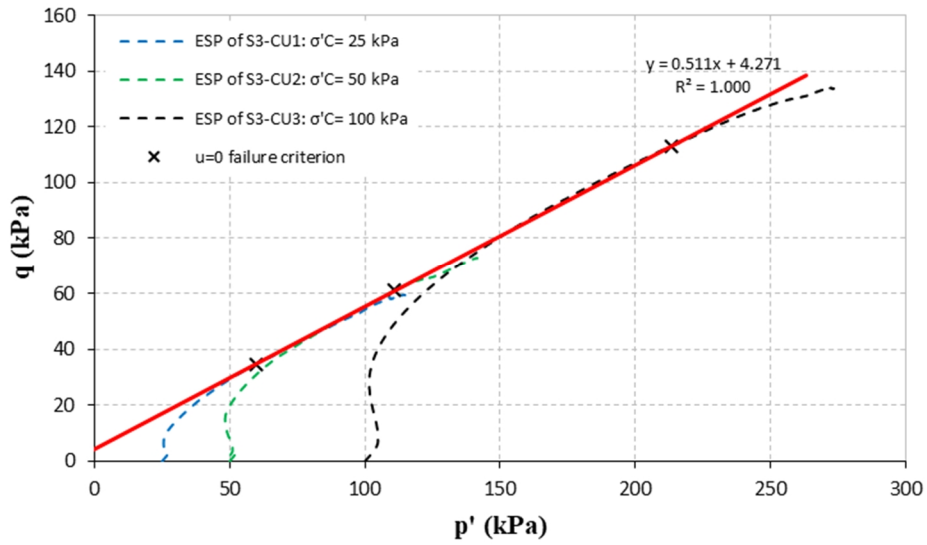
Figure C.5. Effective stress path and failure line for CU tests on Soil 3 Randolph - samples compacted at standard energy
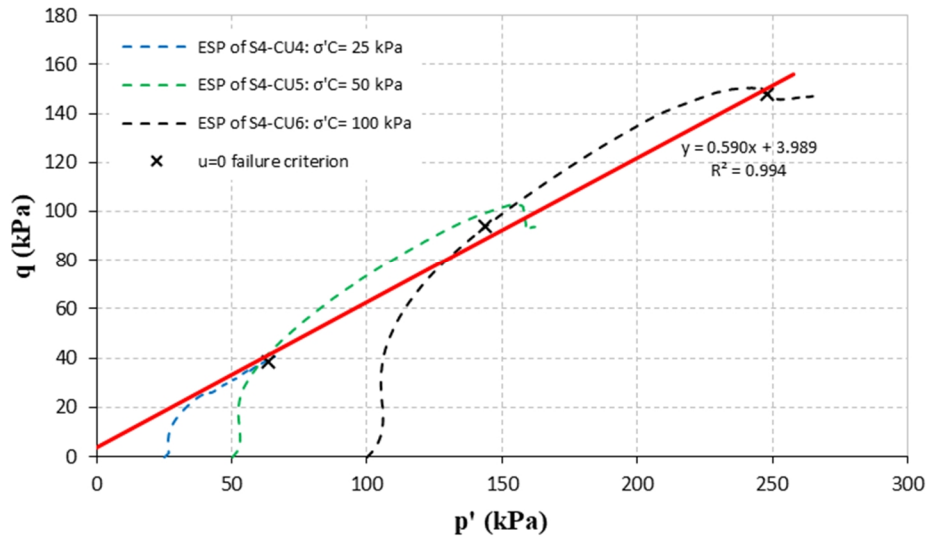

Figure C.6. Effective stress path and failure line for CU tests on Soil 3 Randolph - samples compacted at intermediate energy
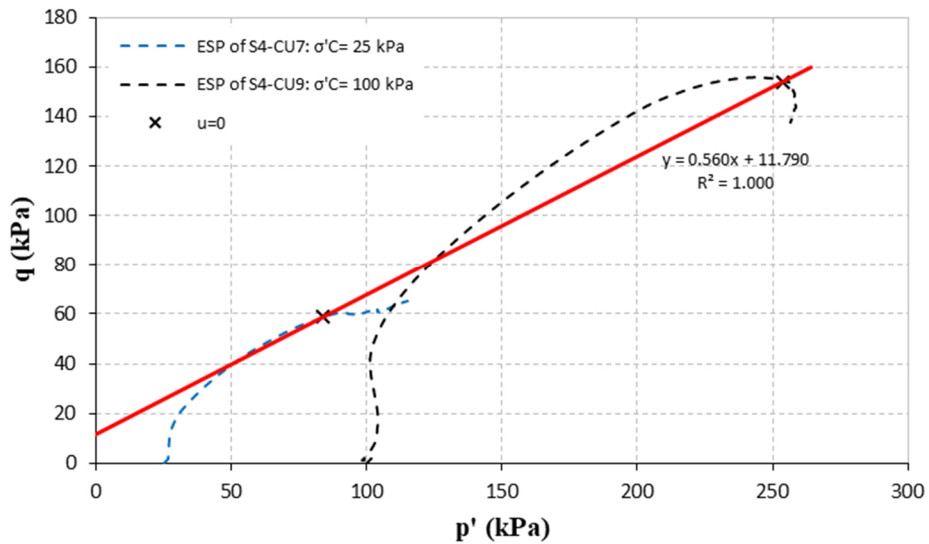
Figure C.7. Effective stress path and failure line for CU tests on Soil 3 Randolph - samples compacted at modified energy
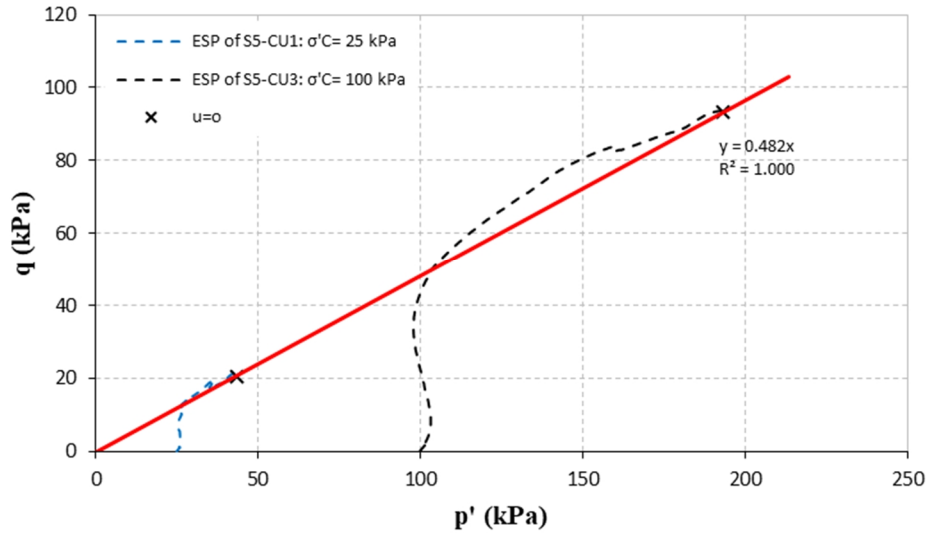

Figure C.8. Effective stress path and failure line for CU tests on Soil 4 Rowan - samples compacted at standard energy

Figure C.9. Effective stress path and failure line for CU tests on Soil 4 Rowan - samples compacted at intermediate energy

Figure C.10. Effective stress path and failure line for CU tests on Soil 4 Rowan - samples compacted at modified energy

198

Figure C.11. Effective stress path and failure line for CU tests on Soil 5 Mecklenburg - samples compacted at standard energy
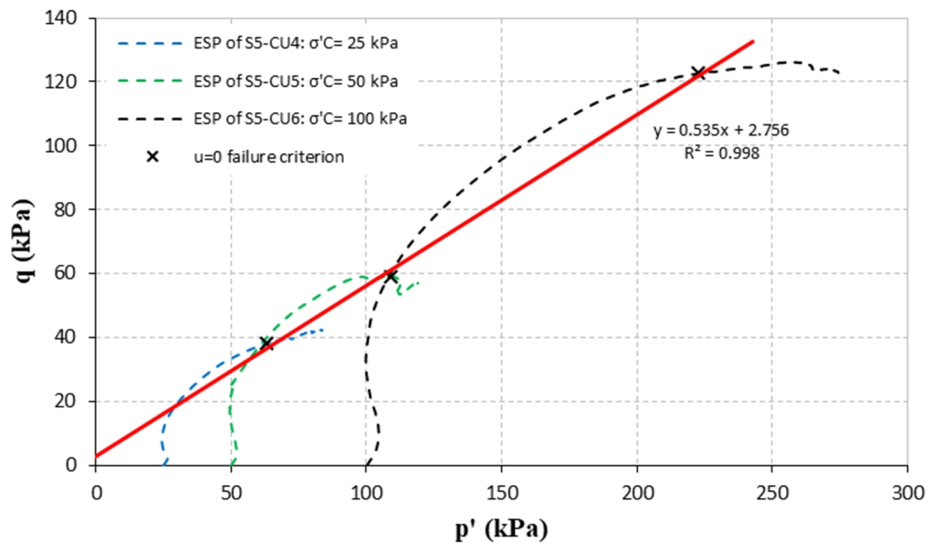

Figure C.12. Effective stress path and failure line for CU tests on Soil 5 Mecklenburg - samples compacted at intermediate energy
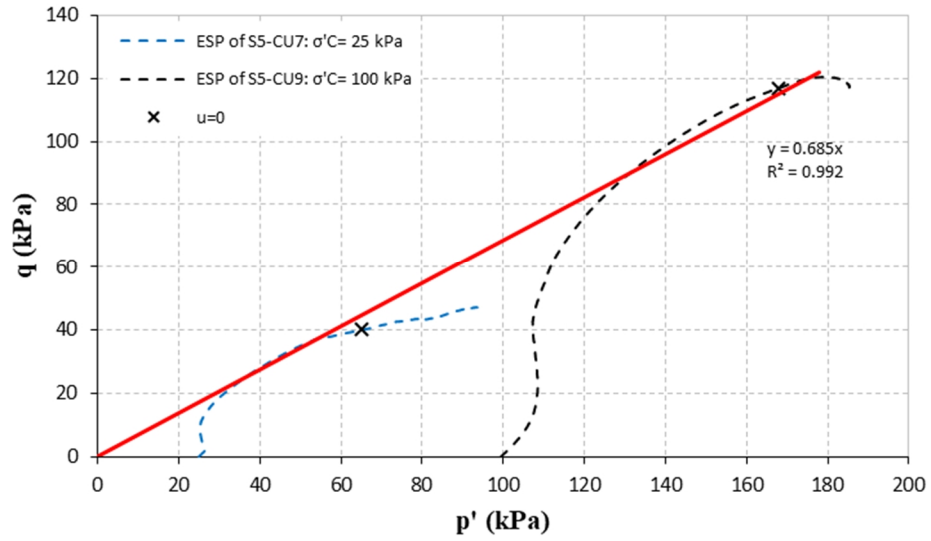
Figure C.13. Effective stress path and failure line for CU tests on Soil 5 Mecklenburg - samples compacted at modified energy